# DOWNEY PLANT

RESEARCH DIVISION

EVALUATION OF THE BLAST
PARAMETERS AND FIREBALL CHARACTERISTICS
OF LIQUID OXYGEN/LIQUID HYDROGEN PROPELLANTS

Final Report On

Contract No. NAS 9-4355

Report No. 0954-01(01)FP / April 1967 / Copy 36

AEROJET GENERAL TIRE GENERAL

AEROJET-GENERAL CORPORATION

DOWNEY, CALIFORNIA

AEROJET-GENERAL CORPORATION
Research Division
11711 Woodruff Avenue
Downey, California

EVALUATION OF THE BLAST
PARAMETERS AND FIREBALL CHARACTERISTICS
OF LIQUID OXYGEN/LIQUID HYDROGEN PROPELLANT

Final Report On

0954-01(01)FP

Contract No. NAS 9-4355

Prepared For

Apollo Program Office
National Aeronautics and Space Administration
Manned Spacecraft Center
Houston, Texas

Prepared by: R. E. Pesante
M. Nishibayashi

Contributors: B. L. Cooper
D. G. Frutchey
A. F. VanRyckeghen

Reviewed by: *M. Nishibayashi*
M. Nishibayashi, Head
Explosive Kinetics Dept.
Ordnance Division

Date: 7 April 1967

No. of Pages: 138

Approved by: *H. J. Fisher*
H. J. Fisher, Manager
Research Division

Classification: UNCLASSIFIED

ACKNOWLEDGEMENTS

CONTENTS

ILLUSTRATIONS

ILLUSTRATIONS (Cont)

TABLES

1.   INTRODUCTION

The current use of liquid oxygen/liquid hydrogen (LOX/LH_2) propellant in large space-vehicle booster systems and its proposed utilization for man-rated booster systems requires a realistic assessment of the potential explosion, fire, and thermal radiation hazards. Accurate assessment of these hazards is especially important for providing design criteria to assure the safety of astronauts in the event of any malfunction of a man-rated propulsion system requiring a mission abort. Accurate evaluation of these hazards is essential for the safety of test personnel and launch equipment, and for the effective accomplishment of space missions with the economic utilization of appropriate funds and land areas. Launch hazards information concerning LOX/RP-1 propellant systems is available from observations of actual malfunctions that have occurred in full-scale missile test flights. Although some information is available for the malfunction of LOX/LH_2 propellant systems, complete information is not available for accurate assessment of the potential hazards. The purpose of this study was to obtain estimates of the potential hazards to personnel and equipment that result from using LOX/LH_2 propellants as compared with actual experiences gained from the explosions of LOX/RP-1 propellants.

It was not the intent of this program to obtain data to be extrapolated for missile size quantities of propellant, nor was it intended for the experimental data to be considered as the complete answer to full-scale evaluation of the explosive characteristics of a launch vehicle.

2.   OBJECTIVE

The objectives of this program were: (1) to study the basic parameters of LOX/LH_2 propellant, and (2) to compare the basic blast characteristics of LOX/LH_2 propellant systems with LOX/RP-1 and nitrogen tetroxide/Aerozine-50 (N_2O_4/A-50) propellant systems. (Aerozine-50 is a 1:1 mixture of hydrazine and unsymmetrical dimethyl hydrazine propellants.) Specific characteristics considered in evaluating the propellant systems were peak overpressure, shock wave velocity, positive pressure impulse and duration, fragment velocity, thermal radiation and temperature, initial fireball growth rate, and fireball size and duration.

3.   SUMMARY

Ten tests were conducted with cryogenic (LOX/LH_2 and LOX/RP-1) and hypergolic (N_2O_4/A-50) propellants from 1 June to 24 September 1965 to evaluate the explosive and thermal characteristics of these materials. The propellants were combined using a mixing technique that permitted variation of the oxidizer/fuel contact area and the weight of propellant for a specific oxidizer/fuel ratio. The oxidizer and the fuel were mixed by placing oxidizer-filled glass dewars in a fuel-filled pan and shattering the dewars with an explosively generated shock wave.

The cryogenic propellants reacted spontaneously when the dewars were shattered. Since this prevented the evaluation of an optimum mixing time before initiation, all tests were conducted without an initiation delay period after initial contact.

The overpressure test results indicated that the explosive yield of LOX/LH_2 increased as the distance from the event increased. The impulse TNT equivalences increased with increased distance to approximately 60 ft from the test fixture and decreased thereafter within the limits of the test area. Maximum overpressure and impulse test equivalences follow:

Propellant Type (1 lb)	Equivalent lb TNT	
	Overpressure	Impulse
LOX/LH_2	0. 6 to 0. 8	0. 8 to 0. 9
LOX/RP-1	0. 6 to 0. 8	0. 8 to 1.05
N_2O_4/A-50	0.42	0. 52

Analysis of test films revealed that most of the fireball's growth occurred during the first 20 msec after propellant initiation.

Examination of the initial fireball growth rate data from test to test indicated a similarity of growth rates for the LOX/LH_2 propellant. Initial fireball growth rates of 0. 92 and 0.46 ft/msec per $lb^{1/3}$ of propellant were observed for the fireball diameters and heights, respectively. The diameter and height growth rates attenuated to approximately 0. 18 and 0. 14 ft/msec per $lb^{1/3}$ of propellant after approximately 15 msec. The maximum fireball diameters varied from 64 to 91 ft and the maximum height ranged from 38. 5 to 73 ft.

4.   TECHNICAL DISCUSSION

4.1   APPROACH

Several programs have been conducted by various agencies (References 1 to 8) to assess explosion hazards associated with catastrophic failures of missile-launch vehicles containing both cryogenic and hypergolic propellants.   None of these studies has evaluated the effect of a change in the initial contact surface area between the oxidizer and the fuel and its influence on the explosion parameters of a LOX/LH_2 propellant system.

In this study it was intended to extend the controlled contact area tests with $LOX/RP-1$ and $N_2O_4/A-50$ propellants in previous studies (Reference 9) to LOX/LH_2 propellant for comparison.

4.2   TEST CONFIGURATION DESIGN

Contact interface area was controlled by placing one-liter cylindrical glass dewar flasks in an aluminum pan.   The oxidizer was placed in the glass dewar and the fuel was placed in the pan surrounding the dewars. The oxidizer and fuel were mixed by transmitting an explosively generated shock wave into the bottom of the aluminum pan; the shock wave shattered the glass dewars and provided nearly simultaneous contact of the fuel and oxidizer.   The contact area was computed from the mean radius of the double-wall glass dewars.   The shock wave was generated by a double length of 20-gr/ft mild detonating fuze (MDF) placed against the bottom on the outside of the aluminum pans directly underneath each row of dewars.   The MDF was initiated at two central points on opposite sides of the pan to make shock wave transmission into the pan nearly simultaneous.   The construction of a LOX/LH_2 dewar pan assembly with the MDF protruding through the foam insulation is shown in Figure 1. The MDF was initiated with a small quantity of Composition C-4 explosive and two DuPont X-98 blasting caps were used to ensure initiation system reliability.

To determine the effect of the LOX/LH_2 explosion parameters with respect to initial propellant contact area, a test plan was devised that evaluated three different contact areas (25. 12, 36. 81, and 56. 23 sq ft) for a fixed oxidizer to fuel ratio (5:1) or total propellant weights of 100, 150, and 225 lb, respectively.   A constant ratio of 1 sq ft of contact area to 4 lb of propellant was maintained for all LOX/LH_2 tests.

HYDROGEN VENT STACK

POLYETHYLENE DIAPHRAGM

CORK STOPPER

LOX IN DEWAR

MILD DETONATING FUZE

ALUMINUM PAN

10 LITER GLASS DEWAR

FOAM INSULATION

LH$_2$ IN PAN
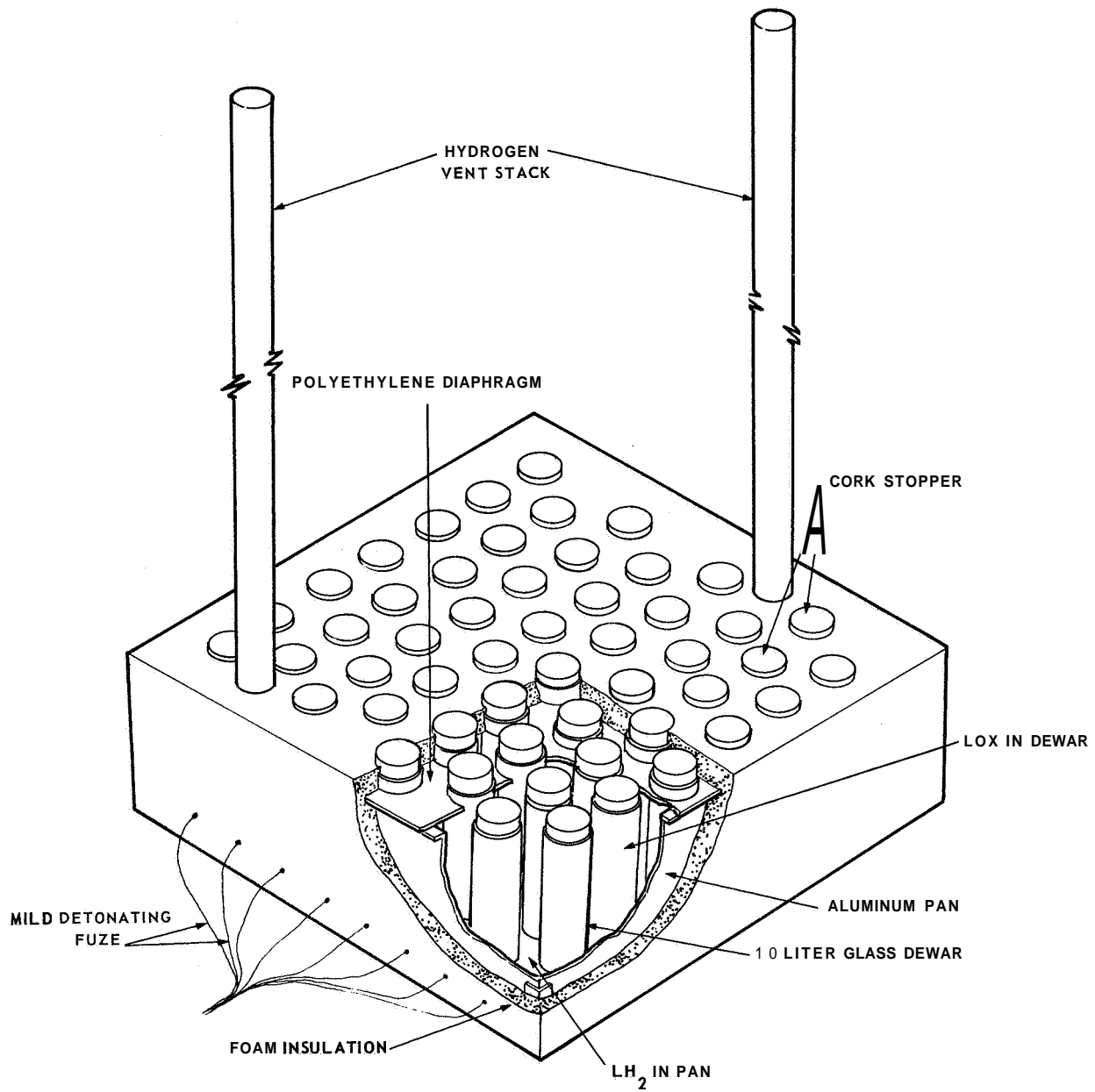
Figure 1. LOX/LH$_2$ Dewar Pan Assembly.

Table 1 Propellant Test Plan*

Propellant	Oxidizer/Fuel Weight Ratio	Propellant Weight (lb)	Contact Area (ft2)	Contact Area To Total Propellant Weight Ratio	Number of Dewars
LOX/LH$_2$	5:1	225	56.23	1:4	81
		150	36.81	1:4	52
		100	25.12	1:4	36
LOX/RP-1	2 5:1	171	36 a1	1:4.54	52
N$_2$O$_4$/A-50	2:1	229.5	36 81	1:6.25	52

*Two tests for each c ation:

Ten tests total.

Comparison tests were conducted with LOX/RP-1 and N_2O_4/A-50 propellants with a contact area of 36. 81 sq ft to permit correlation of the three propellant systems with data obtained in previous studies (Reference 9).   The mixture ratios, initial contact interface areas, and total quantities of propellant are presented in Table 1.   Each of the five test conditions was conducted in duplicate for a total of ten tests.

The dewar pan configuration was designed to provide a symmetrical arrangement.   The number of dewars and the depth of liquid in the pans and dewars was determined with a computer program developed in a previous study (Reference 9).   The pan size, dewar arrangement, and depth of propellants are given in Table 2.

The aluminum pans to contain the dewars and fuel were fabricated to the sizes indicated by the computer program.   The sides of the pans were 1/8 in, sheet welded to a 3/16-in. sheet aluminum bottom.   All joints of the pans were welded and reinforced with 1/8-in. -thick aluminum angle.

Because LH_2 was used in these tests, the pans were insulated with a minimum 2-in. thickness of urethane foam ($\rho \approx$ 2. 0 lb/ft^3) on all sides. A typical LOX/LH_2 dewar pan is shown in Figure 2.   The bottoms of the LOX/RP-1 and N_2O_4/A-50 dewar pans were insulated with approximately 2 in. of foam.   This foam was utilized to ensure that the shock wave trans- mitted into the LOX/RP-1 and N_2O_4/A-50 pans had the same magnitude as that in the LOX/LH_2 tests.   A typical LOX/RP-1 dewar pan is shown in Figure 3.

The pans were designed to remain intact after initiation of the MDF. The shock wave was transmitted into the bottom of the pan without rup- ture of the aluminum sheet; the bottom of a typical pan with its sides blown away after propellant reaction is shown in Figure 4.

4.3   TEST OPERATION

4.3. 1   LOX/LH_2 Tests

The dewars were supported in a vertical position by a 1/16-in. poly- ethylene membrane secured to the top edges of the pan to prevent spillage. The bottom tips of the dewars rested on the bottom of the pan.   Each dewar was closed with a cork stopper to prevent the oxidizer from evaporating.

Table 2   Dewar Pan Data.

Propellant	Total Propellant Weight (lb)	Number of Dewars	Dewar Arrangement*	Pan Size Width (in.)	Pan Size Length (in.)	Height (in.)	Height of Fuel in Pan (in.)
LOX/LH$_2$	225	81	9 by 9	44-3/16	44-3/16	12	11.3
	150	52	4 rows of 7 4 rows of 6 Alternated	35-3/4	35-3/4	12	11.4
LOX/RP-1	100	96	6 by 6	24-1/2	29-7/16	12	11.3
	171	72	4 rows of 7 4 rows of 6 Alternated	23-23/32	24	12	11.4
N$_2$O$_4$/A-50	229.5	52	4 rows of 7 4 rows of 6 Alternated	25-1/32	25	12	11.4

*All dewars were glass, one-liter size, cylindrical with hemispherical bottoms
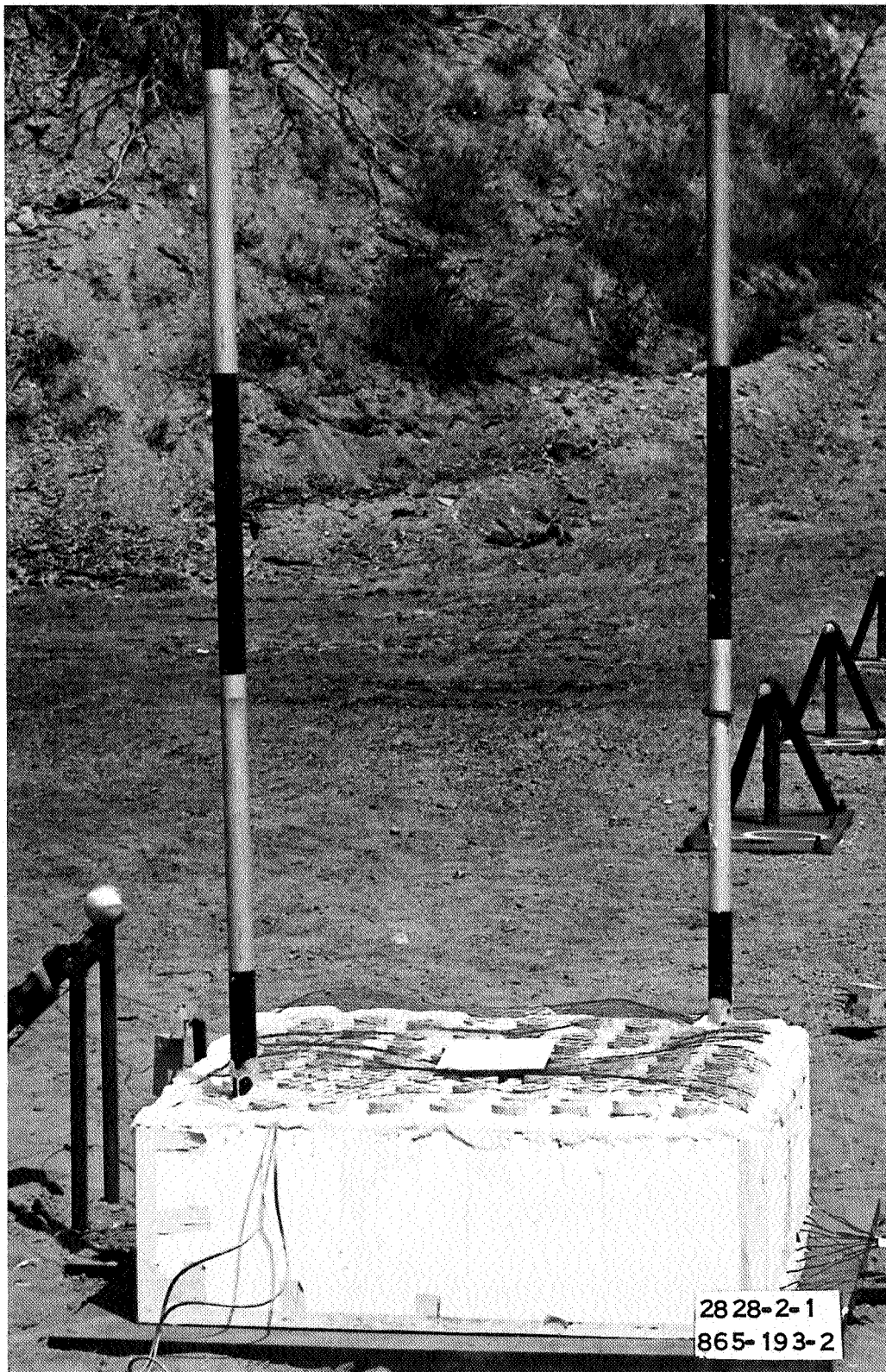
Figure 2. Typical LOX/LH$_2$ Test Setup.
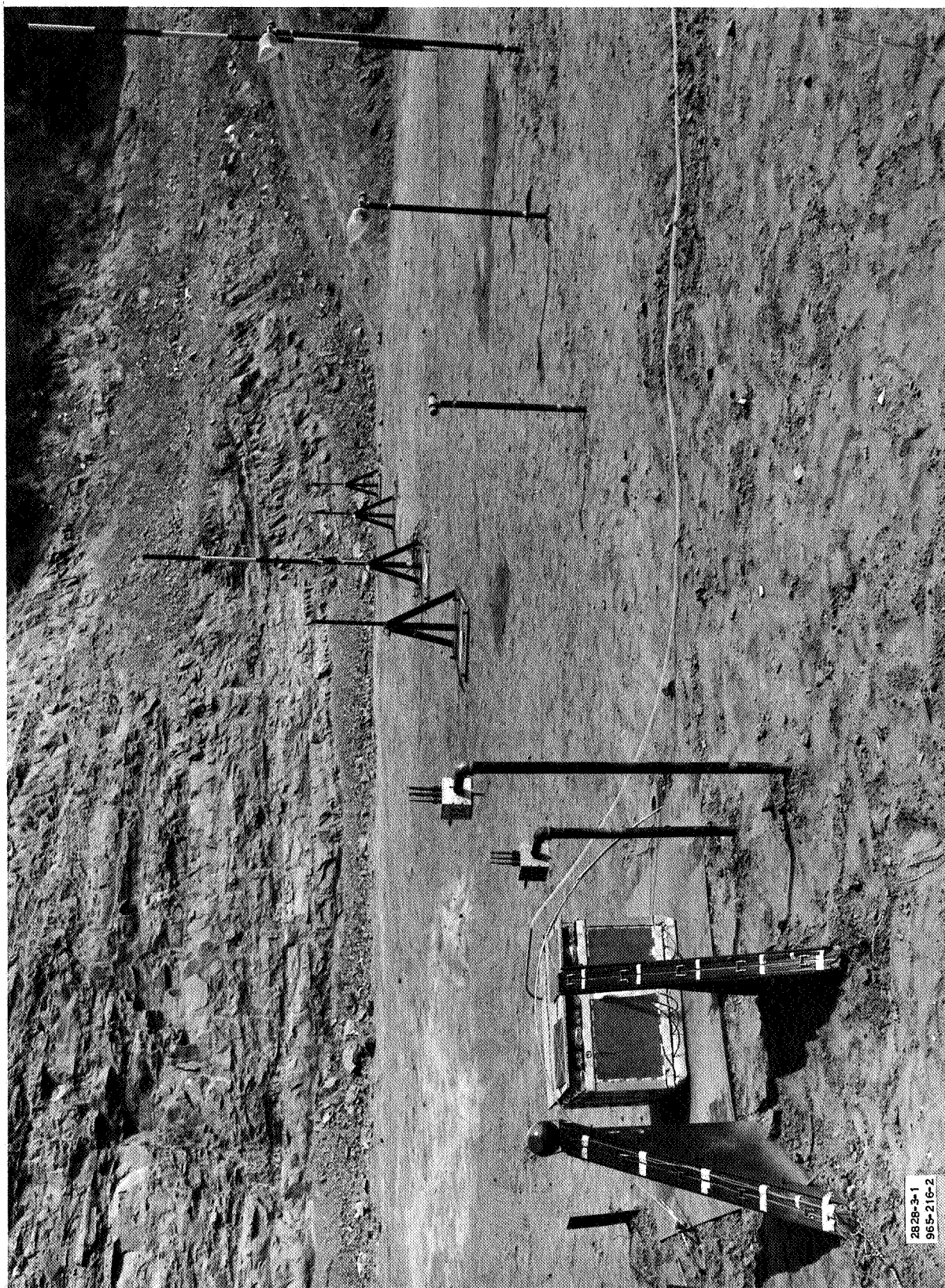
Figure 3. Typical LOX/RP-1 Test Setup.
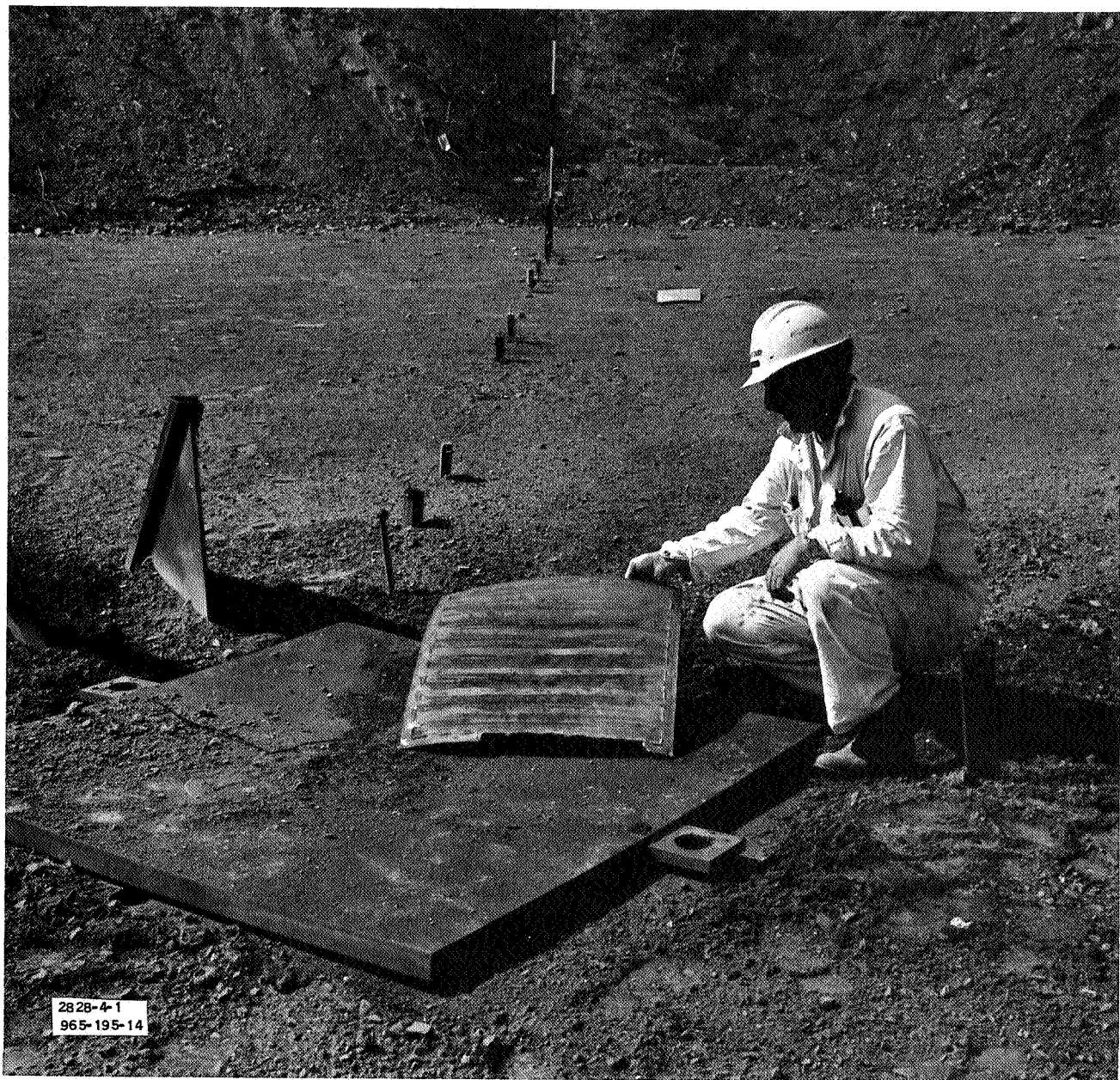
Figure 4.   Aluminum Pan Bottom After Test.

To provide personnel safety, the LH$_2$ was added by remote control. The loading operation was conducted from a reinforced building for instrumentation and personnel approximately 125 ft from the test fixture. The fuel was transferred from a 1000-liter LH$_2$ trailer (Linde LSH-1000) to the test pan through a 175-ft long, 3/4-in. diameter foam-insulated aluminum line. An LH$_2$ loss of approximately 200% occurred during transfer.

The fuel depth in the pan was sensed by a carbon-resistor type level indicator. The level indicator consisted of a 47K and a 1K resistor in series. The voltage drop across the 1K resistor was monitored when 22.5 volts were applied to the system. A 30 millivolt differential (approximate) was observed when the 47K resistor was completely immersed in the liquid hydrogen vs the gaseous hydrogen.

A schematic drawing of the probe circuit is shown in Figure 5. Four probes were placed in each pan at different levels to permit monitoring of the fuel level during the loading operation.

A typical test was conducted in the following manner:

a.   The MDF was attached to the pan bottom and the pan was covered with insulation.

b.   The dewars were secured in the pan and a layer of insulation was placed on the top of the pan.

c.   The dewars were filled with enough LOX to provide the desired contact area with the surrounding fuel.

d.   The dewars were stoppered with the corks to reduce evaporation.

e.   The dewar pan was secured to a 2 in. steel witness plate with a 1/2 in. diameter cable to prevent upward movement of the pan after initiation of the MDF.

f.   The LH$_2$ was added remotely to the pan until its depth equalled that of the oxidizer in the dewars.

g.   The MDF under the pan was initiated, sending a shock wave into the pan to shatter the dewars.
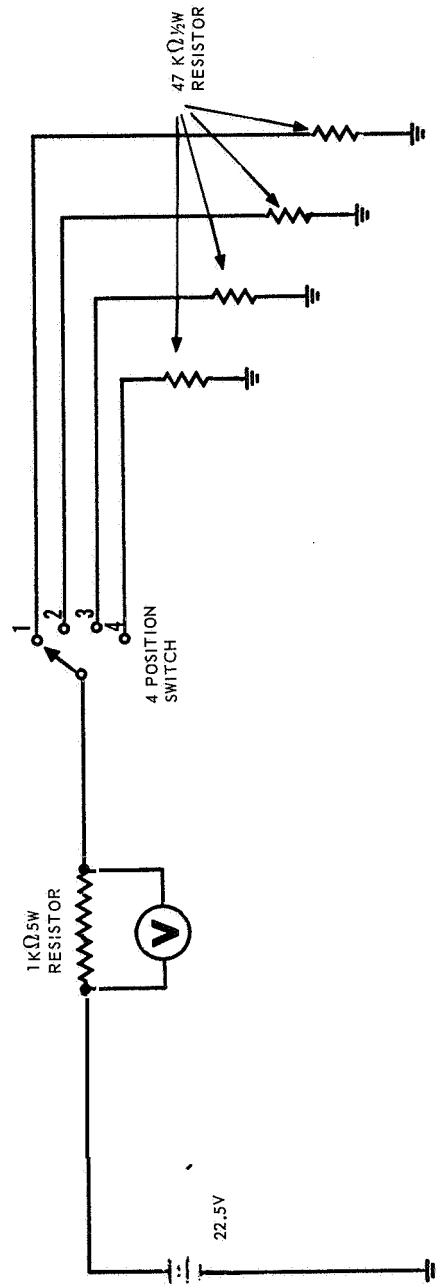
Figure 5   LH$_2$ Level Indicator.

4.3.2 LOX/RP-1 Tests

The LOX/RP-1 test pan was essentially the same as the LOX/LH$_2$ test pan except only the bottom was foam insulated and the method of securing the dewars in the pan differed. The dewars did not require a supporting membrane because the pan size was just sufficient to contain the dewars. **As** in the LOX/LH$_2$ tests the dewars were stoppered with corks to prevent evaporation of the LOX. **A** plywood cover was placed on top of the stoppers to maintain their seal during the fuel loading operation. **A** pan assembly ready for fuel loading is shown in Figure 3.

A typical test was conducted in the following manner:

a. The fuel reservoir and a nitrogen gas supply (required for pumping the RP-1 into the test pan) were located in a pit adjacent to the test fixture.

b. The fuel, which had been carefully measured previously in a separate vessel, was added to the fuel reservoir.

c. The dewars were manually filled with LOX to the depth required for the specified contact area.

d. The fuel loading operation was conducted from the control building for personnel safety. The desired amount of fuel was forced from the supply reservoir to the dewar pan assembly with gas pressure.

e. At a predetermined time the MDF under the pan was initiated and the various blast and thermal parameters were measured.

4.3.3 N$_2$O$_4$/A-50 Tests

The hypergolic propellant tests were conducted in the same manner as the LOX/RP-1 tests except for added precautions to prevent pre-ignition of the fuel and oxidizer. The method of sealing the dewars was improved by using a Saran-covered foam-rubber stopper bonded to a cork stopper. The N$_2$O$_4$ was precooled to prevent excessive vaporization by passing its supply line through an ice bath. The dewars were precooled with liquid nitrogen which evaporated during the N$_2$O$_4$ loading operation. **A** plywood lid covered with aluminum foil was placed on the pan to prevent the stoppers from becoming dislodged after loading. The top of the pan was purged with gaseous nitrogen to prevent oxidizer vapor accumulation. The propellant loading operation is shown in Figure 6. **A** pan assembly ready for the fuel loading operation is shown in Figure 7. Despite the precautions taken, the propellants ignited prematurely in the end of the loading period during the first hypergolic test.

Figure 6.   Propellant Loading.
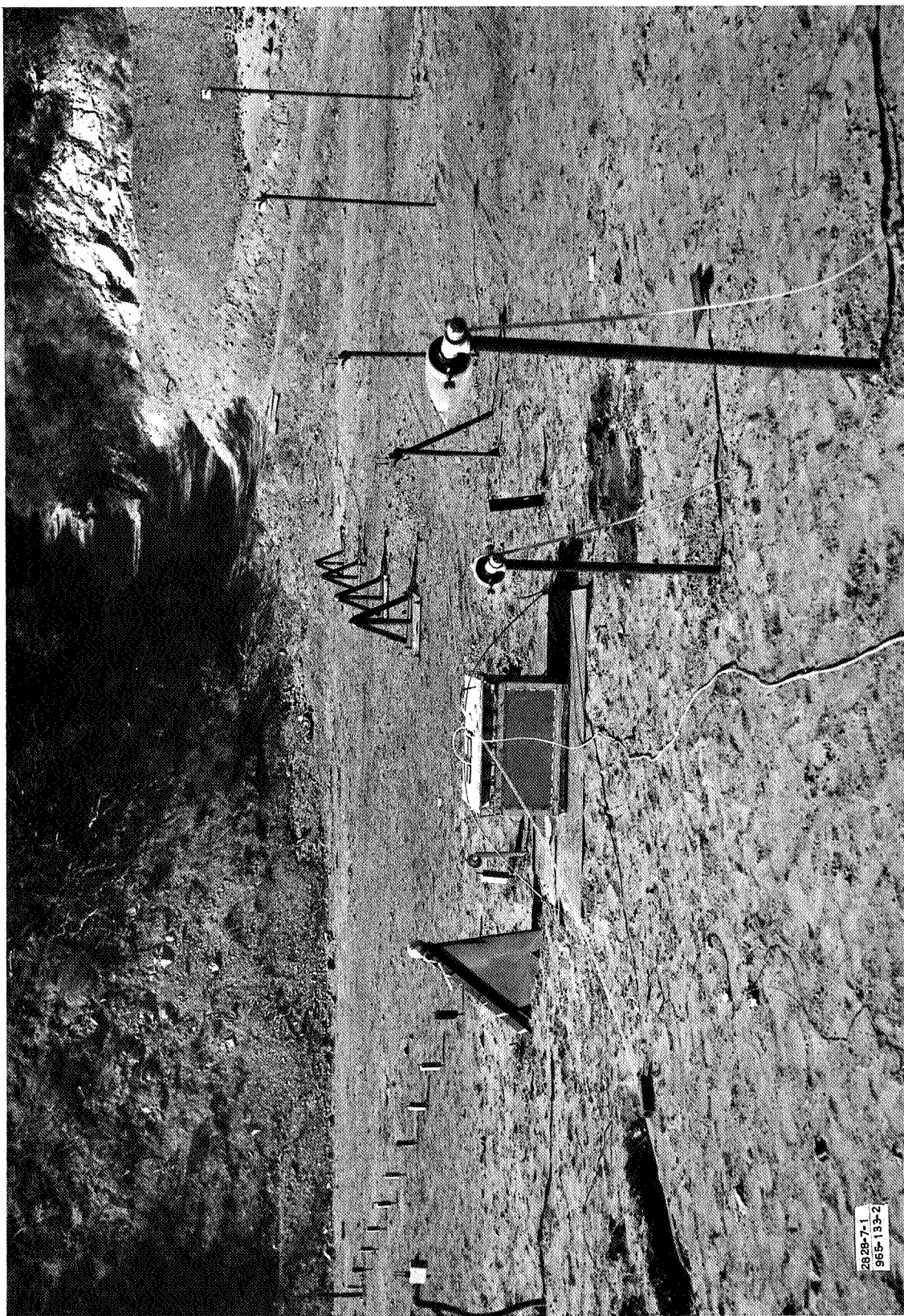
Figure 7. Pan Assembly Ready for Loading.

In the second test, the plywood cover was removed and the gaseous nitrogen purge to the top of the pan was eliminated. There were no premature ignitions after these two modifications were incorporated in the propellant handling procedure. Removing the plywood cover apparently permitted oxidizer vapors escaping from the dewars to disperse into the atmosphere before reaching sufficient concentration to ignite with the Aerozine 50 fuel.

4.4 PRELIMINARY SHATTER TESTS

A series of preliminary tests was conducted to determine the efficiency of the proposed shock wave shattering technique. Various thicknesses of aluminum plate and types of explosive materials were tested to determine a configuration for efficiently shattering the dewars with a minimum amount of explosive material and damage to the pan. Several weights of DuPont explosive sheet and Primacord were rejected because they caused excessive damage to the pan bottoms. Tests with 10 gr/ft MDF and 3/16-in.-thick aluminum pan bottoms produced the desired result when the pan was situated on a steel plate. Since the foam insulation caused a 2-in. separation between the pan bottom and the steel plate, 20 gr/ft MDF was used. In a trial test 49 dewars filled with RP-1 were placed in an air-filled pan (3/16 in. bottom thickness) and shattered into small pieces (approximately 2 by 4 in.). A duplicate test configuration with water in the pan produced smaller dewar fragments because of the incompressibility of the water. The water and air in the pans were used to evaluate the shatter characteristics of the glass dewars under density extremes. A Fastax camera recorded the shatter tests at 2300 frames/sec. Analysis of the films indicated the mixing time between the fuel in the pan and the oxidizer in the dewars was less than 10 msec.

4.5 INSTRUMENTATION

4.5.1 Layout

Four overpressure instrumentation stations were located in each of three gage lines radiating from the test fixture at distances of 25, 40, 60, and 80 ft. The gage lines were 120° apart. A layout of the test area instrumentation is shown in Figure 8 and a photograph of the test area is shown in Figure 9. All instrumentation cables were buried approximately 6-in. to prevent any damage from the blast overpressure and test pan fragments. Two additional overpressure stations were located at a distance of 98 ft. from the center of the test area.
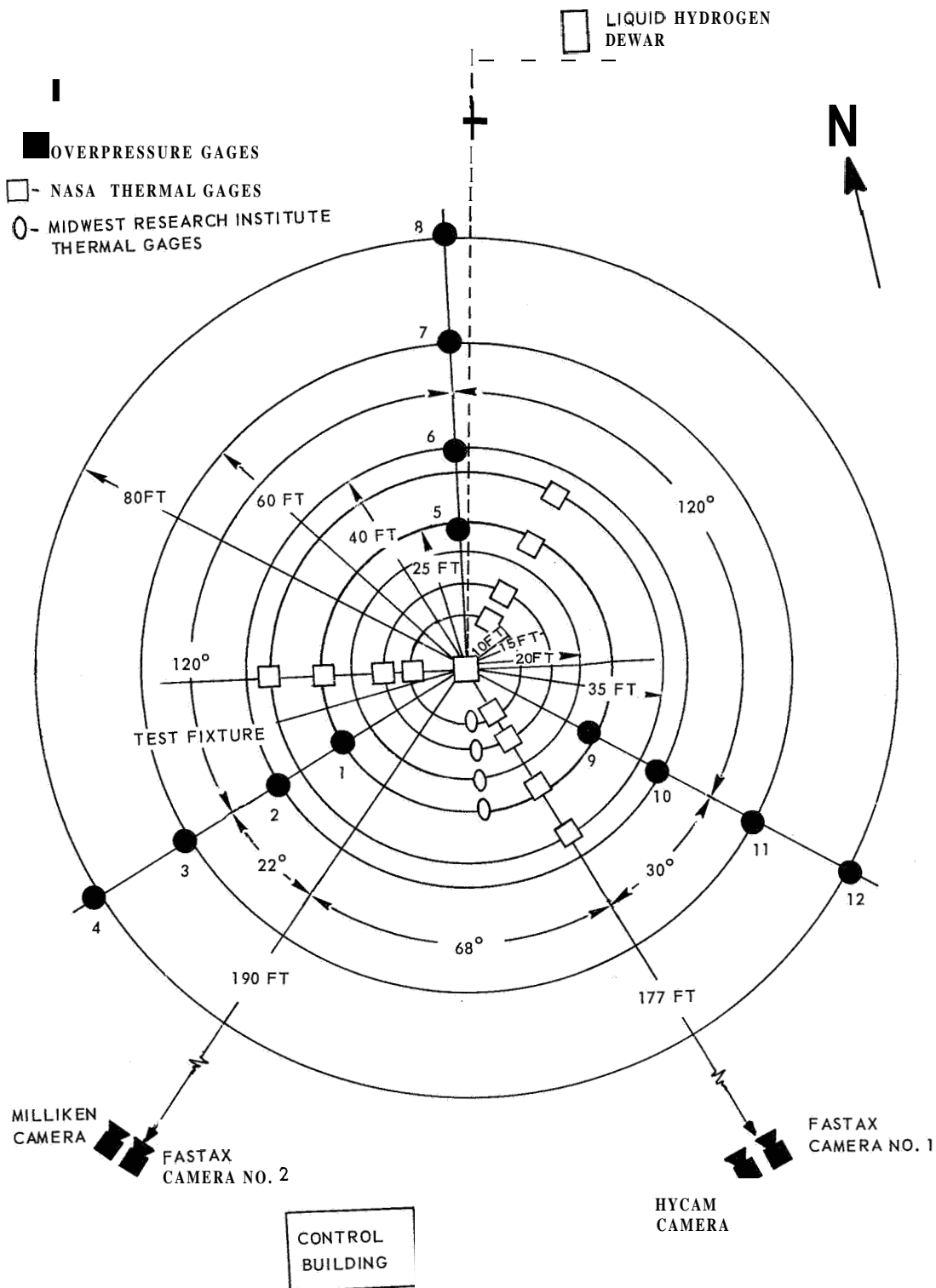
Figure 8. Instrumentation Layout.
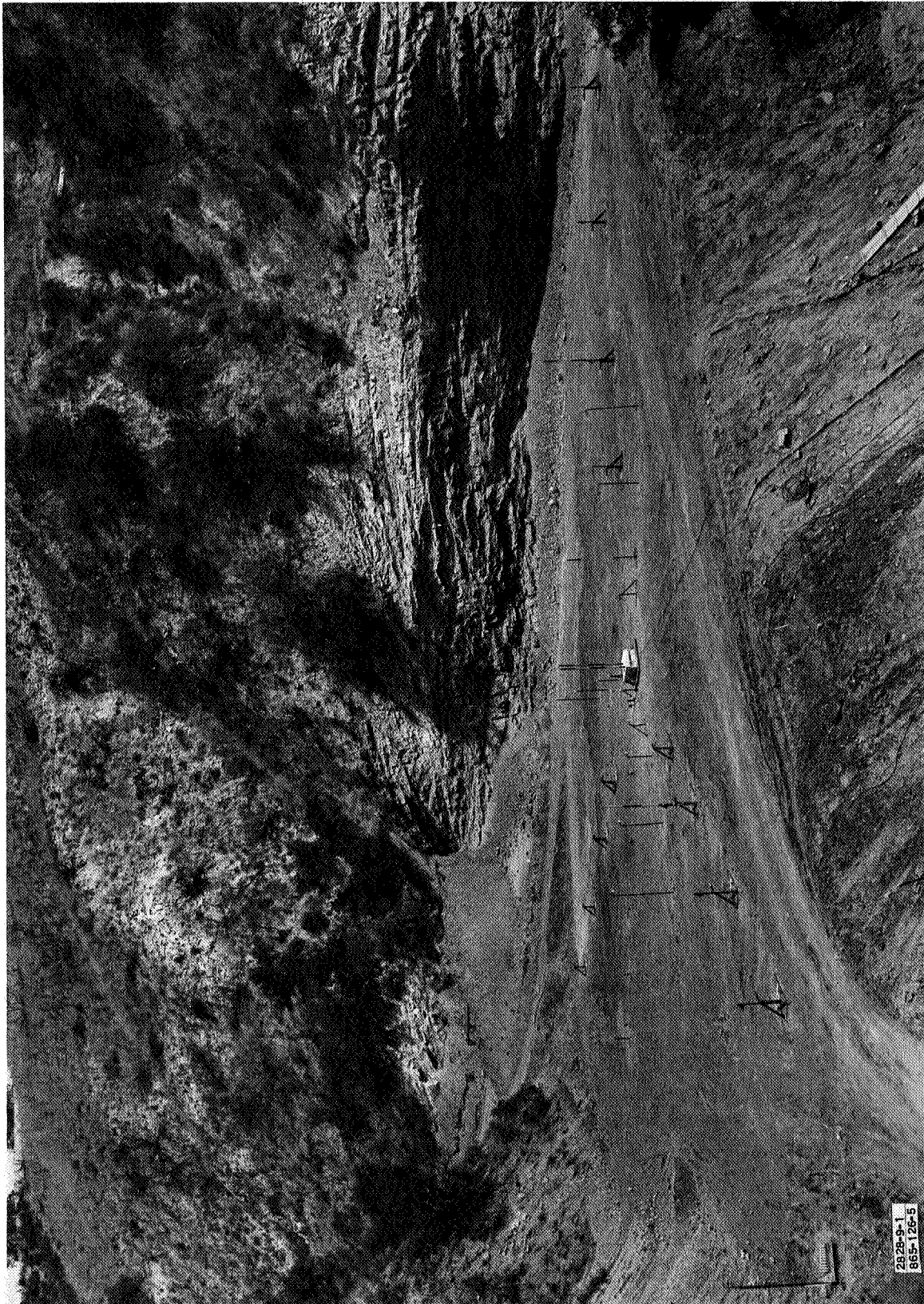
Figure 9. Test Area.

Four thermal radiation stations were established on each of three gage lines radiating from the test fixture at distances of 10, 15, 25, and 35 ft. These gage lines were offset from the overpressure gage lines by 30°. **A** fourth line of four thermal gages (Midwest Research Institute) was located at distances of 10, 15, 20 and 25 ft from the center of the test area. This line was also located 30° from one of the previously indicated thermal gage lines.

Two camera sites were established at distances of 117 and 190 ft from the center of the test area and were separated by 68°. Both camera sites were located approximately 11° above the test area level.

The data-recording equipment was located in an underground control building located approximately 125 ft from the center of the test arena. This building was occupied by all test personnel during the fuel loading operations and actual tests. Closed circuit television permitted observation of test arena from the control building.

4.5.2 Air-Blast Measurements

The air-blast overpressures were measured with Atlantic Research Corporation (ARC) Model LC-33 pencil piezoelectric transducers, and Ballistic Research Laboratory (BRL) self-recording pressure gages.

The ARC pencil gages were placed 2 ft above the ground in rigid pipe stands (Figure 10). Peak pressure, shock wave velocity, positive impulse, and positive overpressure duration were determined from the data recorded with these gages. The gage output was fed through low-noise cable into a calibration unit and then into ARC low impedance amplifiers (Model 104A). The amplifier output was recorded on a 14-channel magnetic tape recorder (Precision Instruments Model 214) operating at 60 in./sec. To obtain readable records for data reduction, it was necessary to play the tape back at 15 in./sec into a recording oscillograph (CEC Model 5-114) operating at 57.6 in./sec. CEC Type 7-343 oscillograph galvanometers were used for the record playback. The graph records represented a four-to-one time expansion playback advantage for data reduction purposes.

Prior to each test, a calibration was recorded on the magnetic tape system for data reduction purposes. The calibration was obtained by applying a square-wave puise of known voltage through a known-value capacitor (including the gage and gage cable capacitances) for each pressure-gage channel. This calibration procedure limits the input capacity of the channel to the expected blast pressure for the particular type and weight of explosive material at a specific distance from the event. The recorder output represented, in pico-coulombs, the expected
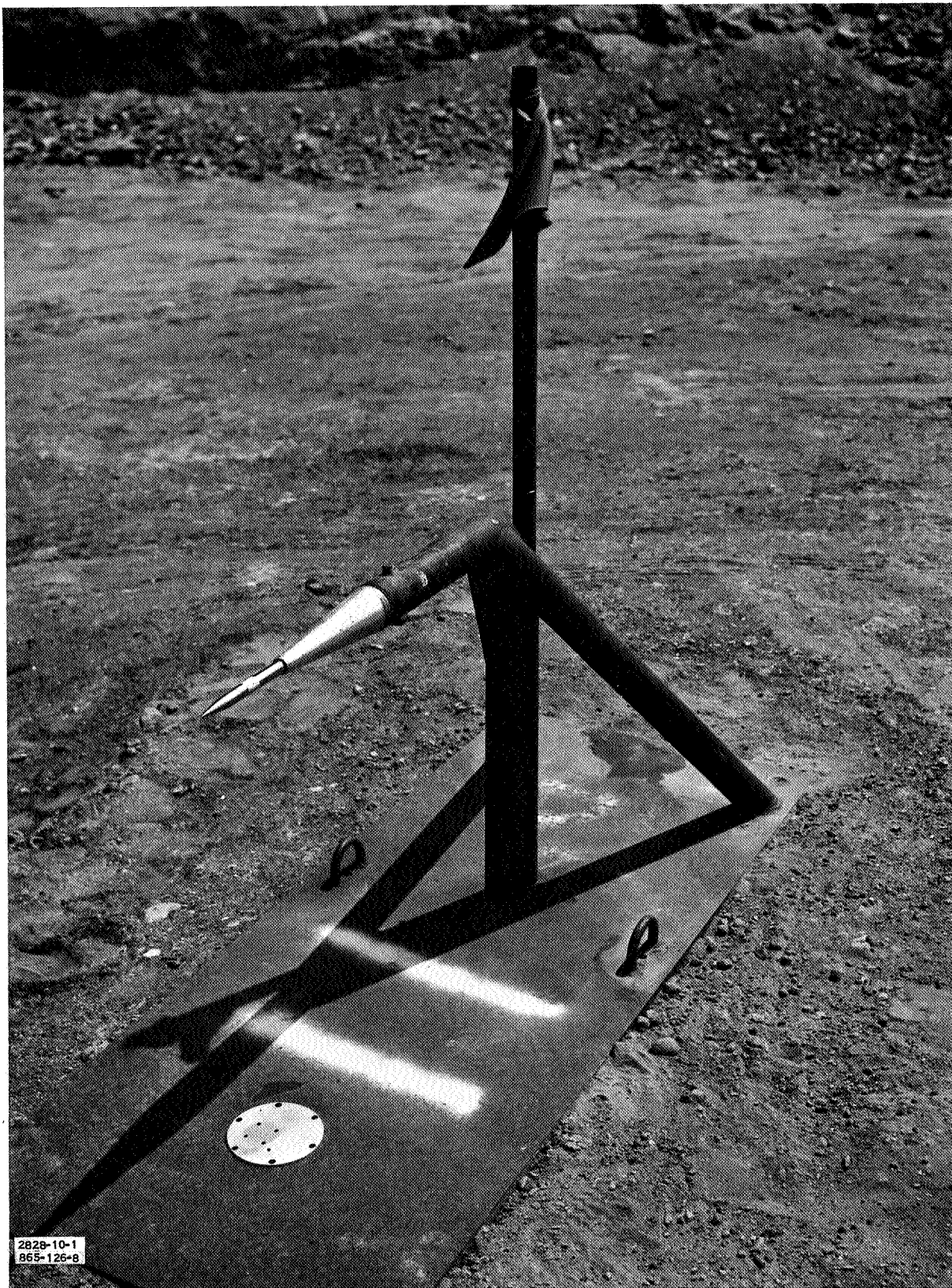
Figure 10. Blast Overpressure Gage Stand.

charge output of the gage on that channel. Data reduction was accomplished by determining what part of the calibration the event represented and then dividing this amount by the gage sensitivity (pico-coulomb/psi) to obtain the overpressure (psi). By varying the calibration voltage (5 to 50 v) and the calibration capacitance (240 to 8000 μμf) it was possible to obtain records for the wide range of overpressures experienced with only small differences in wave amplitude for any of the tests.

No correction was made in the air blast measurements for the effect of atmospheric pressure variation. Examination of the air blast measurement technique indicated that atmospheric pressure has only a negligible effect for the test site elevation (approximately 900 ft).

On each tape record, 2-msec timing marks were recorded for time history purposes. The marks provided the time base required in determining impulse, shock wave velocity, and positive impulse duration.

Prior to starting the actual experimental studies, a series of calibration tests was conducted with TNT explosive charges having known blast characteristics. These preliminary tests were conducted to check out the instrumentation system and to provide TNT equivalence reference data for comparison with the propellant test results. Results of these tests are discussed in Section 4.6.1.

The TNT equivalence of the propellant is defined as the weight of TNT that will give the same peak overpressure or impulse at the same distance as that obtained from the material under test. The TNT equivalences in this report are expressed as the ratio of pounds of TNT equivalent to a pound of propellant.

The calibration tests were conducted with cylindrical 10-, 25-, 50-, and 100-lb TNT charges having a length to diameter ratio of approximately 1. The charges were fired 6 in. above ground level to approximate the center of the explosion generated from the propellants in the pans and to protect the steel test plate.

A description of the BRL pressure gages is presented in Appendix A.

4.5.3   Overpressure Based Upon the Rankine-Hugoniot Equation

The theoretical basis for determining peak overpressure in the 5- to 90-psi range from shock wave and sonic wave velocity measurements is given by Kalavski (Reference 10). With this approach, it is possible to establish a relation between shock wave velocity and the peak overpressure from the Rankine-Hugoniot equations and the properties of the medium.

With the assumption that the ratio of the specific heat at constant pressure and volume is a constant across the shock boundary, it is possible to derive the following equation which is based on the ideal gas law:

$$\frac{P_s}{P_o} = \frac{2\gamma}{\gamma + 1} \left(\frac{U^2}{C_o^2} - 1 \right) \qquad (1)$$

where

P_s = peak overpressure in the shock front (above atmospheric pressure)

P_o = atmospheric pressure

U = shock wave propagation velocity

C_o = velocity of sound in undisturbed air

γ = ratio of specific heat at constant pressure to specific heat at constant volume

The velocity of sound was determined from the formula

$$C = C \left(+ \frac{T}{273} \right)^{1/2} \qquad (2)$$

where

C = velocity of sound in dry air at temperature, T

C_o = velocity of sound in dry air at 0^oC

T = temperature of air in degrees centigrade

Since humidity has a negligible effect only on γ and not on U, C_o, or P_o (since they are measured quantities at the test humidity), it is possible to eliminate consideration of humidity with only a small overall error of less than 0.1% in the calculated pressure.

The shock wave velocities utilized in Equation 1 were determined from time-of-arrival data at the pencil gages. The velocities were computed by dividing the gage-to-gage distance by the gage-to-gage elapsed time. The velocities as calculated are higher than the actual shock wave velocity because this assumes a linear rate of decay. The actual decay is some exponential function depending on the explosive material and the distance from the event.

4. 5.4   Fireball Size Measurements

The fireball growth rate and history profiles were recorded with four cameras located at two viewing sites (Figure 8). The initial growth rate of the fireball was recorded by two Fastax cameras located 190 and 177 ft from the test fixture. The two cameras were operated at approximately 5500 frames/sec to provide a time resolution that was commensurate with the early fireball growth rate. These two cameras were used to record only the initial growth rate. The entire duration of the fireballs was recorded with a Milliken camera operating at 400 frames/sec and a HyCam camera operating approximately 1000 frames/sec. High-speed infrared film was used in both the Fastax cameras while color film was used in both of the slower speed cameras. One-thousand cycle/sec time marks were recorded on the film records during the test for data reduction purposes.

The fireball dimensions were measured with a Vanguard Motion Analyzer. The analyzer scale was calibrated against the pressure station distances on the film records for size computations. A correction was made in the film data to compensate for the fireball curvature. The correction was accomplished with a computer program which made the correction vs distance from the center of the event and recomputed the fireball size.

Fireball duration was judged to cease when the flame was no longer visible. The end of the propellant reaction was characterized by one or more localized fireballs that were partially obscured by the combustion by-products. The termination point was difficult to determine in most tests due to this cloud of by-products.

The computed fireball data was fed into a point plotter (Electronic Associates, Inc. , Model 3033) for graphical representation of the propellant fireballs on a distance vs time basis.

4.5.5   Fragment Velocity Measurements

One of the major hazards associated with the catastrophic malfunction of a missile propulsion system is the danger from metal hardware fragments. These hardware fragments can travel at high velocities, and even though they are small their kinetic energy can inflict severe damage to nearby facilities or prove lethal to personnel. The prediction of fragment trajectories, arrival times, and velocities is not amenable to analytical techniques with the propellant materials involved. Analytical treatments such as the Gurney formula consider only the initial fragment velocity without regard to the contribution of energy imparted to fragments from the expanding fireball generated by a propellant reaction. There are standard analytical procedures for determining the velocity of a fragment as a function of the distance from the starting point, and as a

function of altitude provided the maximum fragment velocity is known. The purpose of this part of the program was to experimentally determine the rate of energy transmitted to fragments within a propellant fireball and to establish at what distance from the propellant energy source the maximum fragment velocity occurs. Four different experimental measurement techniques were evaluated for determining the fragment velocities.

4.5.5.1 Fragment-Wire Velocity Technique

In this technique a wire track was run from near the dewar pan to the outer edge of the test area. The wire was drawn taut between two anchor posts and a fragment of known mass and cross-sectional area was placed on the wire near the dewar pan. Time-of-arrival switches were located along the wire at known distances. The fragment was projected along the wire after initiation of the propellants by the impulse loading from the propellant reaction. As the fragment passed the time-of-arrival stations, a step function signal was recorded on a oscillograph with a suitable time base for data reduction purposes. Knowing the distance and time between stations, it was possible to compute the average velocity between stations. The fragment and several time-of-arrival stations can be observed just to the left of the dewar pan in Figure 7.

Several types of make and break probes were tried for the velocity stations, but the severe shock environment triggered the probe ahead of the arrival of the fragment. Probes which would withstand initial shockwave passage provided too much resistance to the fragment travel to permit valid velocity measurements. The technique was further hindered by deflection of the taut wire as the fragment traveled down the wire, causing the fragment to miss the probe station entirely or strike the probe stand, terminating any further measurements. Several trials were made with this technique but no fragment velocity data was obtained which was significant to the solution of the fragment problem other than the apparent fact that the shockwave precedes any fragments during the initial fireball growth period.

4.5.5.2 Fragment-Reel Velocity Technique

This measurement technique was based on a method of determining the velocity of a flexible wire attached to a fragment of known mass and shape. A spherical fragment was placed near the dewar pan on a wooden stake and a fine, flexible cable secured to the fragment. The cable was wound on a 6-in. diameter Aluminum drum supported on ball bearings to eliminate as much drag as possible on the wire and fragment. The wire drum was positioned near the dewar pan in a heavy steel enclosure. A magnetic pickup was attached to the drum enclosure to determine the velocity of

the drum as the wire unrolled. The fragment separated from the cable in three trials before the drum could move and no drum velocity data was obtained. Tests with the fragment secured to a short length of cable with the end free yielded the same results; i.e., the fragment was separated from the wire due to the extreme shock environment generated by the propellant reaction before the wire could move.

4.5.5.3   Fragment-Wire-Break Station Technique

The fragment-wire-break station technique consisted of a known mass and shape fragment which was secured to a high tensile strength steel wire. The fragment and wire were located near the test fixture (Figure 3) in a position which would cause the fragment wire to break a series of electrical probes which were separated by known distances as it moved away from the test fixture. The extreme shock environment again prevented useable measurements from the test setup by pretriggering many of the velocity stations before the fragment wire could trigger the stations. Although several trials were made to improve the velocity stations to prevent the pretriggering, no useable data was obtained which was significant or could contribute to the solution of the fragment hazard problem. Use of this technique would also require accurate determination of the direction of the flight of the fragment before flight velocities could be computed.

4.5.5.4   Camera Velocity Measurement Technique

A Fastax camera was positioned to record the travel of several metal fragments which were placed on the top of the dewar pan. However, the fragment velocities were less than the initial fireball growth velocities and the fragments were not visible until the fireball had reached its maximum dimensions.

4.5.6   Meteorological Measurements

Readings of humidity, temperature, atmospheric pressure, and wind velocity were recorded for each test. The humidity and temperature were determined with a Brown chart-type recorder. The atmospheric pressure was measured with a mercury barometer. Wind velocity was determined with an anemometer held next to the test fixture before and after each test.

4.5.7   Thermal Measurements

Fireball temperature and radiation measurements were made by personnel from NASA, Manned Spacecraft Center, Houston, Texas.

Fireball temperature measurements were also made on part of the tests by personnel from the Midwest Research Institute, Kansas City, Mo. using a series of preheated thermocouples. Results of these tests are reported in Reference 11.

4.6   TEST RESULTS

The test results from the experimental studies conducted during this program are presented in Tables 3 through 8,

4.6.1   TNT Calibration Tests

Results of the 10, 25, 50, and 100-lb TNT calibration tests are presented in Table *3* in the form of peak overpressure, positive impulse, and positive pulse duration vs distance from the center of the test area. The peak overpressure values were scaled to a 1 lb equivalence basis and the scaled values were used in establishing a test area TNT calibration curve presented in Figure 11 as scaled distance vs overpressure where the scaled distance (X) is equal to the radial distance (R) from the event divided by the cube root of the charge weight $(W^{1/3})$.

The positive impulse data was scaled to a 1 lb equivalence basis in a similar manner. Results of these computations were used to establish the test area impulse calibration curve presented in Figure 12.

A comparison of the calibration test results with Ballistic Research Laboratory data (References 12 and 13) for similar test conditions indicate only a negligible variation in both pressure and impulse values for the range of reduced distance $(X = > 5$ to $< 40)$.

Results of the calibration tests were utilized in Figures **13** through 22 by superimposing the pertinent TNT equivalence percentage curves over the results of the overpressure and impulse measurements for each of the propellant test conditions. These curves permit a direct evaluation of the TNT overpressure and impulse equivalences in terms of distance from the event for each of the test conditions.

The TNT equivalence comparison of two explosive materials must be made with a simultaneous evaluation of peak overpressure and positive impulse data. The initial air shock produced from an explosive material is increased by the support it receives in the fireball from expanding gases and secondary shocks. Once the shock wave has traveled beyond the fireball limits it no longer receives added energy and assumes the characteristics of a shock wave produced from a point source.

Table 3.   TNT Results.

Charge Weight (lb)	Test No.	Gage Distance from Event (ft)	Gage No.	Peak Over-pressure (psi)	Positive Impulse (psi-msec)	Positive Pulse Duration (msec)
10	1	25	1	--*	--*	--*
			5	7.0	11. 6	4.4
			9	8.5	12.9	4. 5
			mean	7.3	12.3	4.5
		40	2	--*		
			6	--*		
			10	--*		
			mean	N/A	N/A	N/A
		60	3	1.8	6. 8	6. 9
			7	1.9	5. 8	7. 1
			11	1.9	6. 2	7.3
			mean	1.9	6. 3	7. 1
		80	4	1.3	4. 6	8.3
			8	1.3	4. 5	6. 2
			12	1. 1	3.5	7.4
			mean	1.2	4.2	7.3
10	2	25	1	--*	--*	--*
			5	6.8	12.4	4.3
			9	6. 7	12. 6	3.7
			mean	6. 8	12.5	4.0
		40	2	3.3	8.9	5. 7
			6	3.5	8.7	5.6
			10	3.0	7.5	4.2
			mean	3.3	8.4	5.2
		60	3	1.8	5. 6	6. 8
			7	1.8	5.5	6.7
			11	1.7	6.0	7.3
			mean	1.8	5.7	6. 9

---

* Gage not operating properly.

Table 3. (Continued)

Charge Weight (lb)	Test No.	Gage Distance from Event (ft)	Gage No.	Peak Over-pressure (psi)	Positive Impulse (psi-msec)	Positive Pulse Duration (msec)
		80	4	1.2	4.5	8.2
			8	1.3	4.9	6.4
			12	1. 1	3.7	7.0
			mean	1.2	4.4	7.2
25	3	25	1	13. 0	26.4	4.4
			5	14. 5	22. 5	4.4
			9	13.2	23. 3	4.4
			mean	13. 6	24. 1	4.4
		40	2	5.5	15. 5	6. 3
			6	5. 2	16. 2	6. 8
			10	5. 1	14. 5	5.7
			mean	5.3	15.4	6.3
		60	3	2.7	10.8	7. 6
			7	2.5	10.4	9.2
			11	2.9	10.4	8.3
			mean	2. 7	10.5	8.4
		80	4	1.7	8.4	8.4
			8	1.8	8.7	8.7
			12	1.7	7.3	7.3
			mean	1.7	8. 1	8. 1
25	4	25	1	13. 1	21.9	4.5
			5	13.4	20.3	4.4
			9	16. 2	24. 5	6.2
			mean	14. 2	22. 2	5.0
		40	2	5.5	16. 3	6. 1
			6	5.0	15.8	6.9
			10	5.4	13. 2	5.5
			mean	5.3	15. 1	6. 2
		60	3	2. 6	10.1	7. 6
			7	2. 6	10.5	8. 8
			11	2. 8	12.0	8.0
			mean	2.7	10.9	8. 1

Table 3.   (Continued).

Charge Weight (lb)	Test No.	Gage Distance from Event (ft)	Gage No.	Peak Over-pressure (psi)	Positive Impulse (psi-msec)	Positive Pulse Duration (msec)
		80	4	1.7	7.9	8. 8
			8	1.9	9.3	8. 5
			12	1. 7	6. 6	8.3
			mean	1. 8	7.9	8. 5
50	5	25	1	26. 5	37.2	4.5
			5	25.4	36. 6	4.7
			9	25.9	40. 3	4.5
			mean	25. 9	38. 0	4. 6
		40	2	8. 6	22.3	5. 8
			6	8. 5	23. 3	7.7
			10	8.2	19.4	5.2
			mean	8.4	21.7	6. 2
		60	3	4.3	15. 0	8. 9
			7	4.2	15. 8	9.4
			11	4. 8	18. 1	7. 8
			mean	4.4	16. 3	8. 7
		80	4	2.5	12.2	9.3
			8	2.5	13. 2	12.0
			12	2.4	10.4	10.4
			mean	2.5	11.9	10. 6
50	6	25	1	23. 9	36. 0	4.4
			5	29. 2	42. 1	4.8
			9	25. 0	38.2	5.2
			mean	26. 0	38. 8	4. 8
		40	2	8. 5	22.1	6. 1
			6	9.0	24. 7	7. 7
			10	8. 7	19. 5	4. 7
			mean	8. 7	22. 1	6. 2
		60	3	4.0	14. 8	8. 1
			7	3.9	14. 3	9.0
			11	3.9	16. 4	8. 7
			mean	3.9	15. 2	8. 6

Table 3.   (Continued).

Charge Weight (lb)	Test No.	Gage Distance from Event (ft)	Gage No.	Peak Over-pressure (psi)	Positive Impulse (psi-msec)	Positive Pulse Duration (msec)
		80	4	2.6	11.5	9.3
			8	2.6	13.1	9.4
			12	2.3	10.3	10.4
			mean	2.5	11.6	9.7
100	7	25	1	39.0	71.7	4.9
			5	38.0	59.5	4.9
			9	--*	--*	--*
			mean	38.5	65.6	4.9
		40	2	13.8	35.4	6.1
			6	12.5	36.4	7.1
			10	13.8	34.0	5.8
			mean	13.4	35.3	6.3
		60	3	5.8	22.3	8.1
			7	6.0	22.5	9.3
			11	6.1	24.8	8.4
			mean	6.0	23.2	8.6
		80	4	--*	--*	--*
			8	3.4	19.4	13.4
			12	3.8	17.1	12.7
			mean	3.6	38.3	13.1
100	8	25	1	45.2	85.8	5.9
			5	46.7	55.6	4.4
			9	47.1	82.3	5.1
			mean	46.3	75.6	5.1
		40	2	14.2	38.1	5.7
			6	14.4	44.1	7.4
			10	15.2	37.7	9.4
			mean	14.6	40.0	7.5

* Gage not operating properly.

Table 3. (Continued).

Charge Weight (lb)	Test No.	Gage Distance from Event (ft)	Gage No.	Peak Over-pressure (psi)	Positive Impulse (psi-msec)	Positive Pulse Duration (msec)
		60	3	5. 6	26.3	13. 7
			7	5.9	23.9	10.7
			11	5. 1	28. 5	13.4
			mean	5.5	26. 2	12. 6
		80	4	3.2	16. 7	11. 8
			8	3.4	21.0	13. 5
			12	3. 6	17. 3	12.7
			mean	3.4	18. 3	12.7

Table 4.   Fireball Size and Duration.

Propellant	Propellant Weight (lb)	Contact Area (ft^2)	Test No.	Maximum Size		Duration (sec)
				Height (ft)	Diameter (ft)	
LOX/LH$_2$	100	25.12	1	52.0	68.5	1.89
LOX/LH$_2$	100	25.12	2	38.5	64.0	1.70
LOX/LH$_2$	225	56.23	3	57.5	74.5	1.92
LOX/LH$_2$	225	56.23	4	63.0	91.0	2.00
LOX/LH$_2$	150	36.81	5	73.0	66.0	1.90
LOX/LH$_2$	150	36.81	6	68.0	70.0	2.45
LOX/RP-1	171	36.81	8	48.0	83.0	1.80
LOX/RP-1	171	36.81	10	46.0	78.5	1.35
N$_2$O$_4$/A-50	229.5	36.81	9	49.5	70.5	1.28

Table 5.   Propellant Test Results.

Propellant	Propellant Weight (lb)	Contact Area (ft^2)	Test No.	Gage Distance from Event (ft)	Gage No.	Peak Over-pressure (psi)	Positive Impulse (psi-msec)	Positive Pulse Duration (msec)
LOX/LH$_2$	100	25. 12	1	25	1	21.2	47. 5	6 4
					5	20.0	42. 8	7 5
					9	29. 8	83. 8	7 9
					mean	23. 7	58. 0	7 3
				40	2	9.3	34 0	12 2
					6	9.2	36. 5	7. 7
					10	7.7	38. 5	13 8
					mean	8. 7	36. 3	11 2
				60	3	4. 6	24. 1	15.2
					7	5.0	21. 6	9. 8
					11	5.3	23. 0	9 5
					mean	5.0	22.9	11 5
				80	4	2.7	12.3	12.4
					8	3.2	14.7	12 4
					12	3.0	13.3	9.9
					mean	3.0	13.4	11. 6
LOX/LH$_2$	100	25. 12	2	25	1	17. 6	52. 3	6 6
					5	21.7	63. 8	6.0
					9	20. 5	49. 1	7 9
					mean	19. 9	55. 1	6 8
				40	2	8. 2	36. 0	11 6
					6	9.5	37. 3	7 3
					10	8.9	31.3	8 8
					mean	8.9	34.9	9.2
				60	3	4. 6	20.9	9.4
					7	5.0	19. 0	8 7
					11	4.6	22. 5	8.8
					mean	4. 7	20. 8	9.0
				80	4	2.8	18. 2	17 7
					8	3.1	18.3	13 8
					12	3.1	13.1	9.4
					mean	3.0	16.5	13. 6
LOX/LH$_2$	225	56. 23	3	25	1	33.4	92.2	6.0
					5	35.2	84.8	9.0
					9	38. 5	85. 3	8.9
					mean	35. 7	87. 4	8.0
				40	2	14. 8	57.9	12. 3
					6	15.4	64. 2	14. 8
					10	16. I	49.8	7. 2
					mean	15.4	57. 3	11.4
				60	3	7. 2	36. 6	14 1
					7	7.2	--*	--*
					11	7.3	34.0	9 9
					mean	7.2	35.3	12. 0
				80	4	4.3	27.4	14 0
					8	6. 0	--*	--*
					12	5.2	21.2	10. 5
					mean	5.2	24. 3	12 3

* Gage damaged by test fragments.

Table 5. Propellant Test Results (Continued).

Propellant	Propellant Weight (lb)	Contact Area (ft^2)	Test No.	Gage Distance from Event (ft)	Gage No.	Peak Over-pressure (psi)	Positive Impulse (psi-msec)	Positive Pulse Duration (msec)
LOX/LH$_2$	225	56.23	4	25	1	27.4	67.1	6.1
					5	28.2	73.5	9.7
					9	29.4	84.7	9.7
					mean	28.3	75.1	8.5
				40	2	13.0	55.7	11.8
					6	12.7	52.0	11.7
					10	14.0	60.2	14.0
					mean	13.2	56.0	12.5
				60	3	7.3	40.2	15.7
					7	6.8	35.7	15.9
					11	6.3	40.4	16.2
					mean	6.8	38.8	15.9
				80	4	-**	-**	--**
					8	4.3	28.7	13.2
					12	4.2	19.3	10.1
					mean	4.3	24.0	11.7
LOX/LH$_2$	150	36.81	5	25	1	22.1	54.5	6.2
					5	23.4	70.2	11.7
					9	22.7	63.6	9.1
					mean	22.7	62.8	9.0
				40	2	9.3	40.3	11.5
					6	9.8	42.4	10.8
					10	10.0	40.5	12.4
					mean	9.7	41.1	11.6
				60	3	4.8	26.0	14.3
					7	5.1	26.9**	13.6
					11	5.0	29.6	14.7
					mean	5.0	27.5	14.2
				80	4	3.6	22.1	17.3
					8	4.1	21.4	14.4
					12	3.4	15.3	9.4
					mean	3.7	19.6	13.7
LOX/LH$_2$	150	36.81	6	25	1	13.8	37.6	6.3
					5	14.9	39.9	6.2
					9	11.9	40.2	a.7
					mean	13.5	39.2	7.1
				40	2	6.3	26.3	11.7
					6	6.7	30.2	12.4
					10	6.0	36.9	12.8
					mean	6.3	31.1	12.3
				60	3	3.5	19.9	15.4
					7	3.7	19.5	13.9
					11	3.6	21.4	15.6
					mean	3.5	20.3	15.0
				80	4	2.3	14.9	17.0
					8	2.3	15.1	12.6
					12	2.4	16.0	21.0
					mean	2.3	15.3	16.9

* Gage damaged by test fragments.
** Gage not operating properly.

Table 5. Propellant Test Results (Continued).

Propellant	Propellant Weight (lb)	Contact Area (ft²)	Test No.	Gage Distance from Event (ft)	Gage No.	Peak Over-pressure (psi)	Positive Impulse (psi-msec)	Positive Pulse Duration (msec)
N$_2$O$_4$/A-50	229.5	36.81	7		NO DATA			
N$_2$O$_4$/A-50	229.5	36.81	9	25	1	22.2	61.9	8.4
					5	27.8	61.8	7.5
					9	23.9	53.3	7.2
					mean	24.6	59.0	7.7
				40	2	10.1	40.5	11.4
					6	12.5	38.3	9.5
					10	10.7	34.9	8.3
					mean	11.1	37.9	9.7
				60	3	5.1	29.5	19.6
					7	6.1	25.2	11.2
					11	5.0	26.9	11.8
					mean	5.4	27.2	14.2
				80	4	3.6	20.7	15.7
					8	4.0	23.1	13.7
					12	3.3	19.9	16.0
					mean	3.6	21.2	15.1
LOX/RP-1	171	36.81	8	25	1	25.7	54.0	5.6
					5	26.4	38.6	3.4
					9	25.5	54.5***	7.1***
					mean	25.9	49.0	5.4
				40	2	10.4	35.7	10.7
					6	12.2	43.9	11.6
					10	12.0	37.0***	9.1***
					mean	11.5	38.9	10.5
				60	3	5.9	26.7	15.0
					7	5.5	30.7	14.9
					11	6.4	25.2	9.2
					mean	5.9	27.5	13.0
				80	4	3.7	20.4	17.2
					8	3.6	28.9	17.0
					12	3.2	22.6	20.0
					mean	3.5	24.0	18.1
LOX/RP-1	171	36.81	10	25	1	--**	--**	--**
					5	33.2	66.1	4.7
					9	29.8	69.9	8.0
					mean	31.5	68.0	6.4
				40	2	12.0	43.8	12.0
					6	14.6	41.2	6.4
					10	10.7	33.9	5.1
					mean	12.4	39.6	7.8
				60	3	6.7	30.1	11.3
					7	9.2	41.7	8.8
					11	6.2	34.3	11.3
					mean	7.4	35.4	10.5
				80	4	4.3	25.7	16.9
					8	4.7	35.9	21.7
					12	3.6	27.2	17.7
					mean	4.2	29.6	18.8

* Gage damaged by test fragments.
** Gage not operating properly.
*** Gage damaged by test fragments, duration estimated.

Table 6.   Empirical Curve Fits.

Data Set	Coefficient[a]			Average Percent Relative Errors[b]
	A_0	A_1	A_2	
LOX/LH$_2$, Pressure = f (A)	6.403	-2.288	0. 150	5.2
LOX/LH$_2$, Impulse/W$^{1/3}$ = f (X)	3. 184	0. 134	-0.294	7. 5
LOX/RP-1, Pressure = f (A)	6.029	-1.866	0.044	6.4
LOX/RP-1, Impulse/W$^{1/3}$ = f (X)	3. 782	-1. 184	0. 132	9. 6
N$_2$O$_4$/A-50, Pressure = f (λ)	6. 073	-2.243	0. 146	4.9
N$_2$O$_4$/A-50, Impulse/W$^{1/3}$ = f (λ)	3. 738	-1. 147	0.069	4.4

Coefficients for the equation $y = A_0 \ t \ A_1, \ \ln X \ t \ A_2 (\ln \lambda)^2$

Expressed in terms of the logarithmic   pressure or logarithmic impulse scales.

Table 7. Shock Wave Velocities and Rankine-Hugoniot Pressures.

Propellant	Contact Area (ft^2)	Test No.	Position Gage No.	Position To Gage No.	Average Velocity (ft/sec)	Calculated Shock Overpressure (psi)
LOX/LH$_2$	25. 12	1	1	2	1,546	13. 6
			5	6	1,546	13. 6
			9	10	1,492	11. 6
			2	3	1,333	5.7
			6	7	1,365	6. 9
			10	11	1,356	6. 5
			3	4	1,266	3. 5
			7	8	1,294	4. 4
			11	12	1,235	2. 5
LOX/LH$_2$	25. 12	2	1	2	1,500	11.9
			5	6	1,538	13.3
			9	10	1,508	12.2
			2	3	1,325	5. 7
			6	7	1,360	6. 9
			10	11	1,333	5. 9
			3	4	1,258	3. 5
			7	8	1,290	4. 5
			11	12	1,266	3. 7
LOX/LH$_2$	56.23	3	1	2	1,754	22.4
			5	6	1,775	23. 3
			9	10	1,796	24. 3
			2	3	1,449	10. 1
			6	7	1,487	11.5
			10	11	1,460	10.5
			3	4	1,335	6. 1
			7	8	1,384	7. 7
			11	12	1,347	6. 5

Table 7. (Continued).

| Propellant | Contact Area (ft^2) | Test No. | Position | | Average Velocity (ft/sec) | Calculated Shock Overpressure (psi) |
			Gage No.	To Gage No.		
LOX/LH$_2$	56.23	4	1	2	1,667	18.8
			5	6	1,695	20.0
			9	10	1,695	20.0
			2	3	1,444	10.0
			6	7	1,455	10.4
			10	11	1,429	9.4
			3	4	1,316	5.5
			7	8	1,351	6.7
			11	12	1,282	4.4
LOX/LH$_2$	36.81	5	1	2	1,566	14.2
			5	6	1,596	15.4
			9	10	1,563	14.1
			2	3	1,356	6.5
			6	7	1,375	7.2
			10	11	1,361	6.7
			3	4	1,290	4.4
			7	8	1,316	5.2
			11	12	1,278	4.0
LOX/LH$_2$	36.81	6	1	2	1,442	9.8
			5	6	1,485	11.3
			9	10	1,442	9.8
			2	3	1,312	5.2
			6	7	1,312	5.2
			10	11	1,278	4.1
			3	4	1,254	3.4
			7	8	1,274	4.0
			11	12	1,262	3.6
N$_2$O$_4$/A-50	36.81	7*				

*No data.

Table 7. (Continued).

Propellant	Contact Area (ft^2)	Test No.	Position		Average Velocity (ft/sec)	Calculated Shock Overpressure (psi)
			Gage No.	To Gage No.		
N_2O_4/A-50	36.81	9	1	2	1,613	16.0
			5	6	1,630	16.7
			9	10	1,613	16.0
			2	3	1,379	7.2
			6	7	1,418	8.6
			10	11	1,379	7.2
			3	4	1,294	4.4
			7	8	1,329	5.6
			11	12	1,286	4.2
LOX/RP-1	36.81	8	1	2	1,648	19.2
			5	6	1,676	20.4
			9	10	1,630	18.4
			2	3	1,394	9.1
			6	7	1,399	9.3
			10	11	1,429	10.4
			3	4	1,299	5.7
			7	8	1,299	5.7
			11	12	1,270	4.8
LOX/RP-1	36.81	10	1	2	2,000	34.0
			5	6	1,863	27.3
			9	10	1,775	23.3
			2	3	1,460	10.4
			6	7	1,460	10.4
			10	11	1,455	10.3
			3	4	1,316	5.4
			7	8	1,342	6.3
			11	12	1,311	5.2

Table 8. Meteorological Data.

Propellant	Contact Area (ft2)	Test No.	Relative Humidity (%)	Air Temperature (°F)	Wind Direction	Wind Velocity (mph)	Atmospheric Pressure (in. of Hg)
LOX/LH$_2$	25.12	1	44	92	No	10	29.9
LOX/LH$_2$	25.12	2	56	82	North	0-8	28.7
LOX/LH$_2$	56.23	3	61	81	North	10-15	28.7
LOX/LH$_2$	56.23	4	62	80	North	10-15	28.8
LOX/LH$_2$	36.81	5	60	86	North	3-15	28.7
LOX/LH$_2$	36.81	6	60	82	North	0-14	28.8
N$_2$O$_4$/A-50	36.81	7		No Data			
N$_2$O$_4$/A-50	36.81	9	23	88	North	6-9	28.8
LOX/RP-1	36.81	8	94	59	North-west	6-9	28.6
LOX/RP-1	36.81	10	45	81	North-west	0-6	28.7
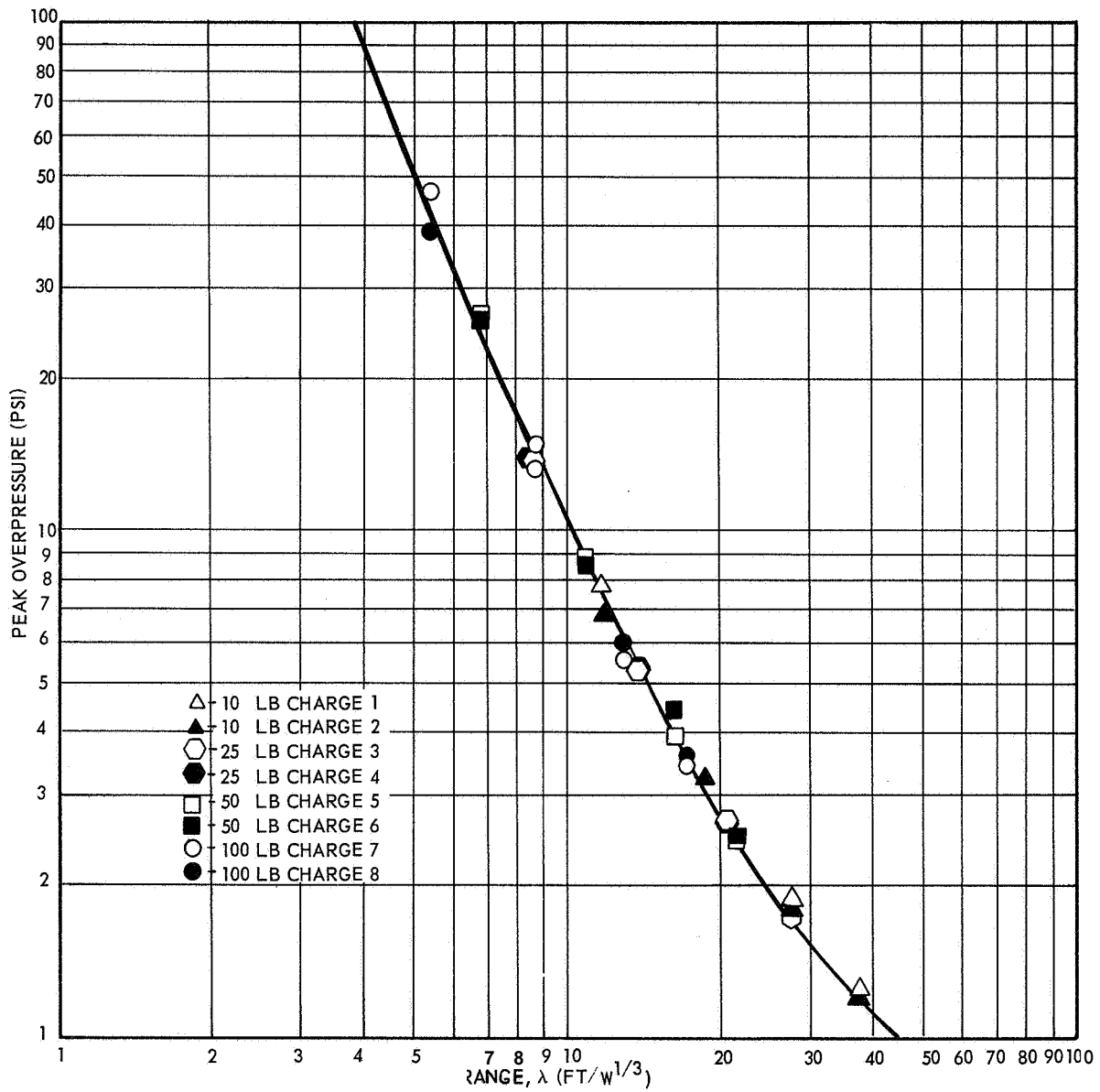
Figure 11. Peak Overpressure vs Scaled Distance for TNT Calibration Tests.

2828-11-1
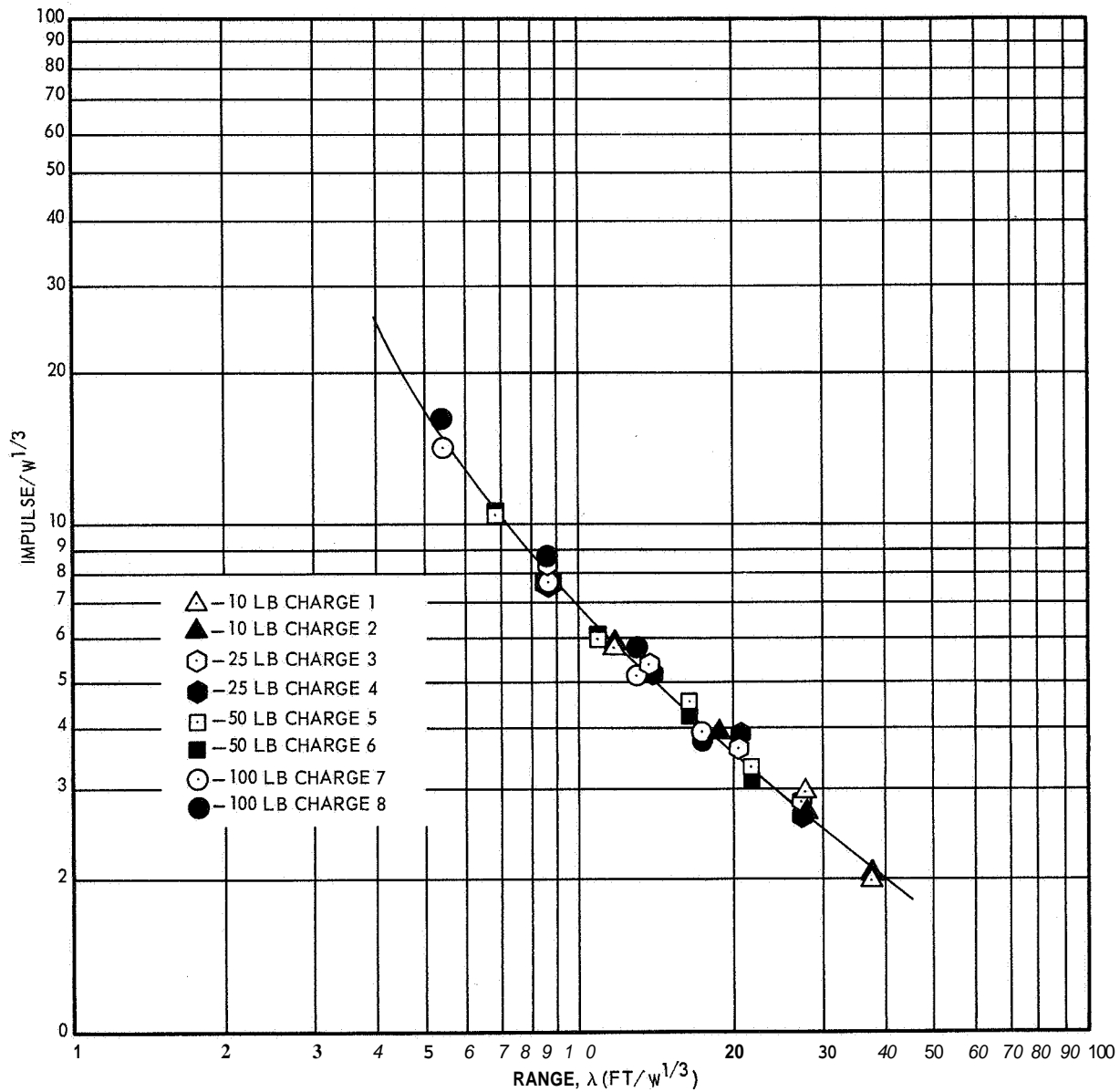
Figure 12. Positive Impulse vs Scaled Distance for
TNT Calibration Tests.
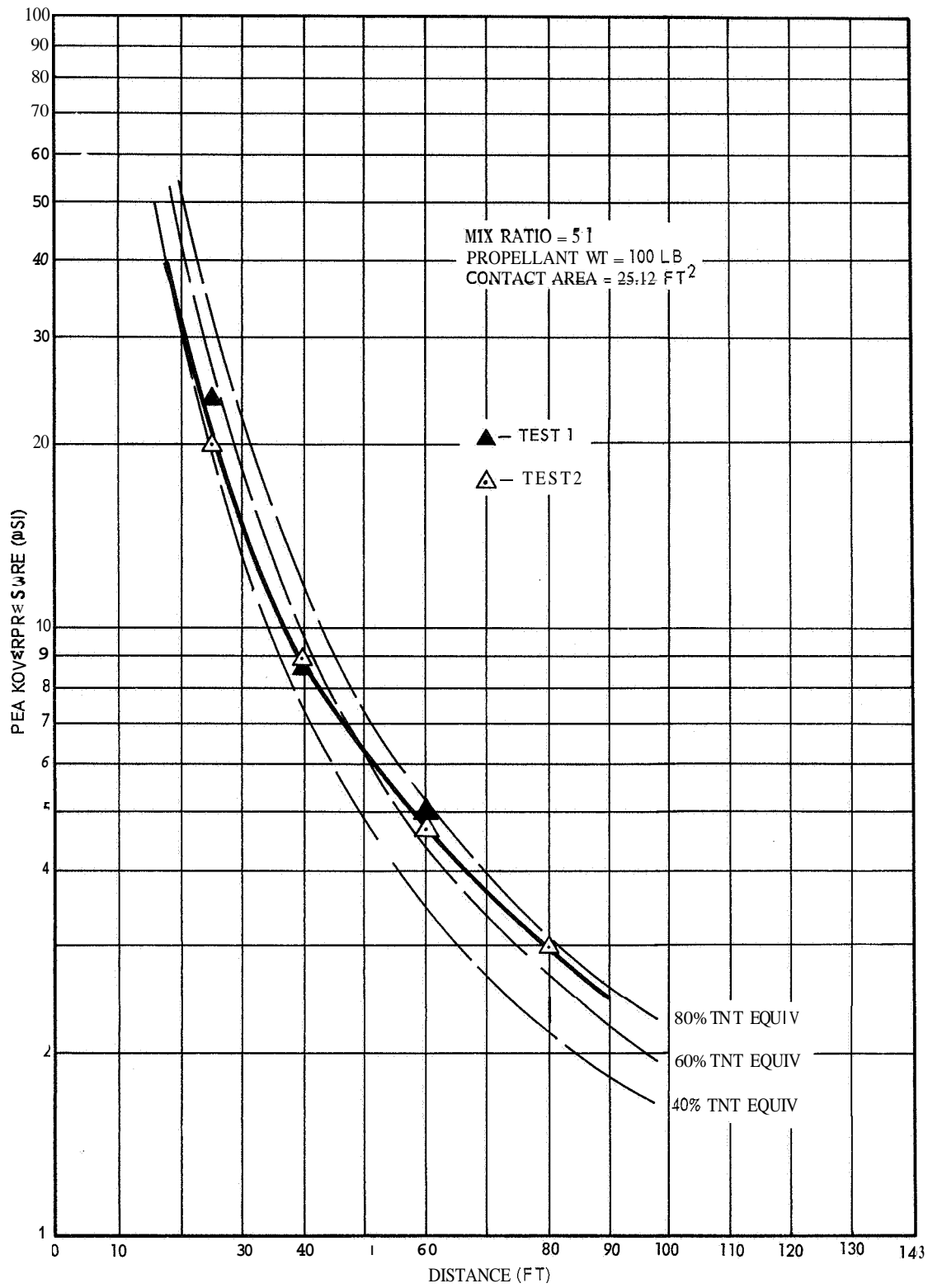
Figure **13.** Peak Overpressure vs Distance **for** LOX/LH$_2$ **(a).**
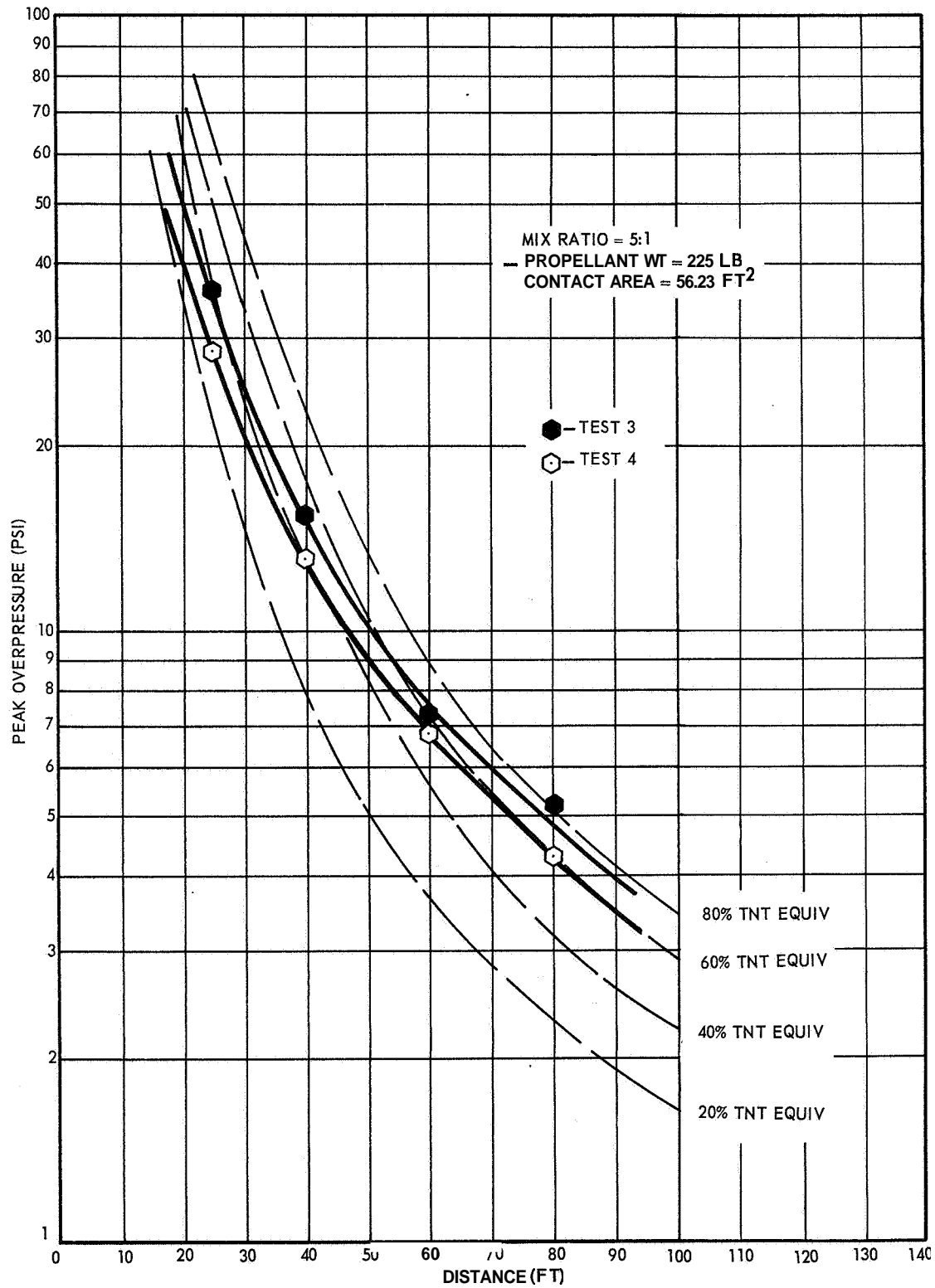
2828-13-1

Figure 14. **Peak** Overpressure vs Distance **for** LOX/LH_2 (b).

MIX RATIO = 5:1
PROPELLANT WT = 150 LB
CONTACT AREA = 36.81 FT^2

■ — TEST 5
□ — TEST 6

80% TNT EQUIV
60% TNT EQUIV
40% TNT EQUIV
20% TNT EQUIV

PEAK OVERPRESSURE (PSI)
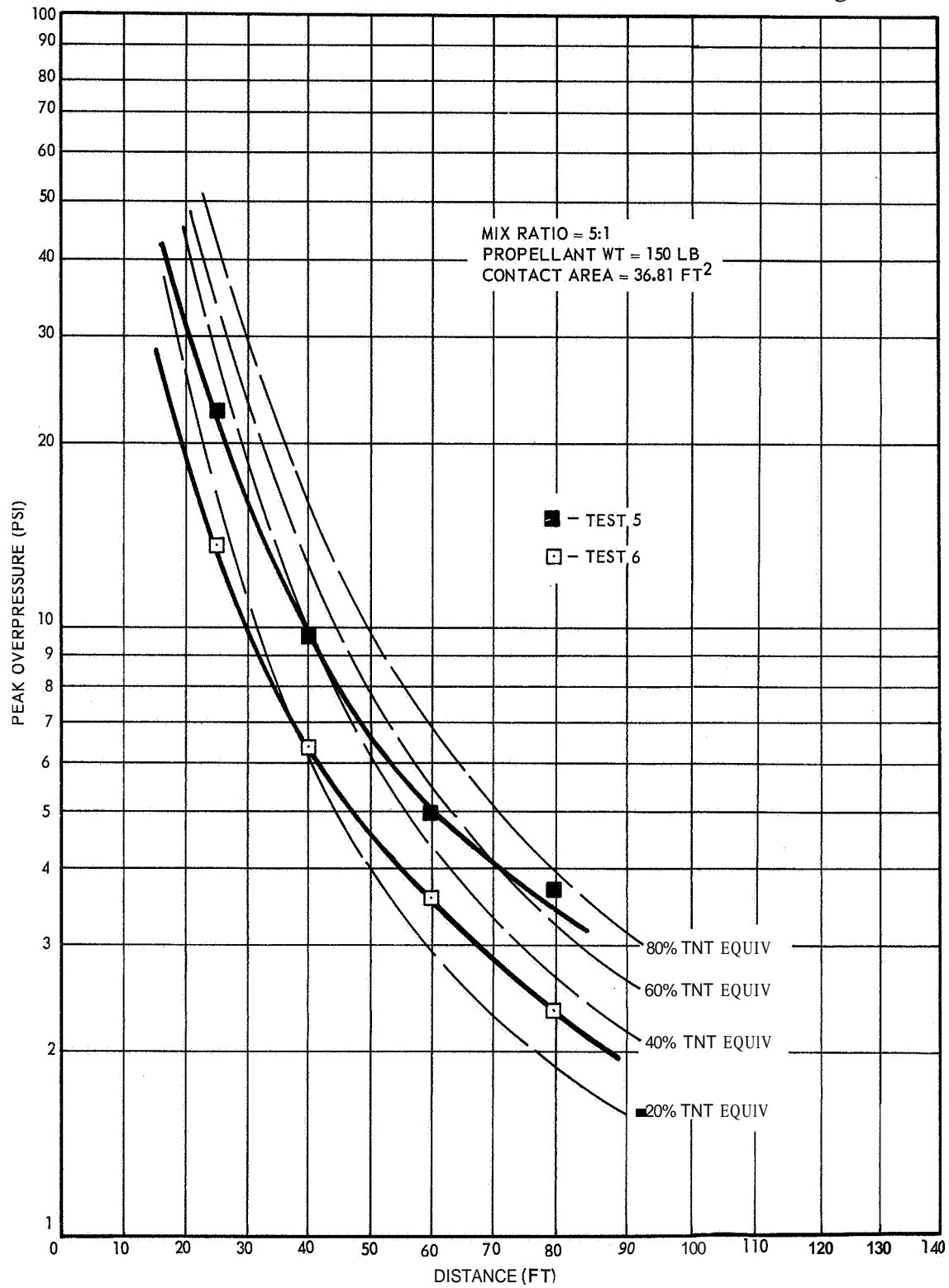
DISTANCE (FT)

2828-15.1

Figure 15. Peak Overpressure vs Distance for LOX/LH$_2$ *(c)*.

MIX RATIO = 2.5:1
PROPELLANT WT = 171 LB
CONTACT AREA = 36.81 FT^2

◇ —TEST 8
◆ —TEST 10

80% TNT EQUIV
60% TNT EQUIV
40% TNT EQUIV
30% TNT EQUIV

PEAK OVERPRESSURE (PSI)
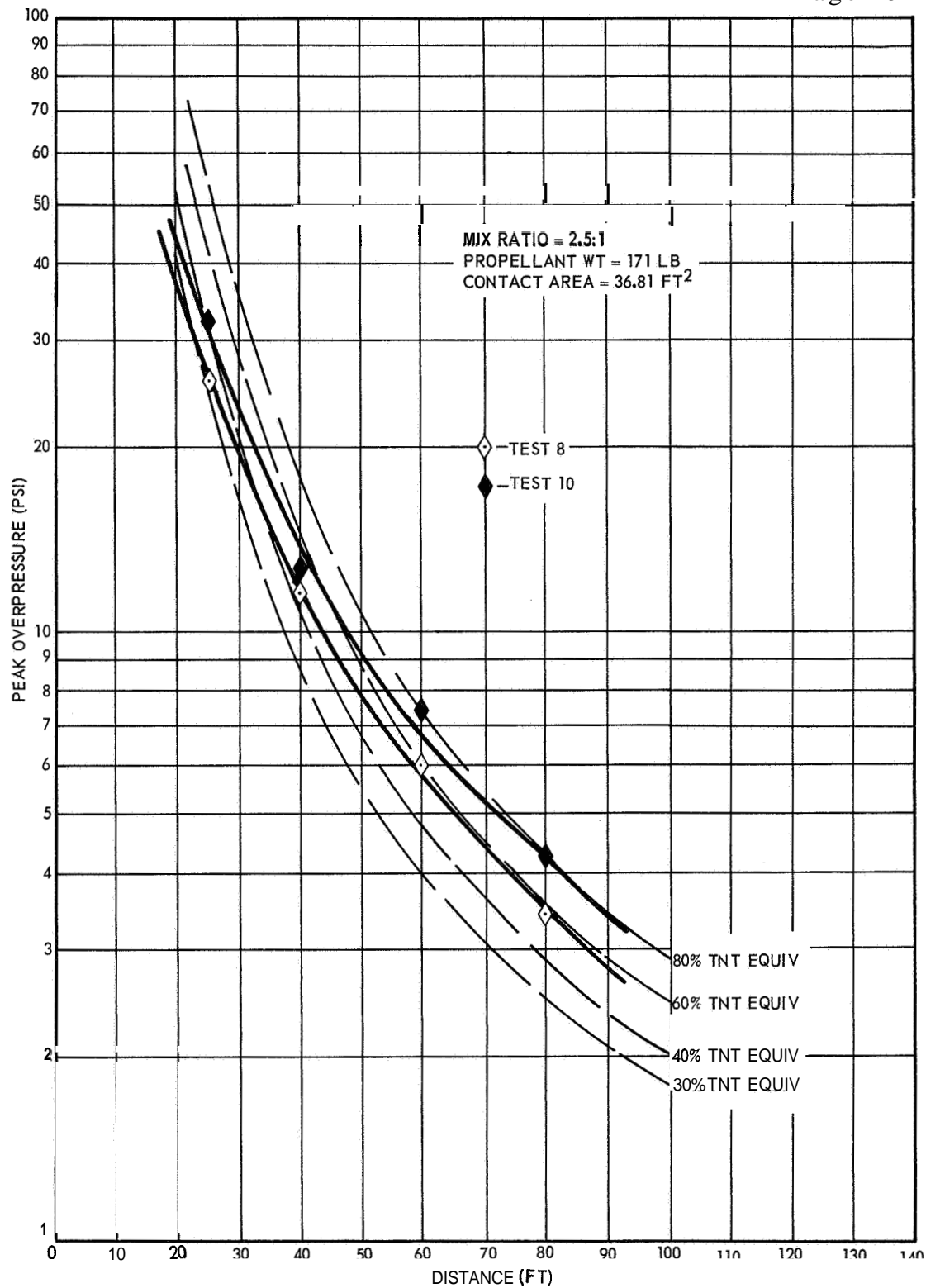
DISTANCE (FT)

2828-16-1

Figure 16.   Peak Overpressure vs Distance for LOX/RP-1.
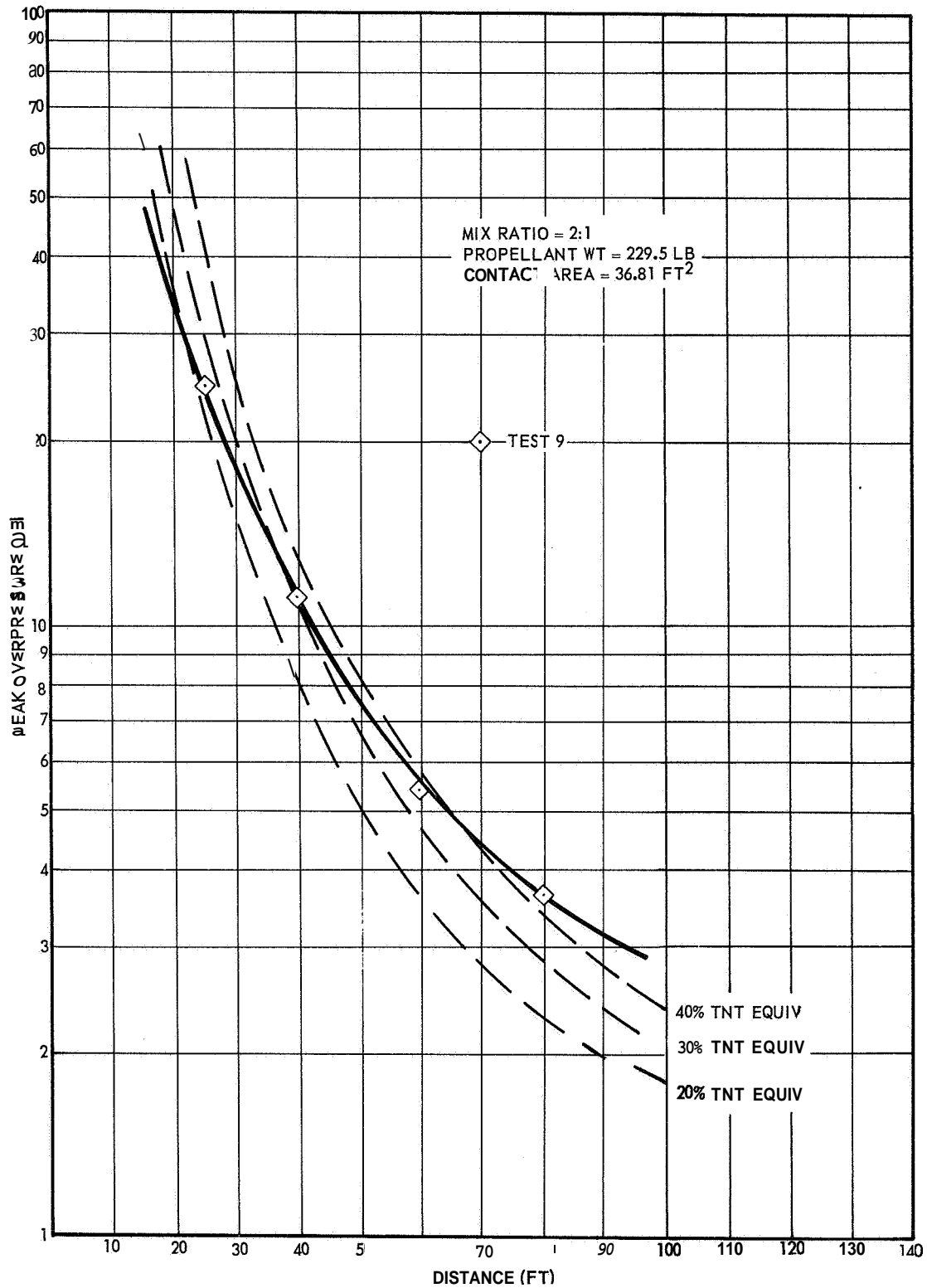
Figure 17. Peak Overpressure vs Distance for N_2O_4/A-50.

MIX RATIO = 5 1
PROPELLANT WT = 100 LB
CONTACT AREA = 25.12 FT^2

▲ — TEST 1
△ — TEST 2

100% TNT EQUIV

30 % TNT EQUIV

50 % TNT EQUIV

IMPULSE (PSI-MS)
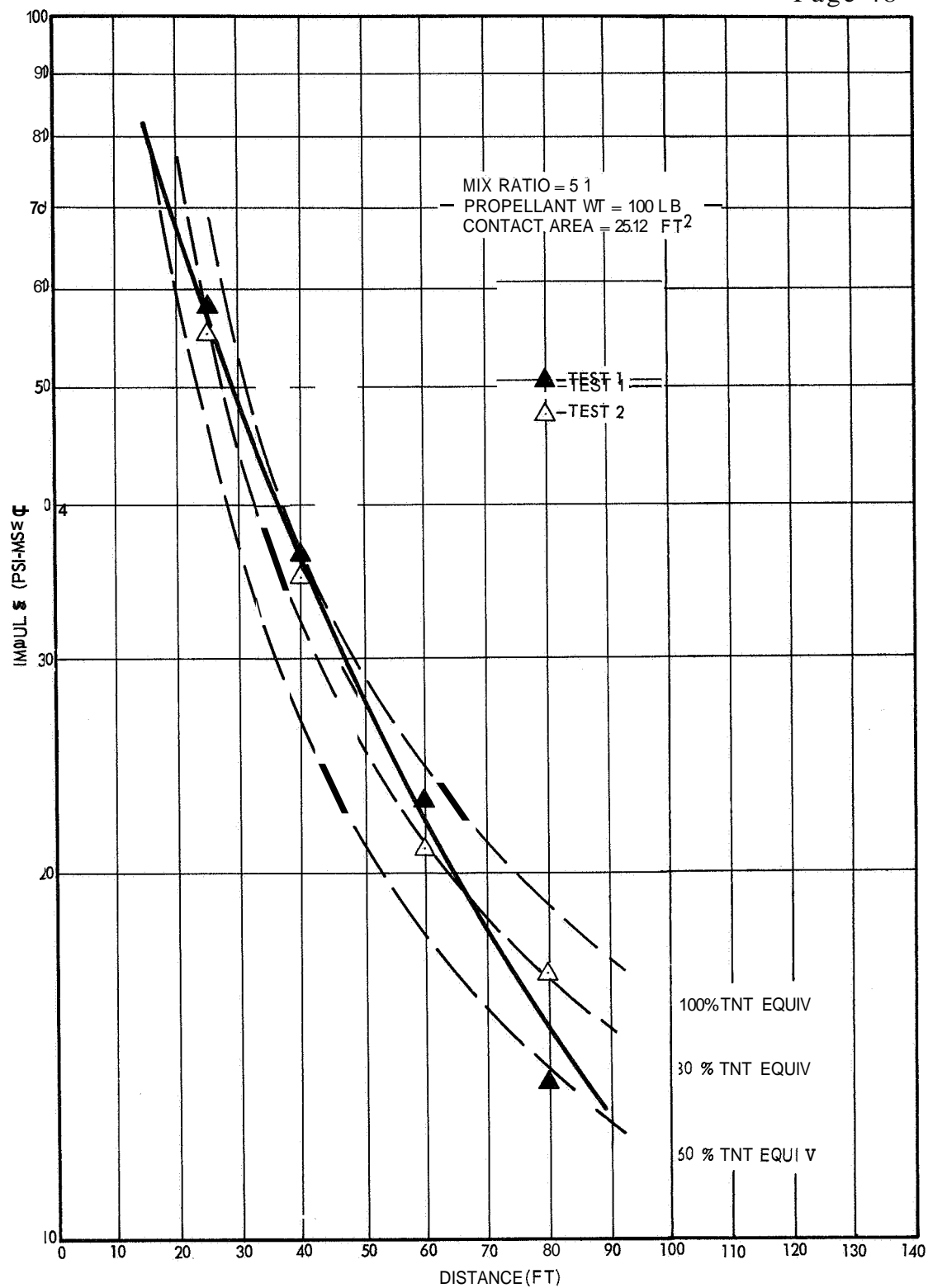
DISTANCE (FT)

2828-18-1

Figure 18.   Positive Impulse vs Distance **for** LOX/LH$_2$ (a).
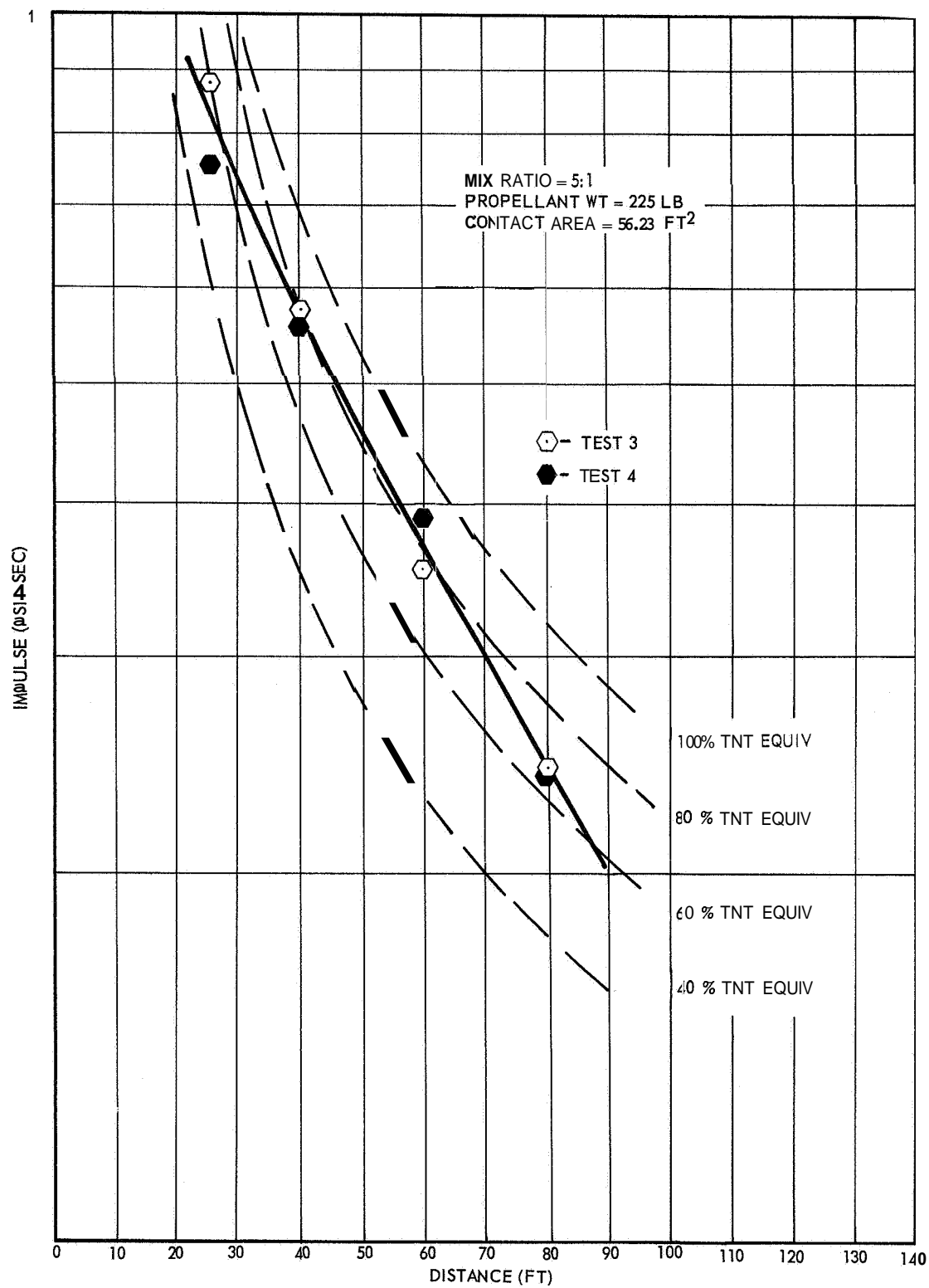
Figure 19. Positive Impulse vs Distance for LOX/LH$_2$ (b).
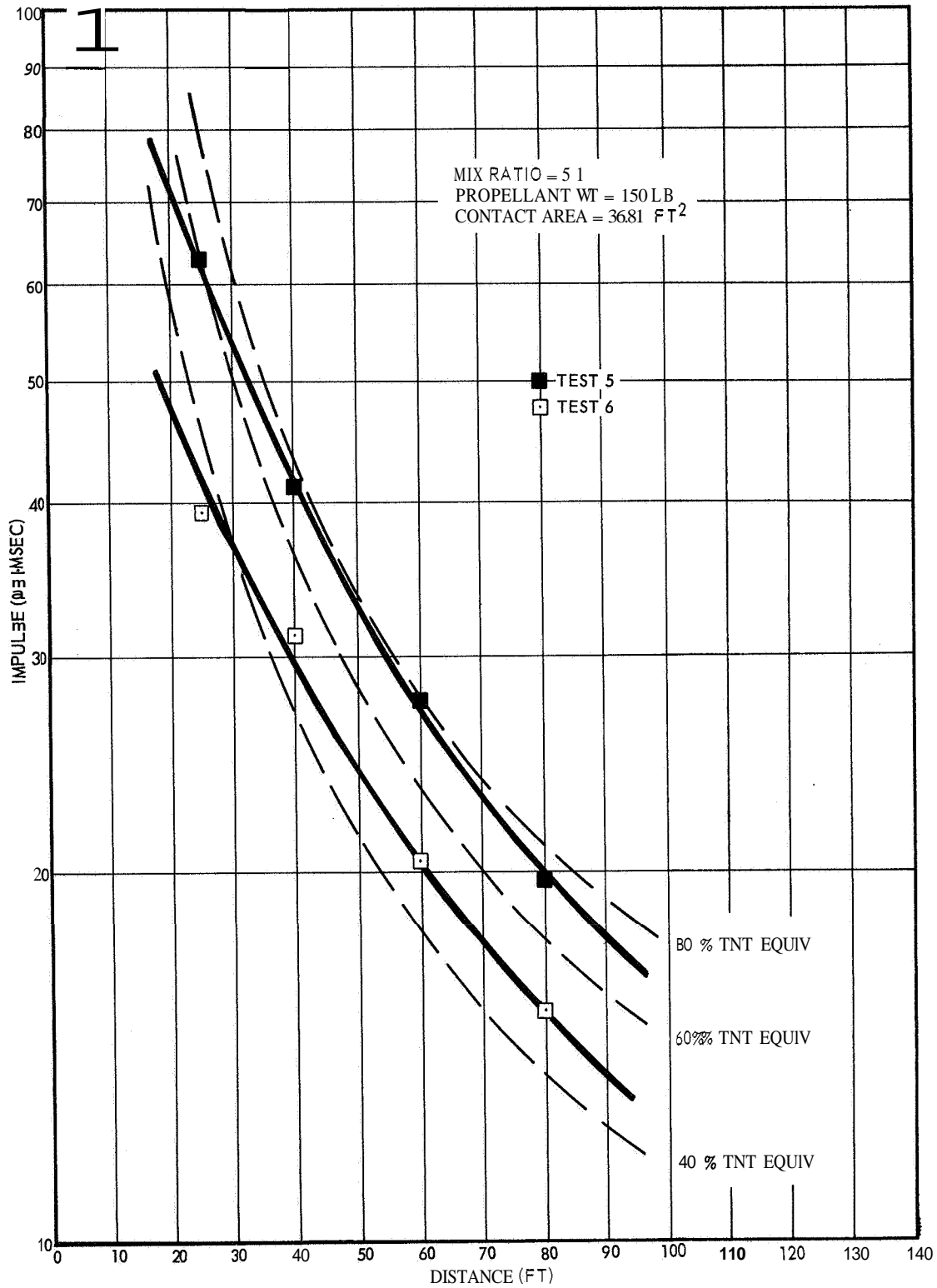
Figure 20.   Positive Impulse vs Distance for LOX/LH$_2$ (c).
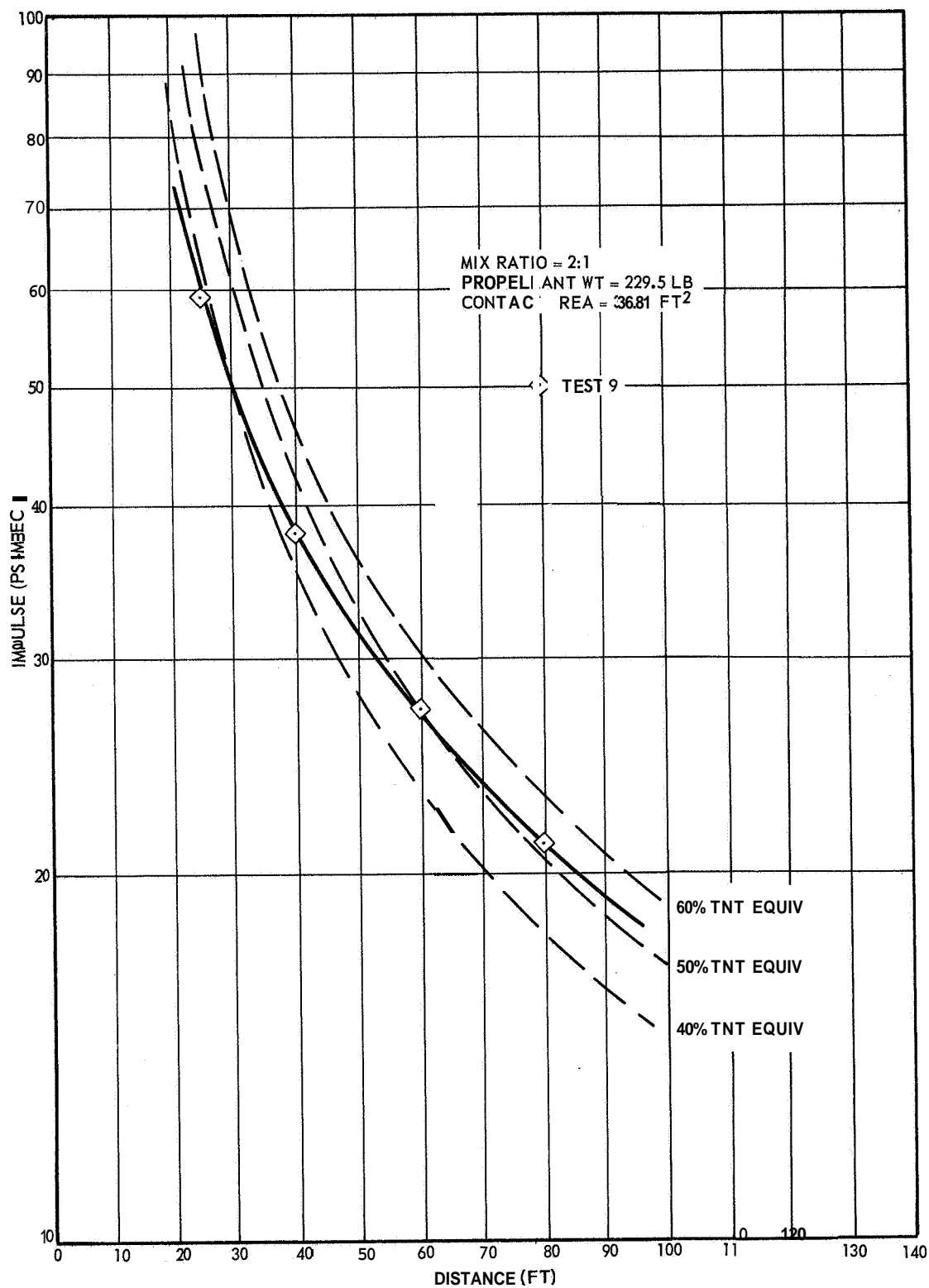
Figure 21.   Positive Impulse vs Distance for N_2O_4/A-50.
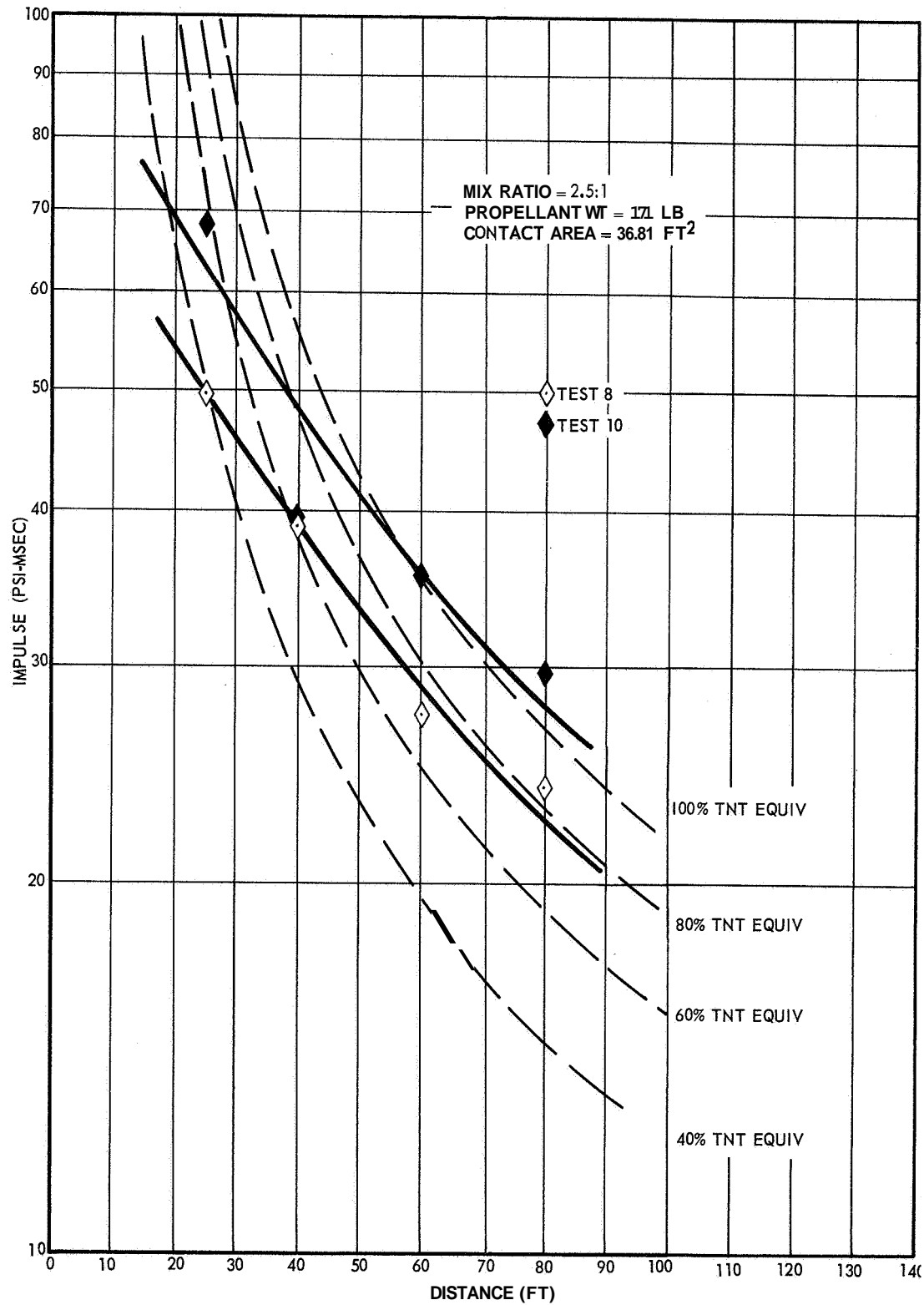
Figure 22.   Positive Impulse vs Distance for LOX/RP-1.

4. 6. 2   Shock Wave Pulse Characteristics

Examination of the positive pressure pulse records indicates that the
pressure time characteristics of the blast waves were closely allied to
those of conventional explosives in initial overpressure rise time,
decay rate, and positive duration for all of the propellant tests.

4. 6. 3   Cryogenic Propellant Initiation

The program plan provided for the evaluation of the LOX/LH_2 initiation
delay after shattering of the dewars.   Previous studies with $LOX/RP-1$
(Reference 9) indicated spontaneous initiation from an undetermined
stimulus when similar dewar pan assemblies impacted a steel plate.
The same spontaneous initiation phenomenon was observed during this
program, thus providing a reproducible type of mixing for the types of
propellants involved.   The source of the initiation stimuli is not known,
but possible causes for the spontaneous initiation are: (1) shock-impact-
caused implosion of the glass dewars, (2) the compression of the pro-
pellant material between the glass fragments and the pan wall or other
fragments, (3) chemical reaction from the silvered glass dewar, or
(4) a combination of all three possible sources.

4. 6.4   Fireball History

The results of the initial fireball expansion, size, and duration measure-
ments are presented in Figures 23 through 31 and are listed in Table 4. A
random variation was observed in the fireball size and duration for the
three propellant combinations.   The maximum fireball diameters varied
from 64 to 91 ft and the maximum heights ranged from 38. 5 to 73 ft.   The
durations varied from 1.28 to 2.45 sec. Examination of the 150 lb
LOX/LH_2 test results and the $LOX/RP-1$ test results indicated a correla-
tion between the fireball duration and blast yield for duplicate test
conditions; i.e. , the longer the duration, the lower the air blast yield.
For the LOX/LH_2 tests, a fireball duration of 1.90 sec was observed for
a TNT blast equivalence of 0. 8 lb of TNT per lb of propellant (Test 5)
while a fireball duration of 2.45 sec was cbserved for a TNT blast
equivalence of 0. 5 lb of TNT per lb of propellant (Test 6).   The LOX/
RP-1 test indicated a duration of 1.80 sec and a blast yield of 0. 6 lb of
TNT per lb of propellant for Test 8 compared to a duration of 1. 35 sec
and a blast yield of 0. 8 lb of TNT per lb of propellant for Test 10. A
similar relationship was observed for the 225 lb LOX/LH_2 propellant
tests although the relationship was not as pronounced.   Examination of
the 100 lb LOX/LH_2 tests indicated equal blast yields with a slightly
longer duration for Test 1 than for Test 2.
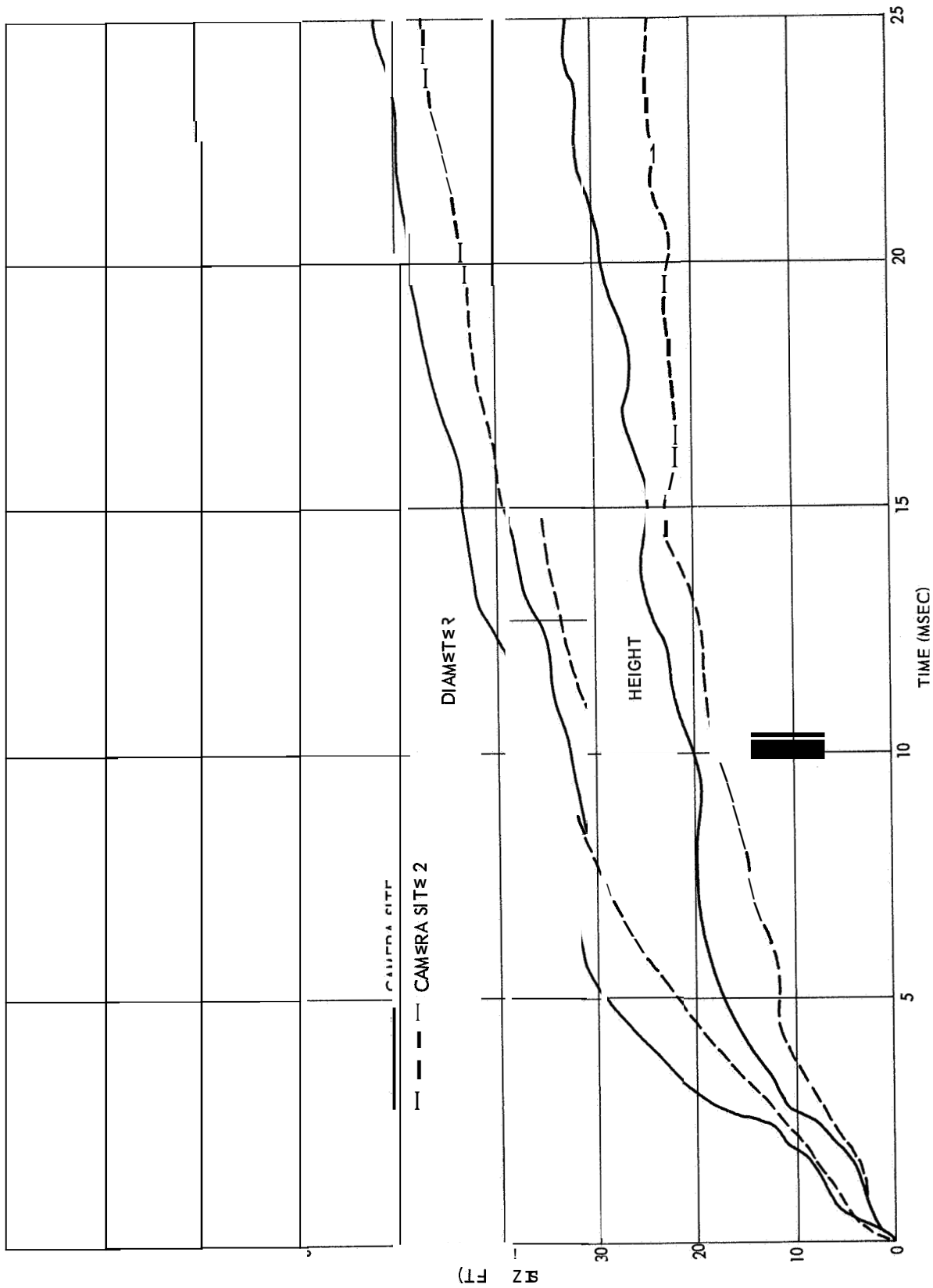
Figure 23a. Fireball History - LOX/LH$_2$ - Initial Growth. Contact Area = 25.12 ft^2 (Test No. 1).
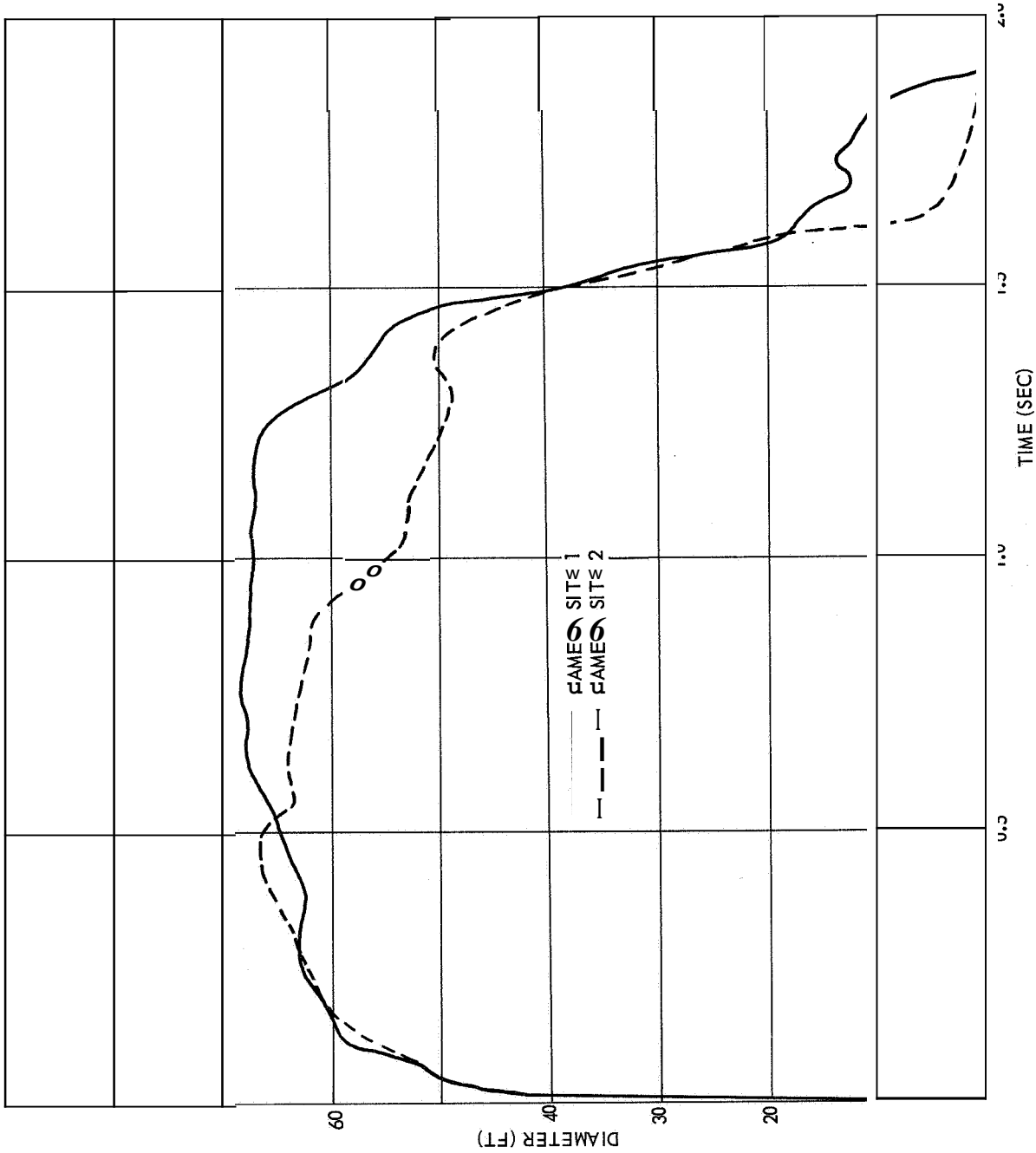
Figure 23b. Fireball History - LOX/LH$_2$ - Diameter.
Contact Area = 25.12 ft^2 (Test No. 1).
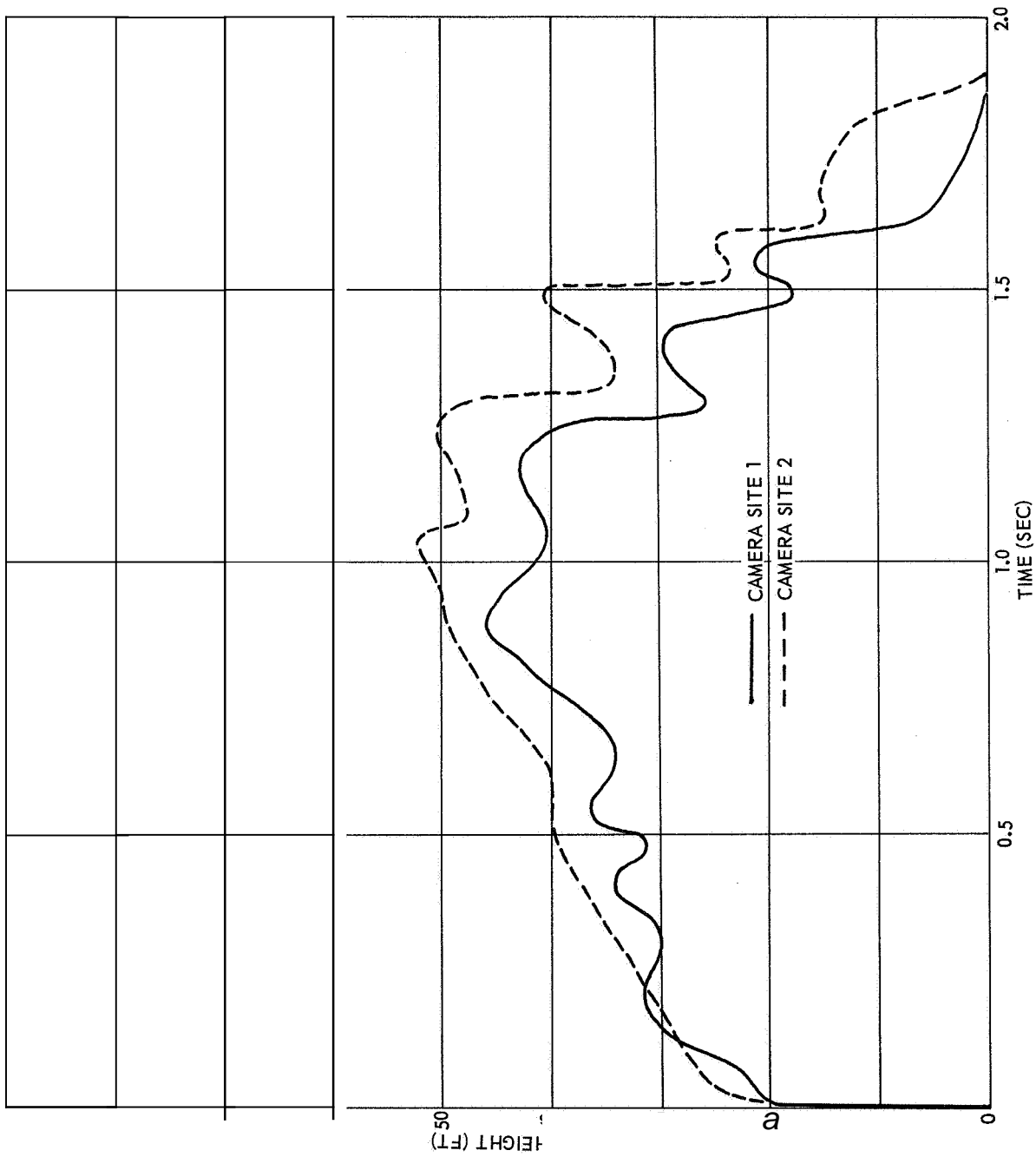
2828-23-1

Figure 23c. Fireball History - LOX/LH$_2$ - Height.
Contact Area = 25.12 ft^2 (Test No. 1).
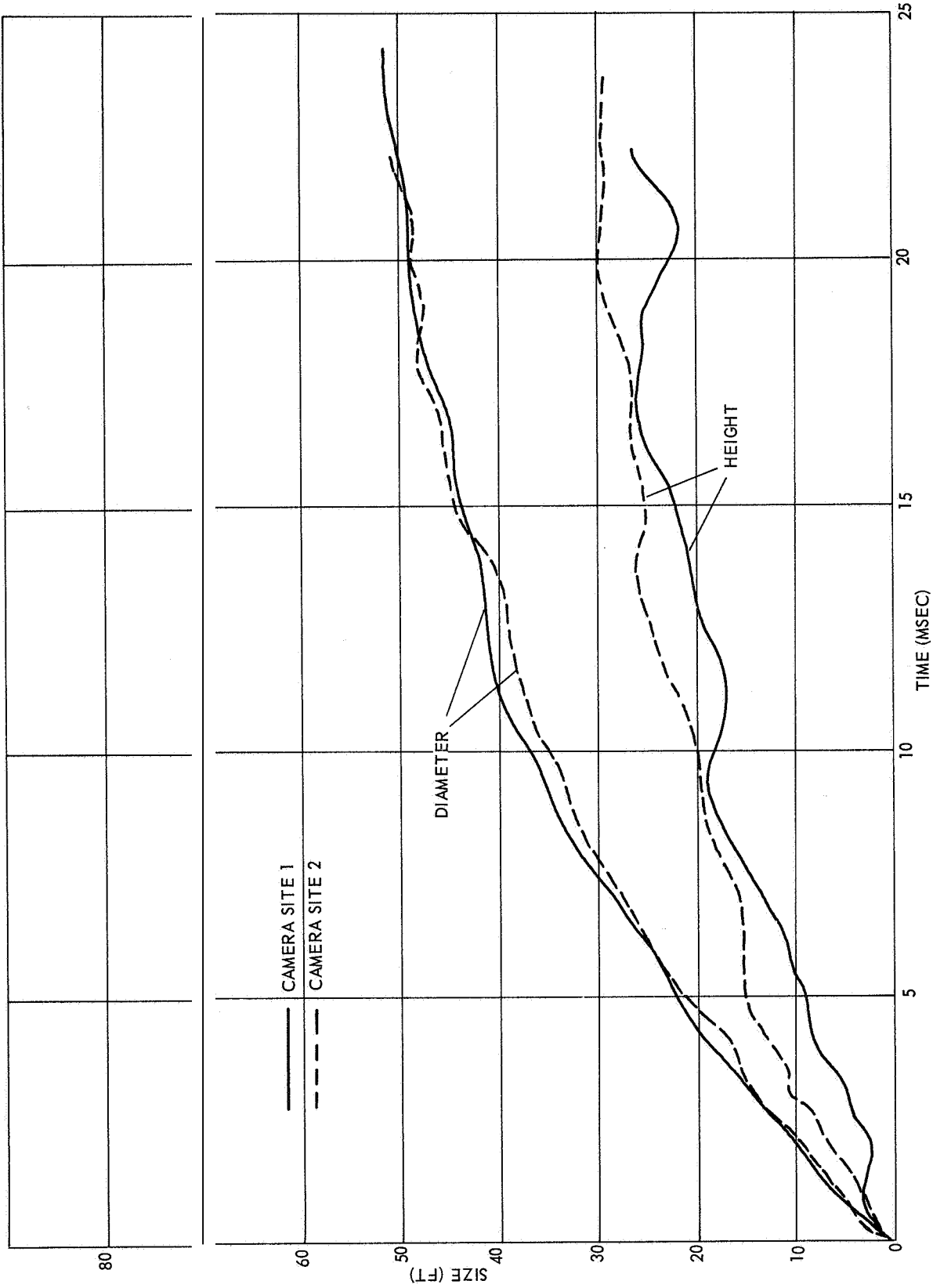
Figure 24a. Fireball History - LOX/LH2 - Initial Growth.
Contact Area = 25.12 ft^2 (Test No. 2).
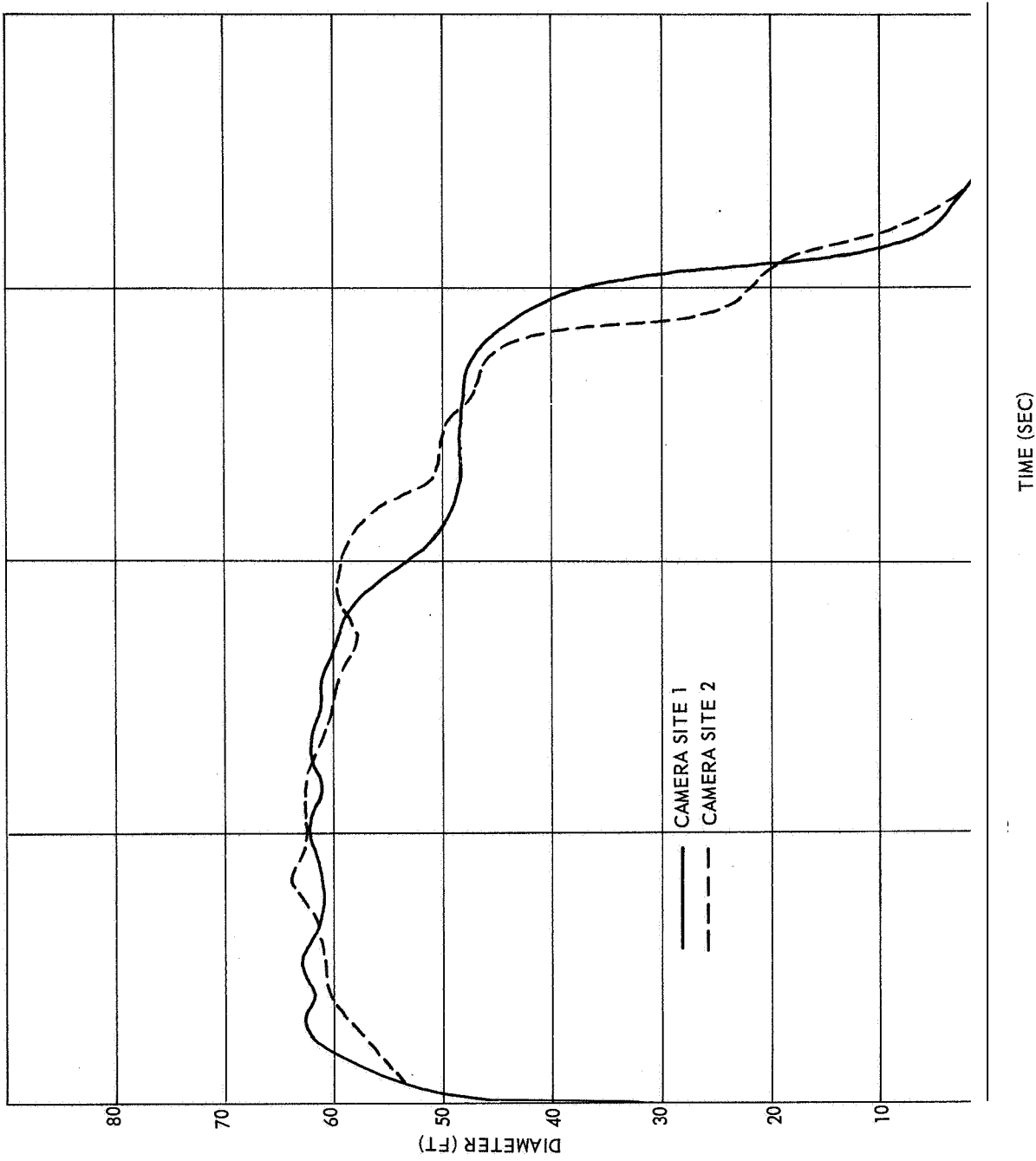
Figure 24b. Fireball History - LOX/LH2 - Diameter.
Contact Area = 25.12 ft² (Test No. 2).
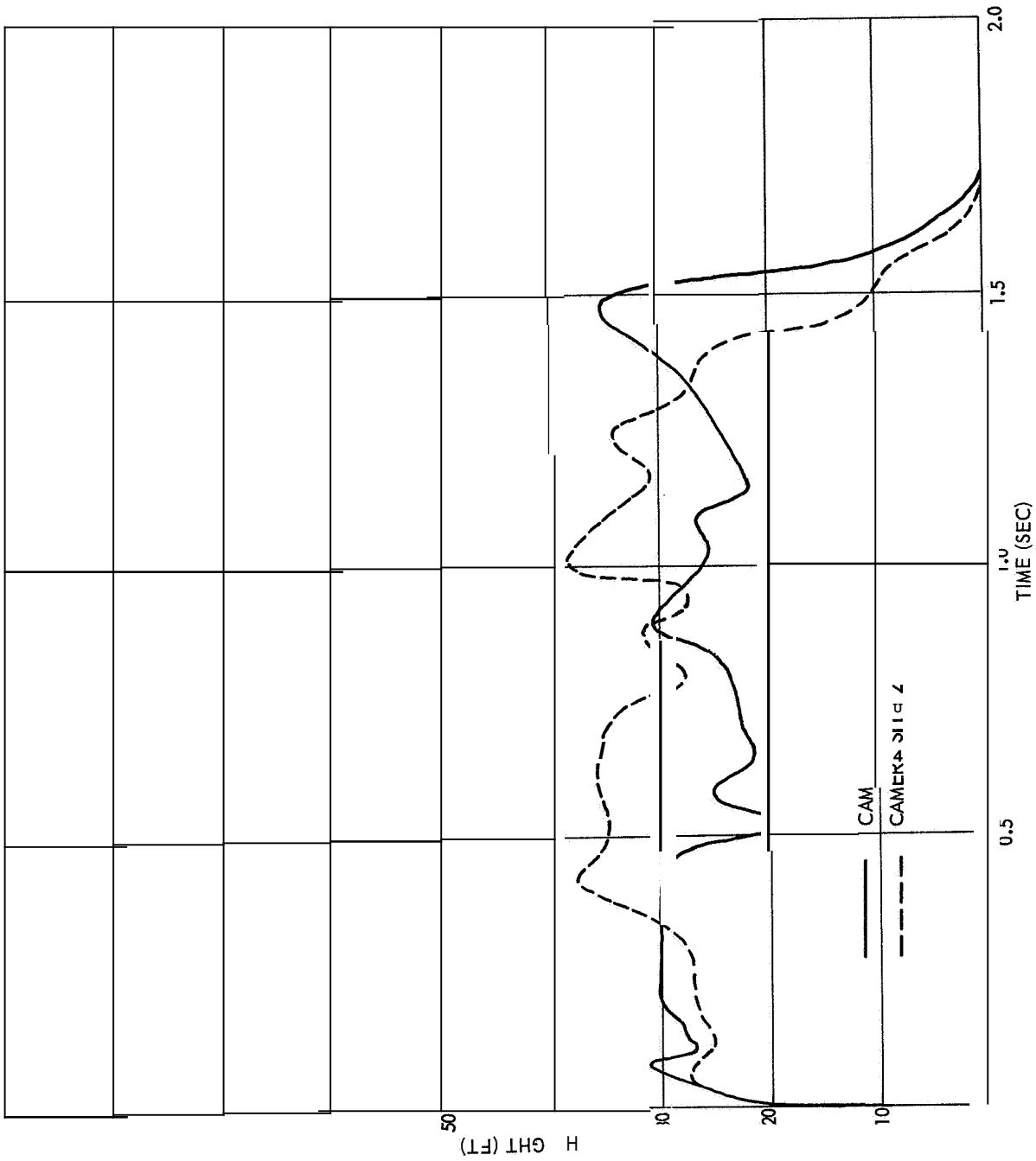
Figure 24c. Fireball History - LOX/LH$_2$ - Height.
Contact Area = 25.12 ft^2 (Test No. 2).
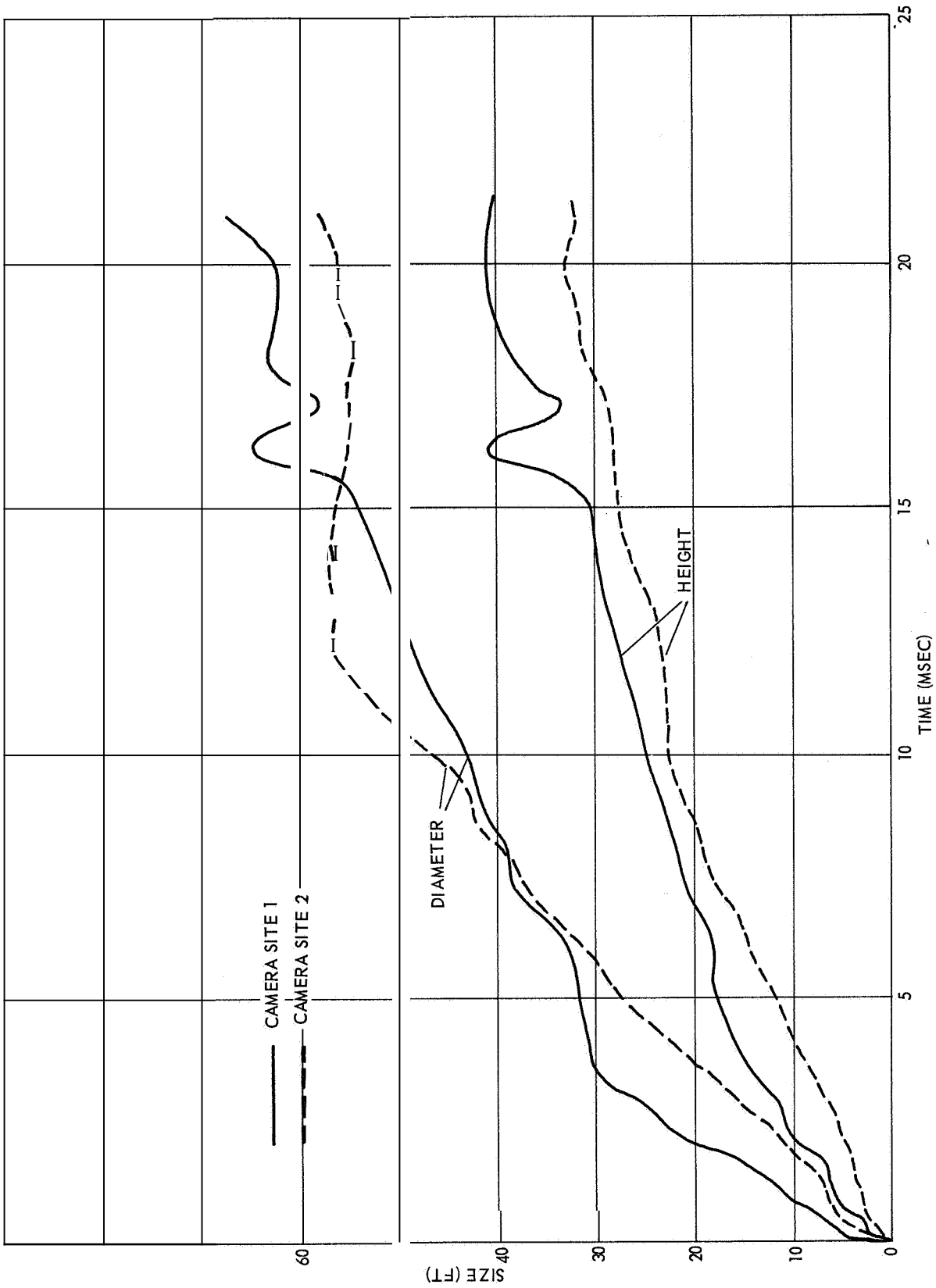
Figure 25a. Fireball History – LOX/LH$_2$ – Initial Growth. Contact Area = 56.23 ft^2 (Test No. 3).
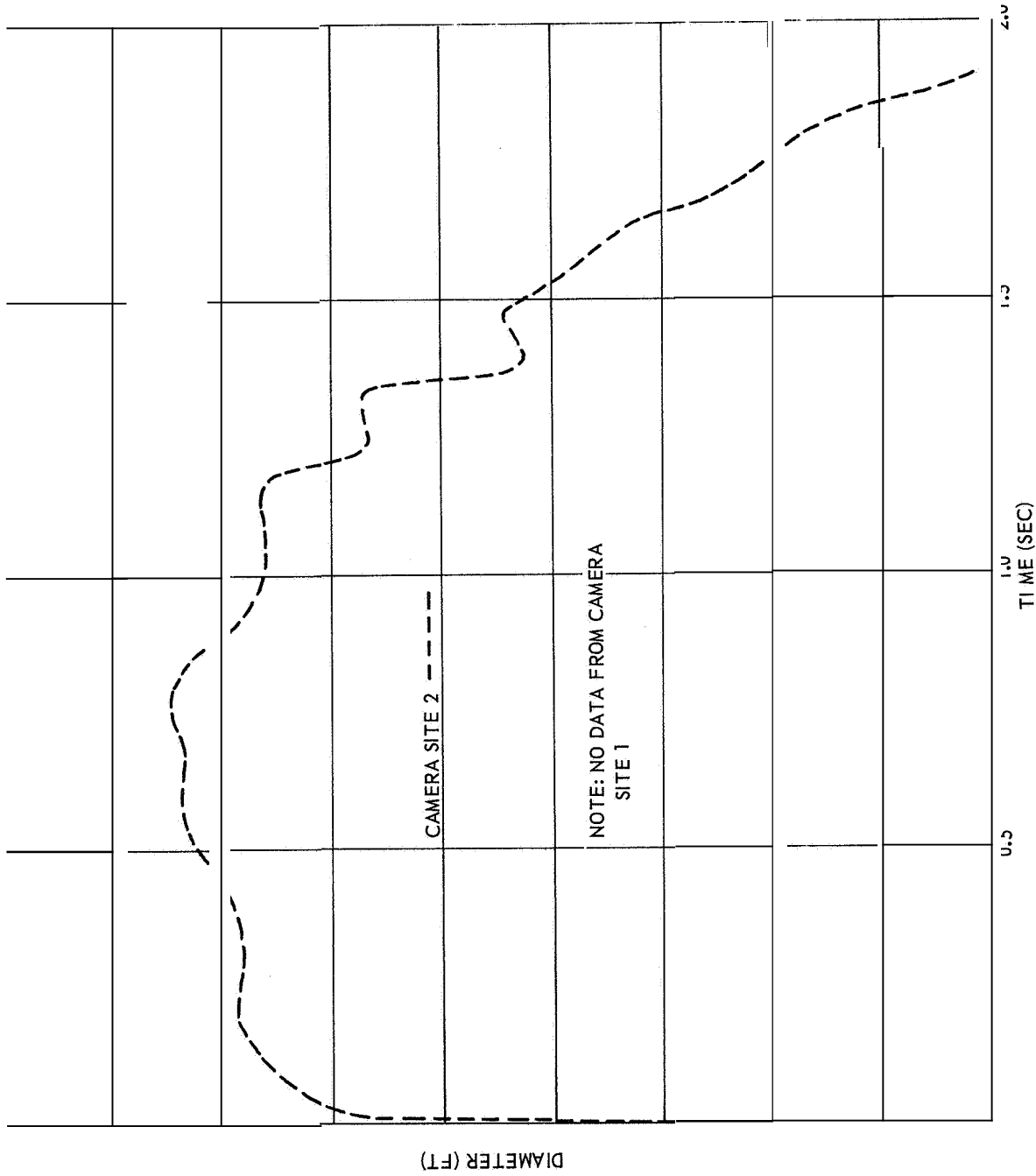
2828-25-1

Figure 25b. Fireball History – LOX/LH$_2$ – Diameter.
Contact Area = 56.23 ft^2 (Test No. 3).

2828-25-1
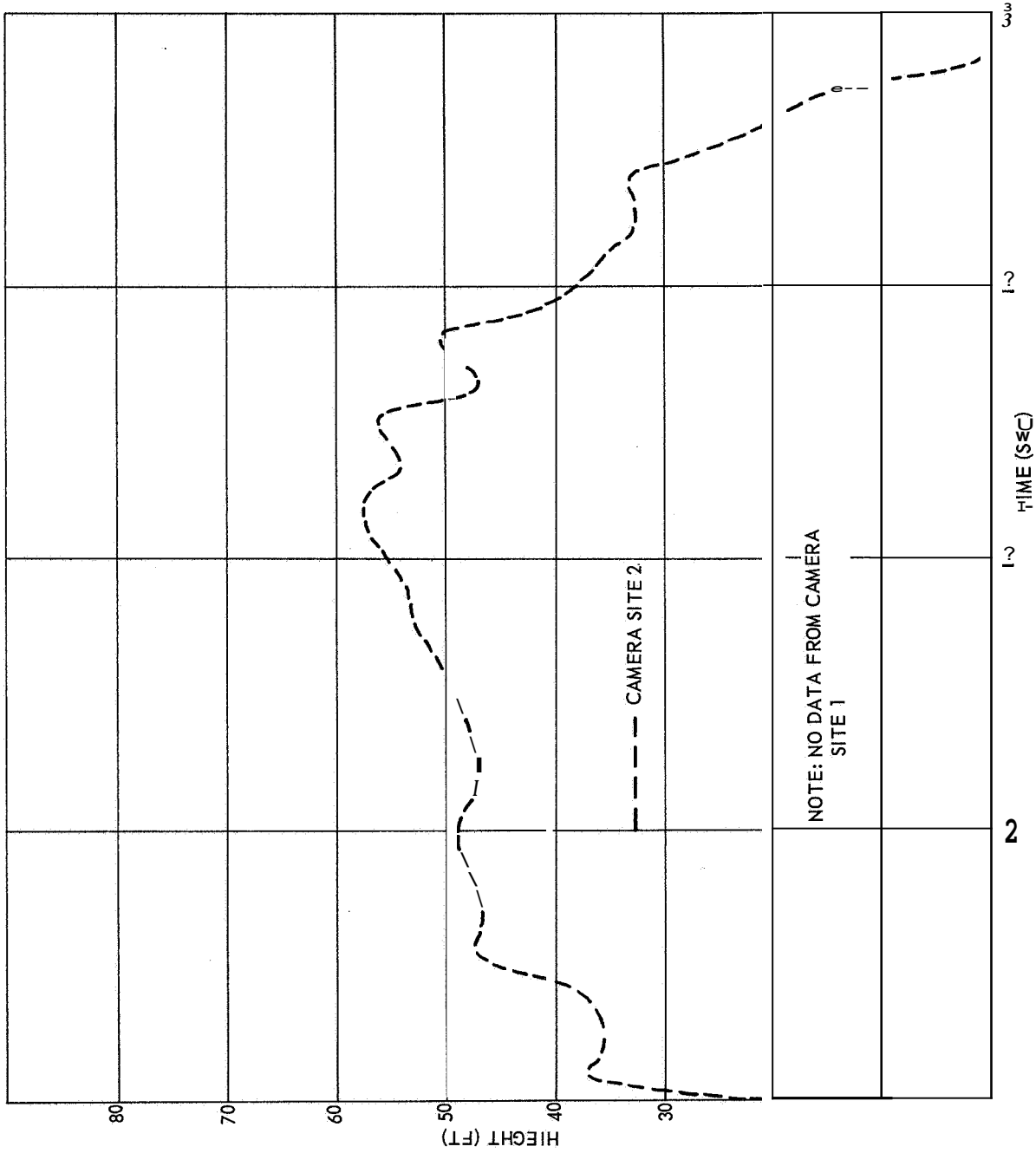
Figure 25c. Fireball History - LOX/LH$_2$ - Height.
Contact Area = 56.23 ft^2 (Test No. 3).

2828-25-1
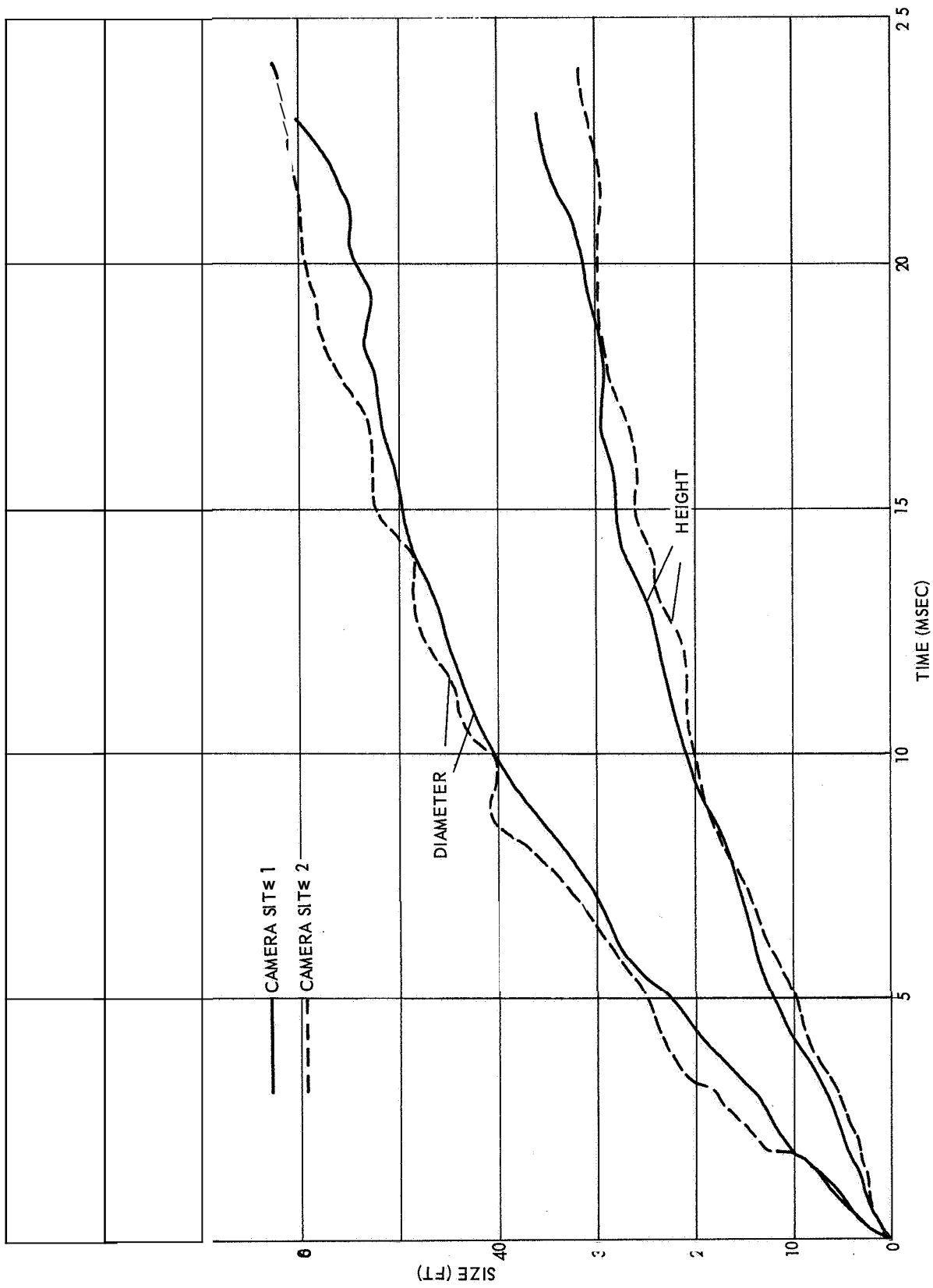
Figure 26a. Fireball History – LOX/LH$_2$ – Initial Growth.
Contact Area = 56.23 ft^2 (Test No. 4).

2828-26-1
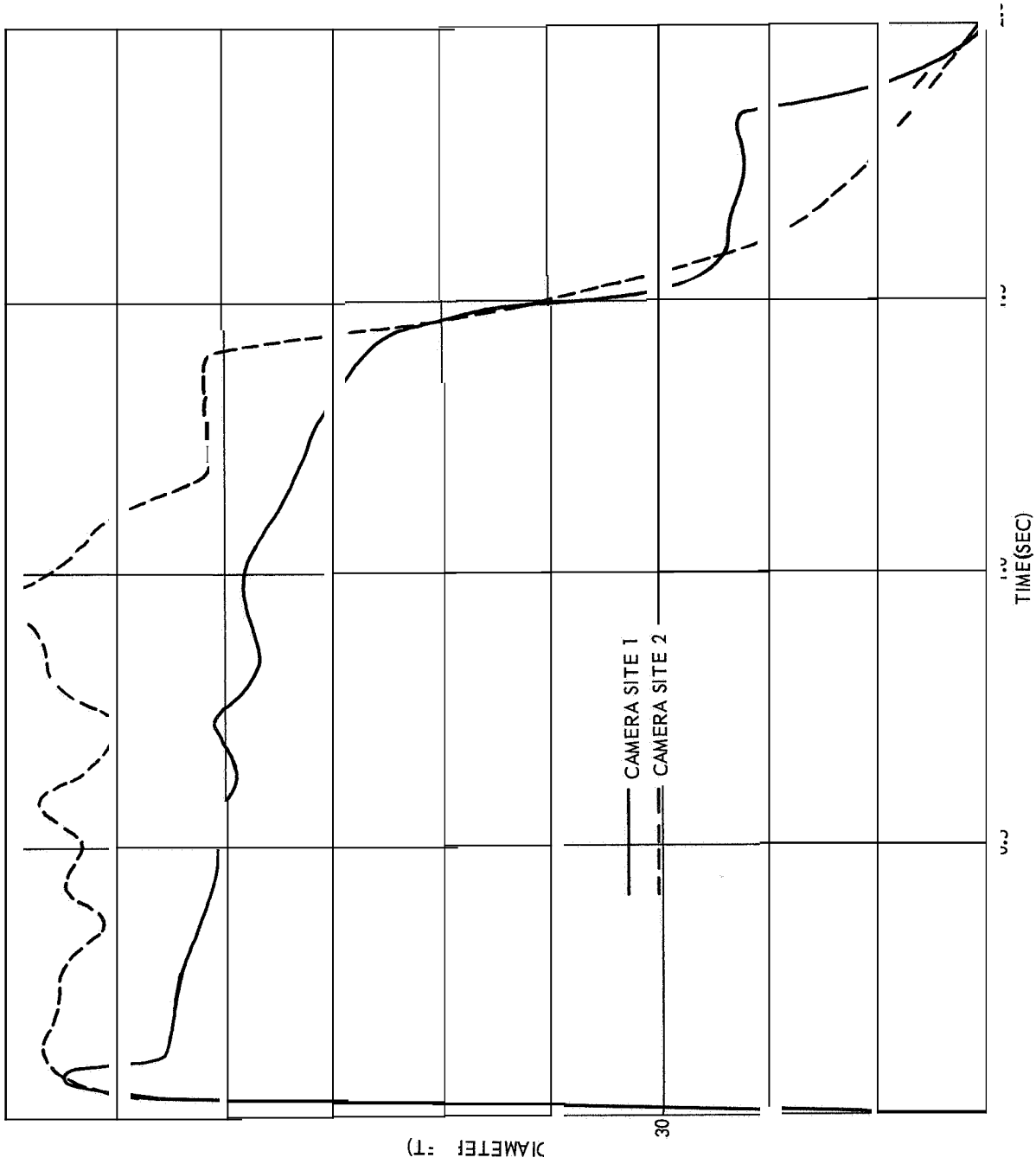
Figure 26b. Fireball History - LOX/LH$_2$ - Diameter. Contact Area = 56.23 ft^2 (Test No. 4).
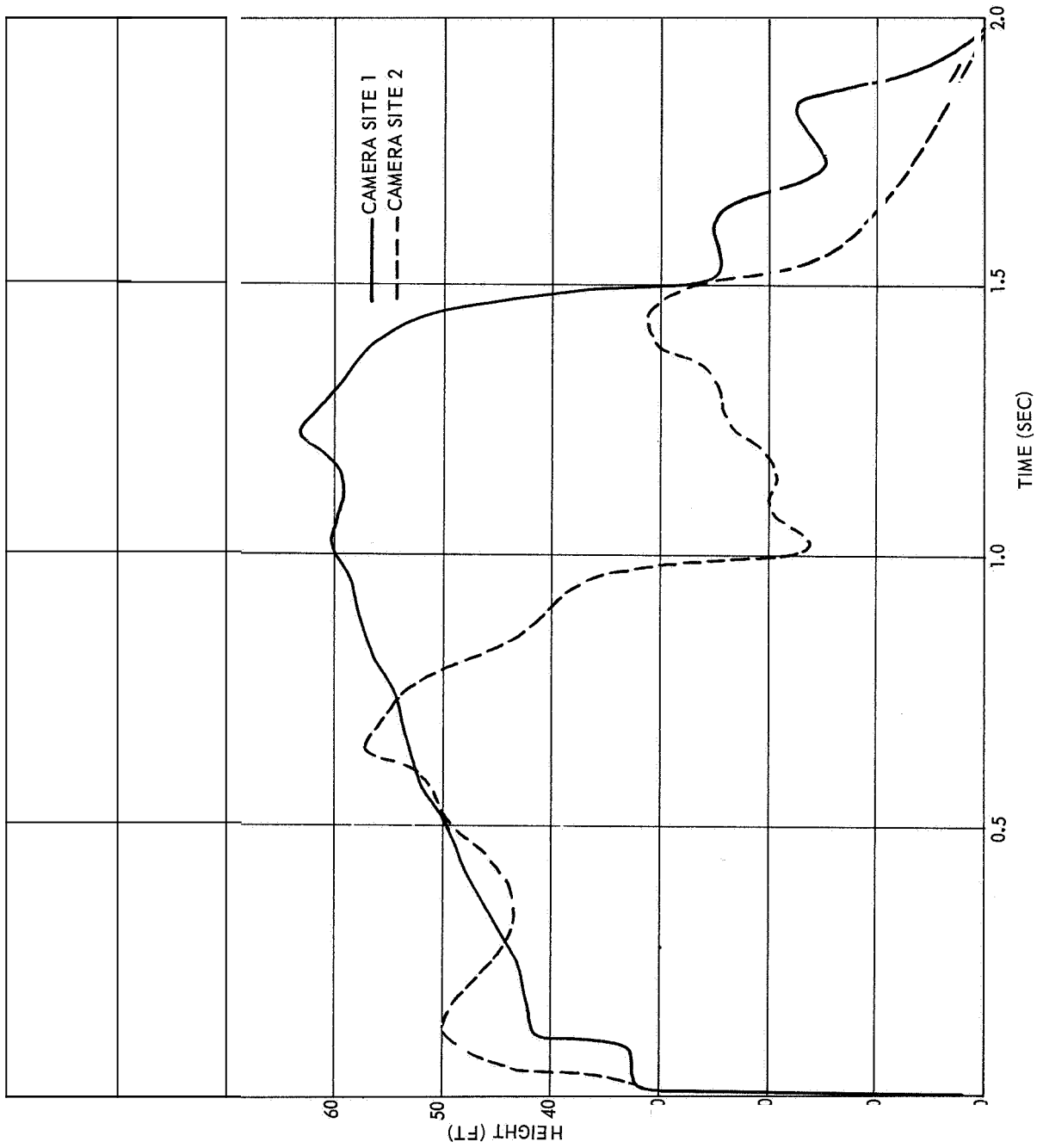
Figure 26c. Fireball History - LOX/LH$_2$ - Height.
Contact Area = 56.23 ft^2 (Test No. 4).
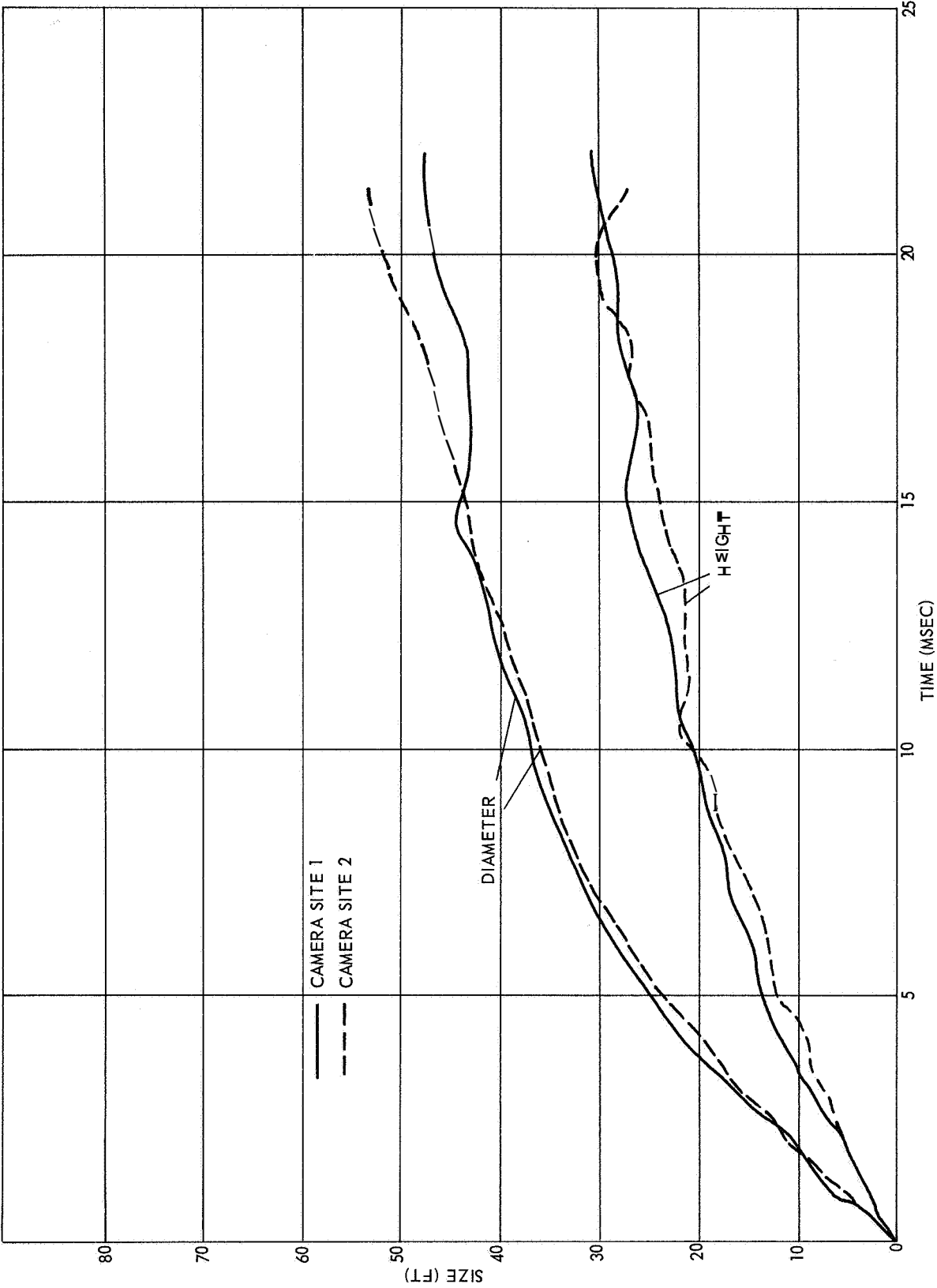
Figure 27a. Fireball History – LOX/LH$_2$ – Initial Growth.
Contact Area = 36. 81 ft^2 (Test No. 5).
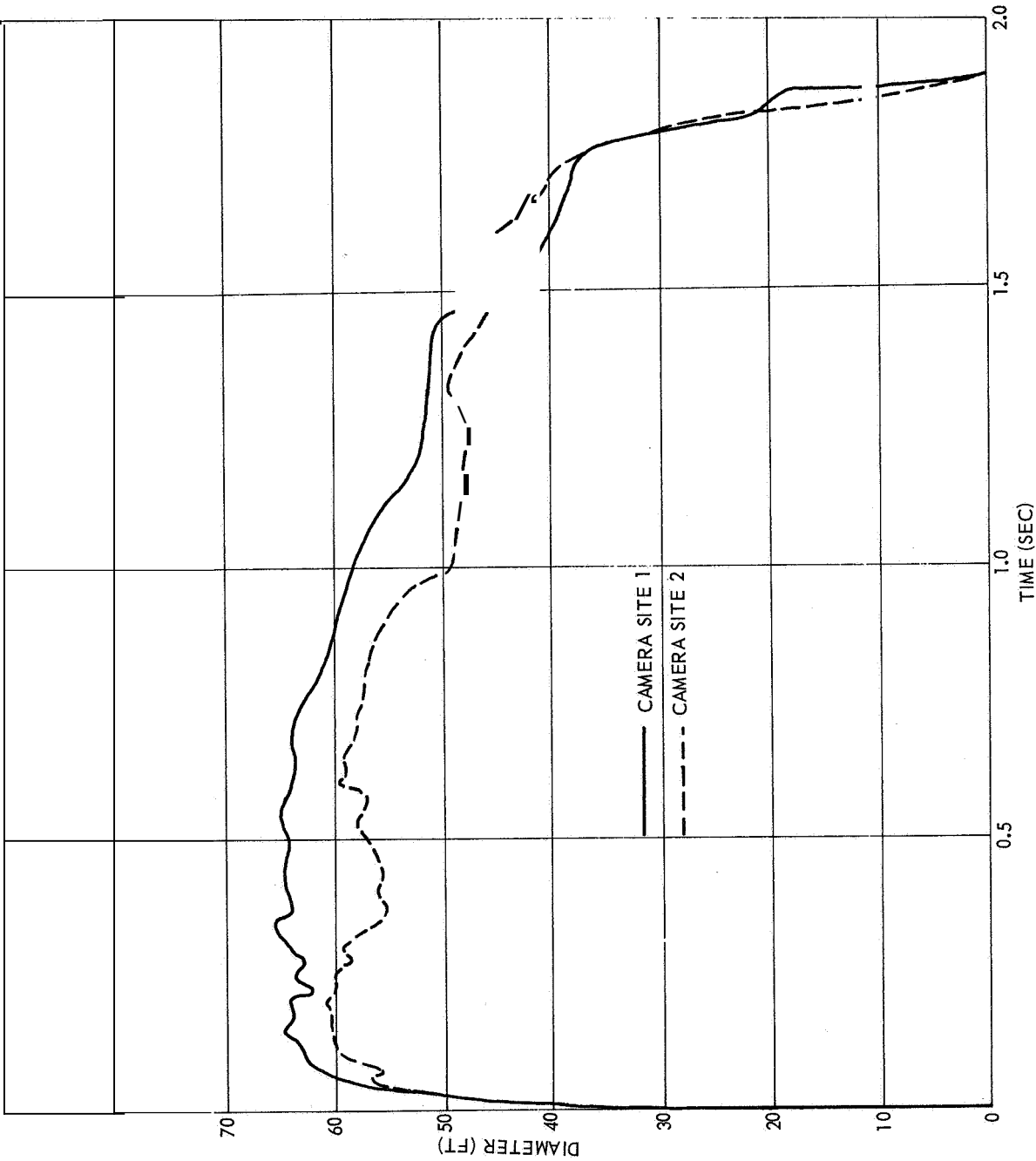
Figure 27b. Fireball History - LOX/LH$_2$ - Diameter Contact Area = 36.81 ft^2 (Test No. 5).
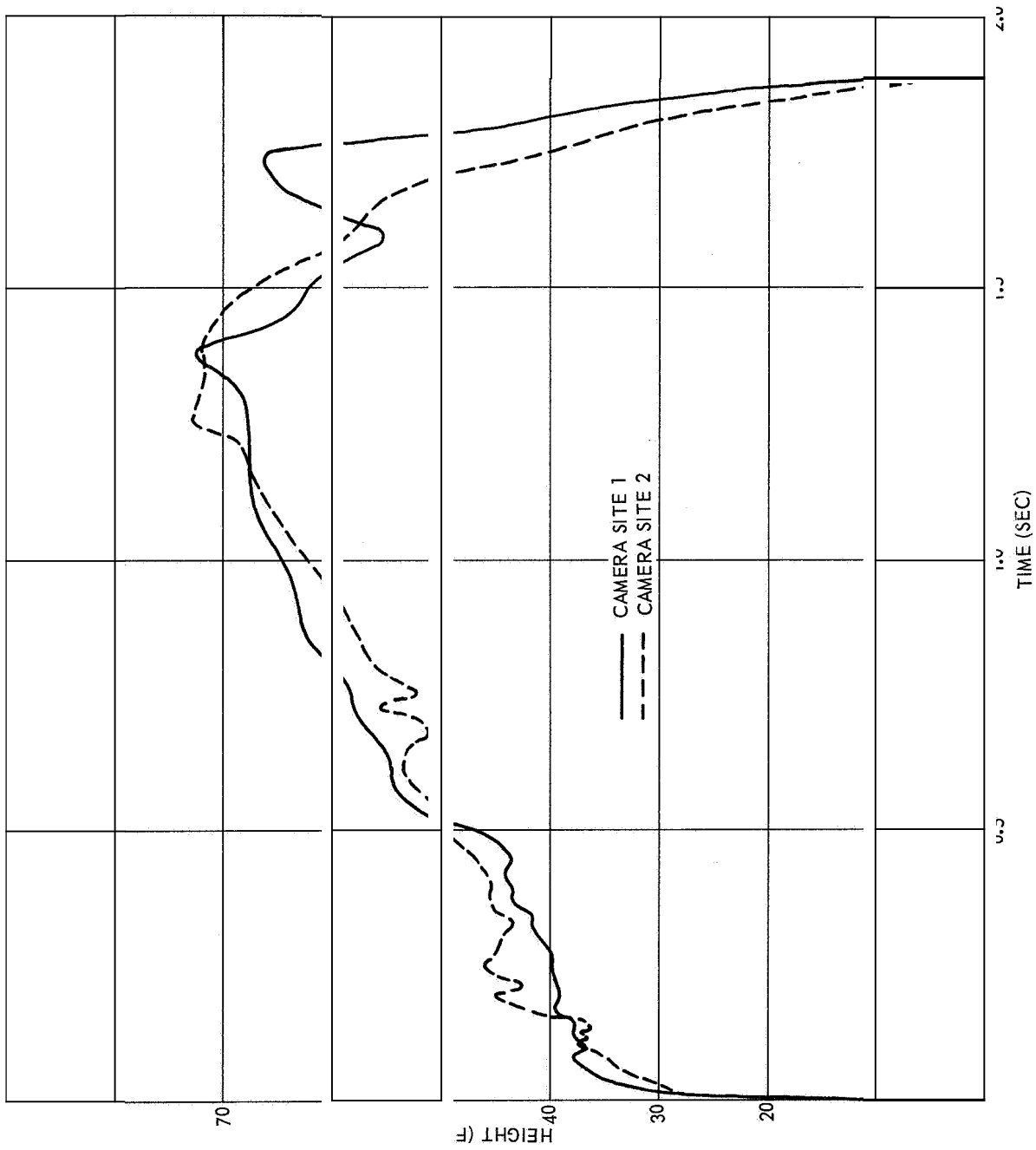
Figure 27c. Fireball History - LOX/LH$_2$ - Height. Contact Area = 36.81 ft^2 (Test No. 5).
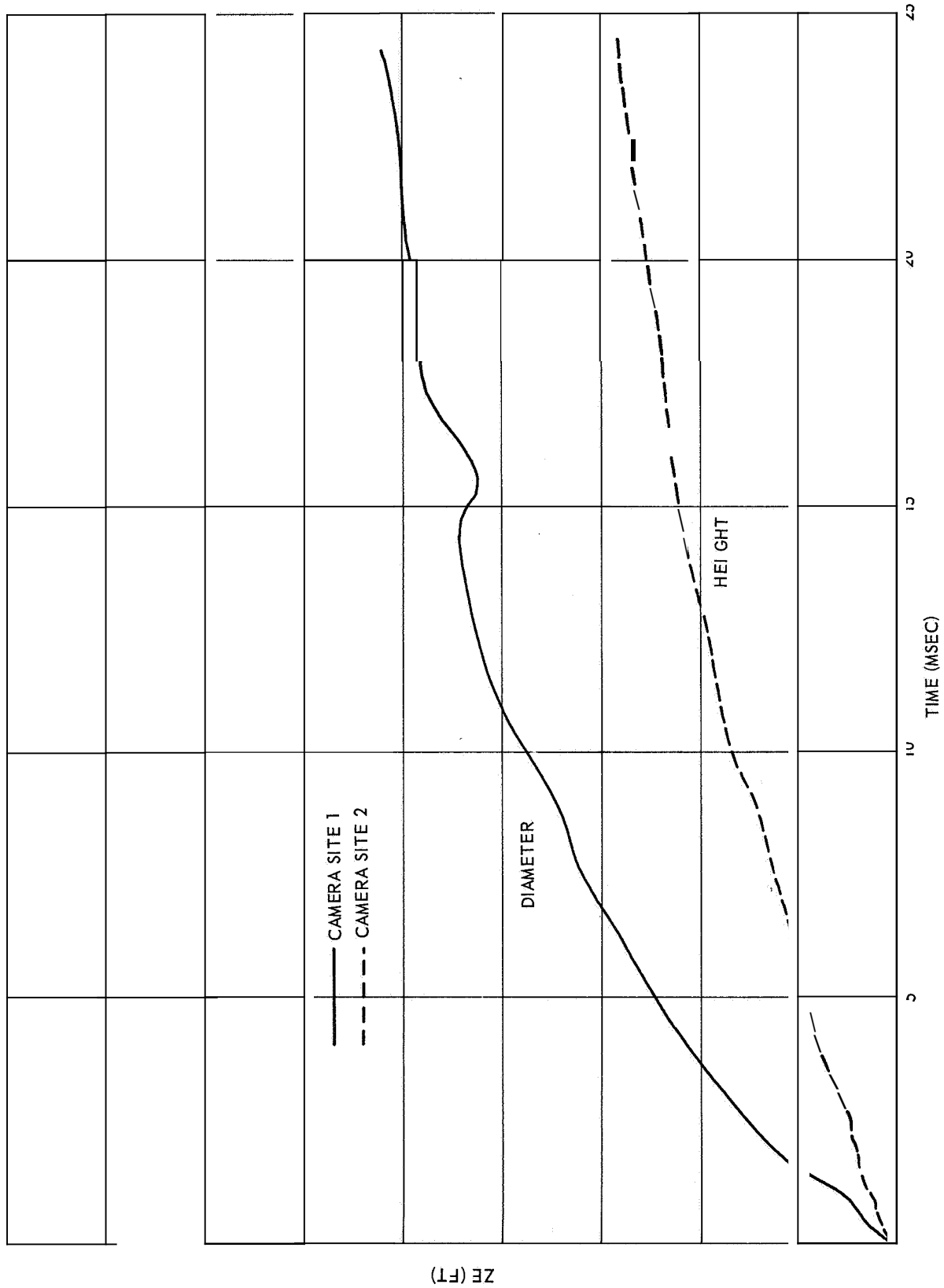
2828-27-1

Figure 28a. Fireball History - LOX/LH2 - Initial Growth.
Contact Area = 36.81 ft2 (Test No. 6).
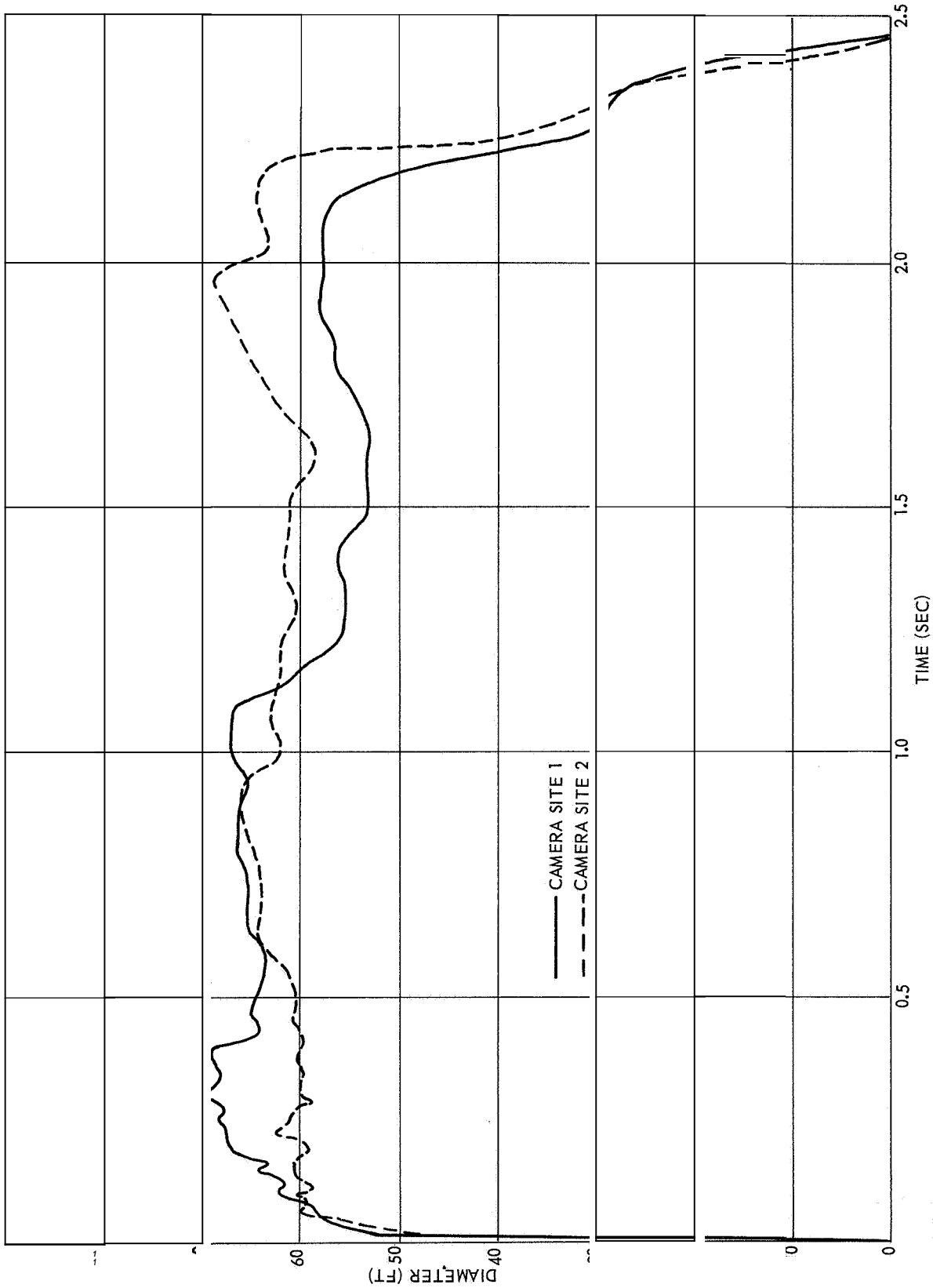
Figure 28b. Fireball History - LOX/LH$_2$ - Diameter
Contact Area = 36.81 ft2 (Test No. 6).
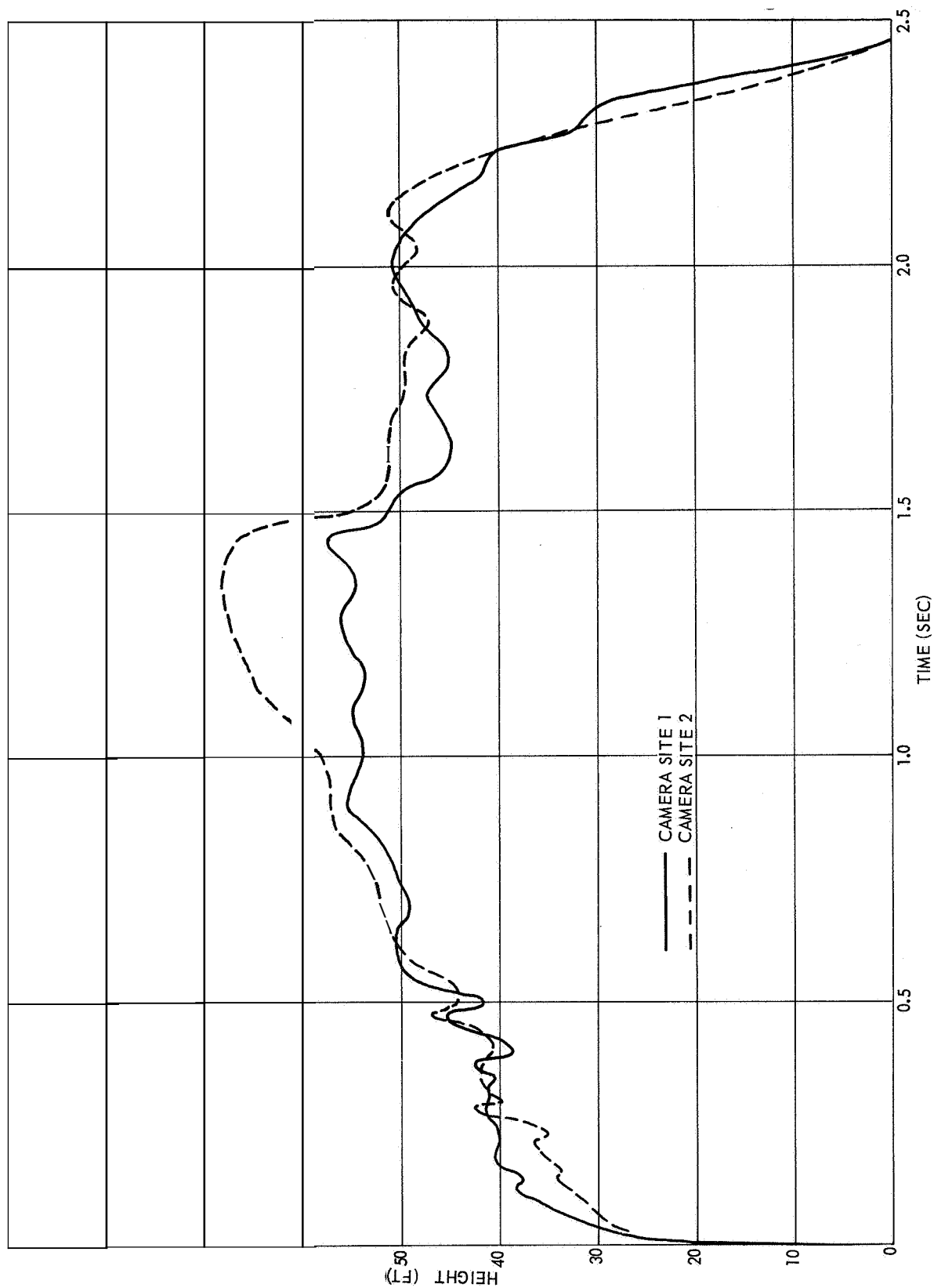
Figure 28c. Fireball History - LOX/LH$_2$ - Height.
Contact Area = 36. 81 ft2 (Test No. 6).
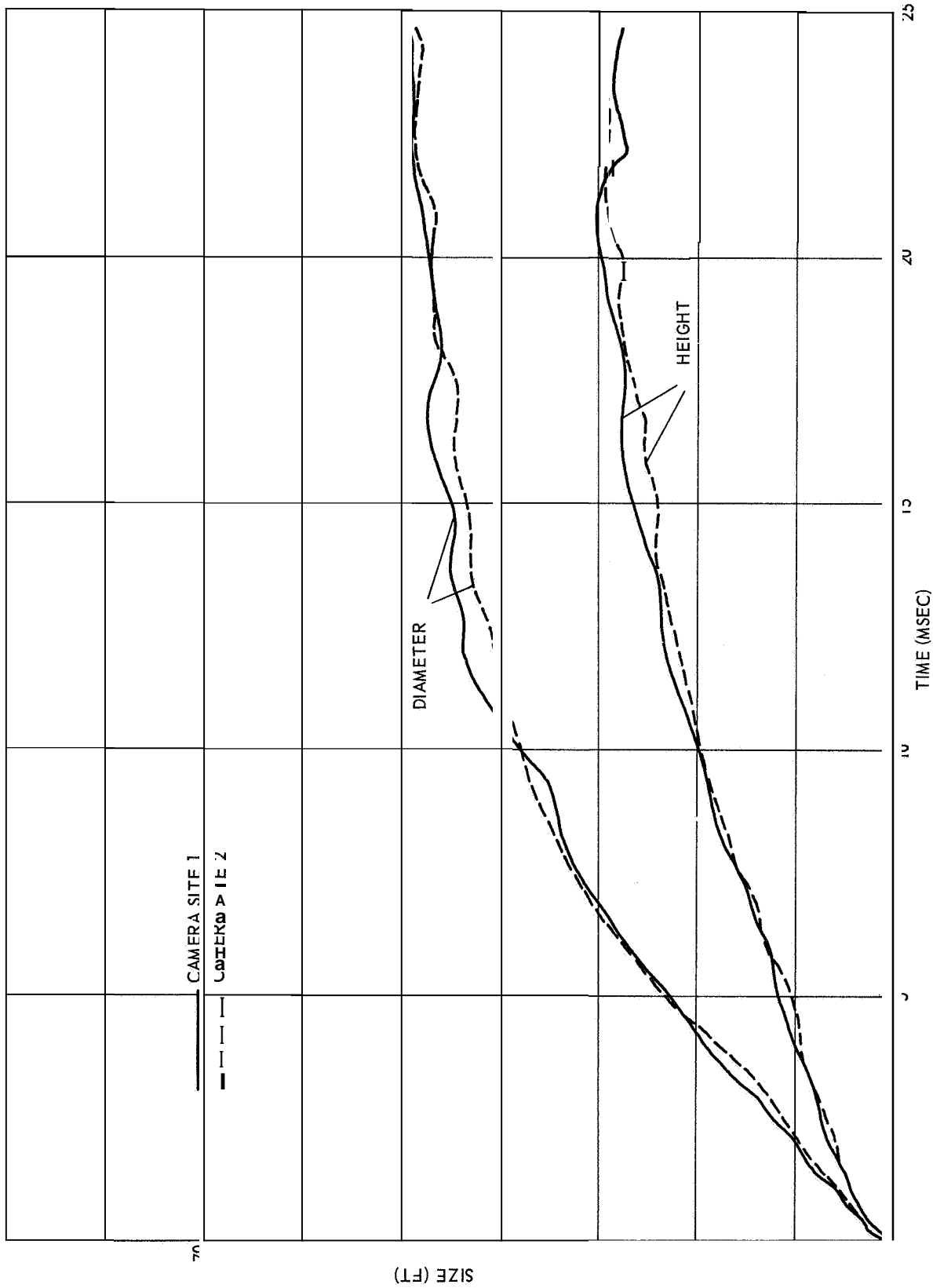
2B28-28-1

Figure 29a. Fireball History - LOX/RP-1 - Initial Growth.
Contact Area = 36.81 ft^2 (Test No. 8).
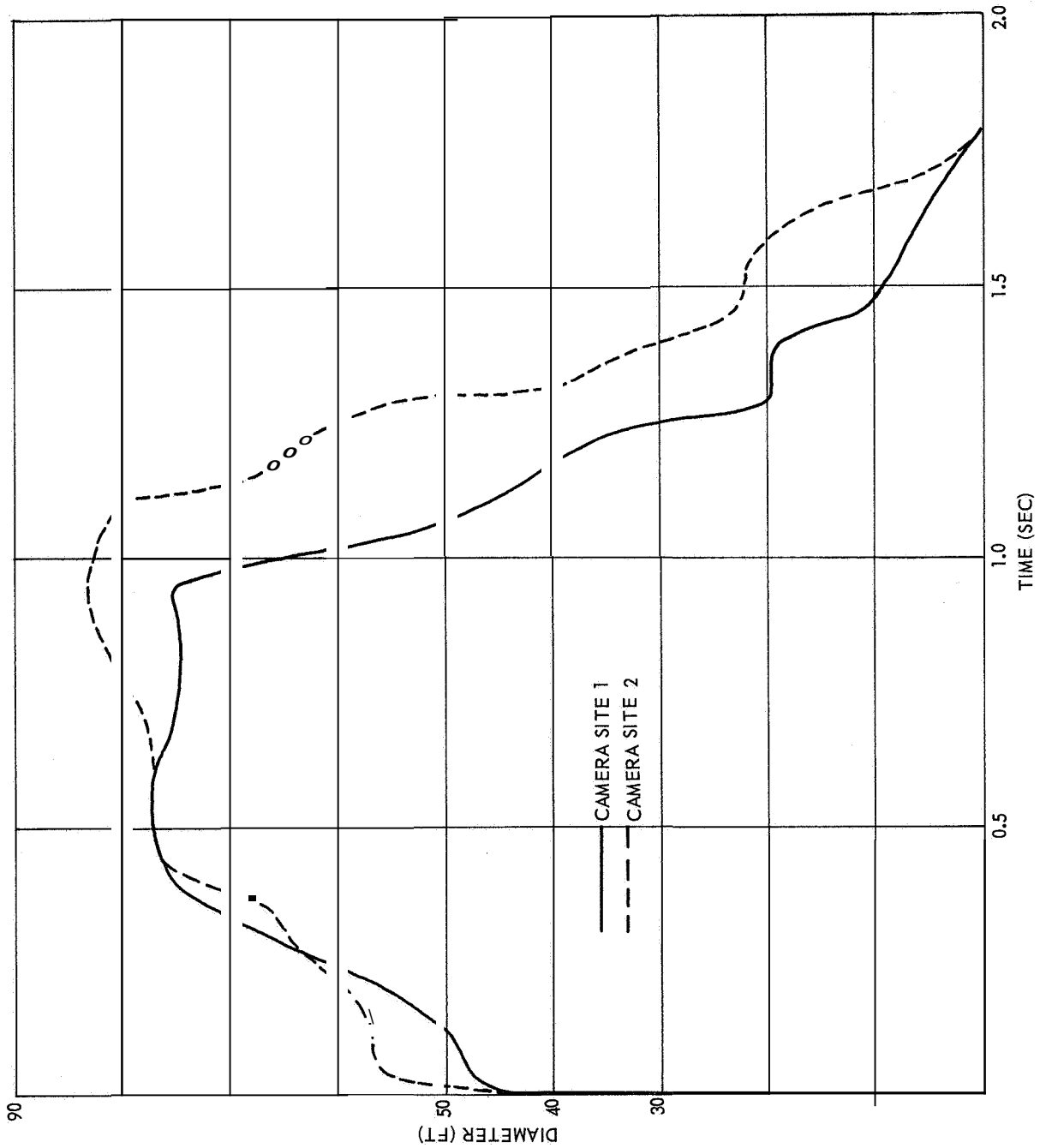
Figure 29b. Fireball History - LOX/RP-1 - Diameter
Contact Area = 36.81 ft² (Test No. 8).

Figure 29c. Fireball History - LOX/RP-1 - Height.
Contact Area = 36. 81 ft^2 (Test No. 8).

2828-29-1
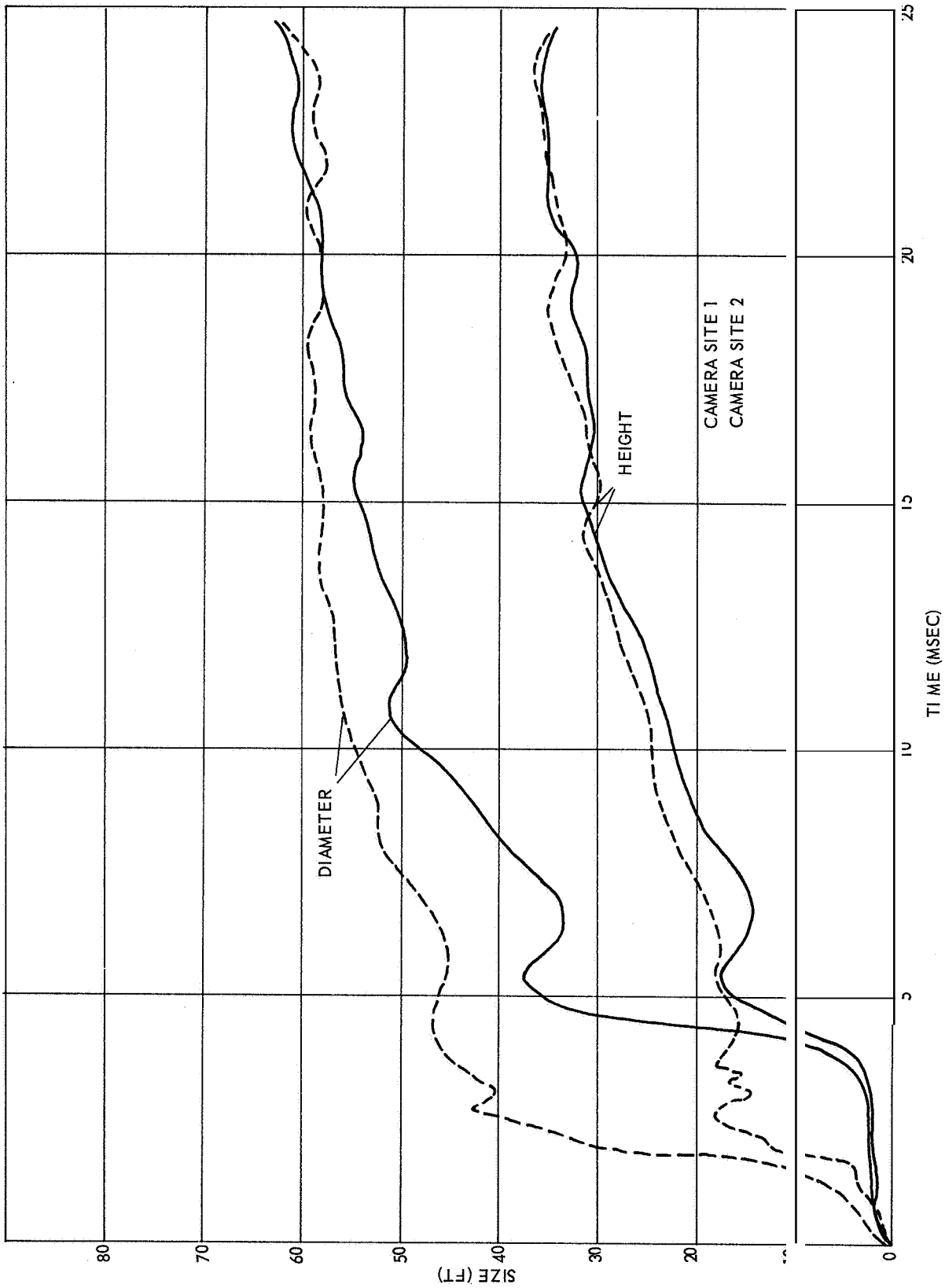
Figure 30a. Fireball History – LOX/RP-1 – Initial Growth.
Contact Area = 36.81 ft2 (Test No. 10).
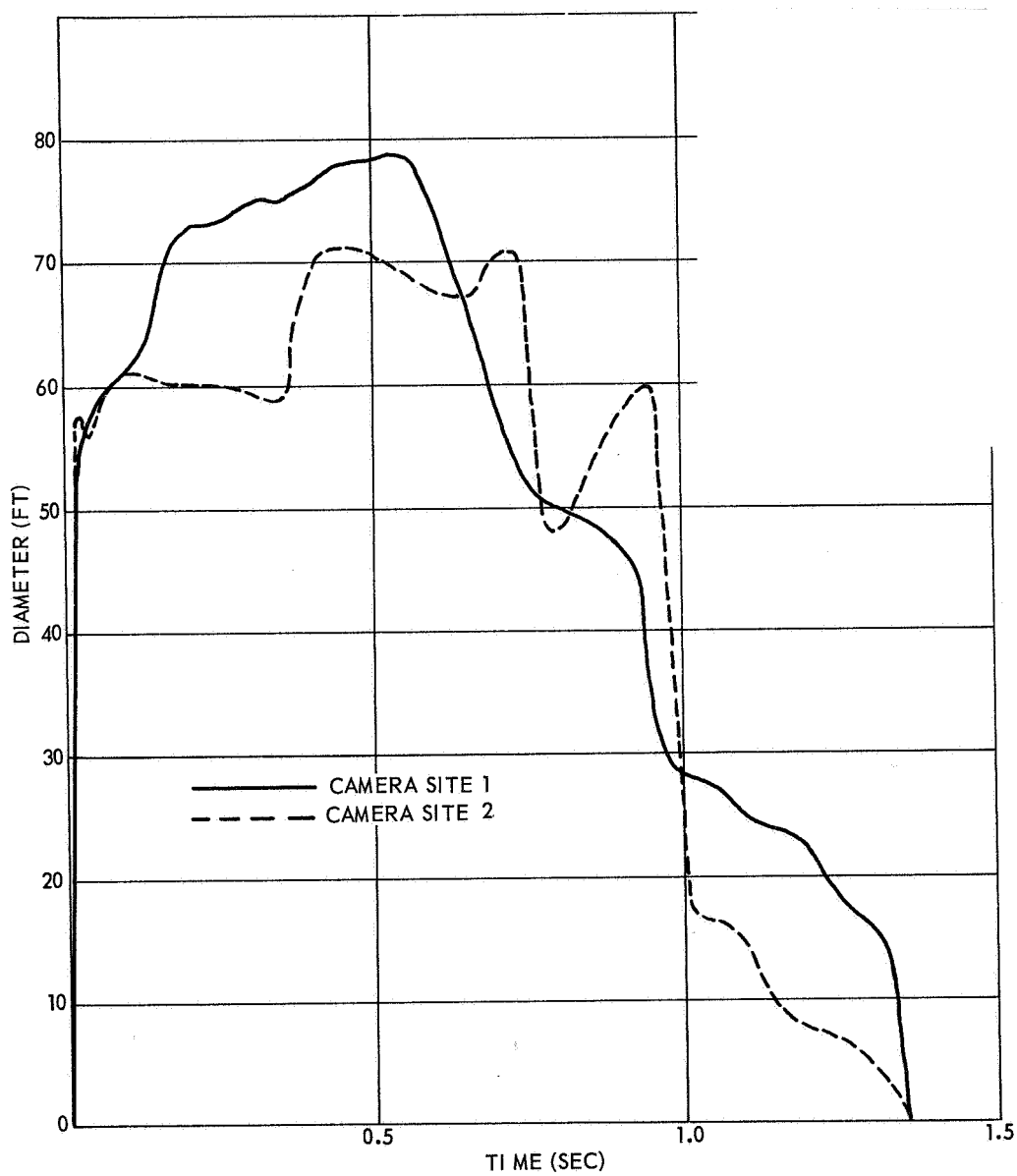
Figure 30b. Fireball History – LOX/RP-1 – Diameter. Contact Area = 36.81 ft² (Test No. 10).
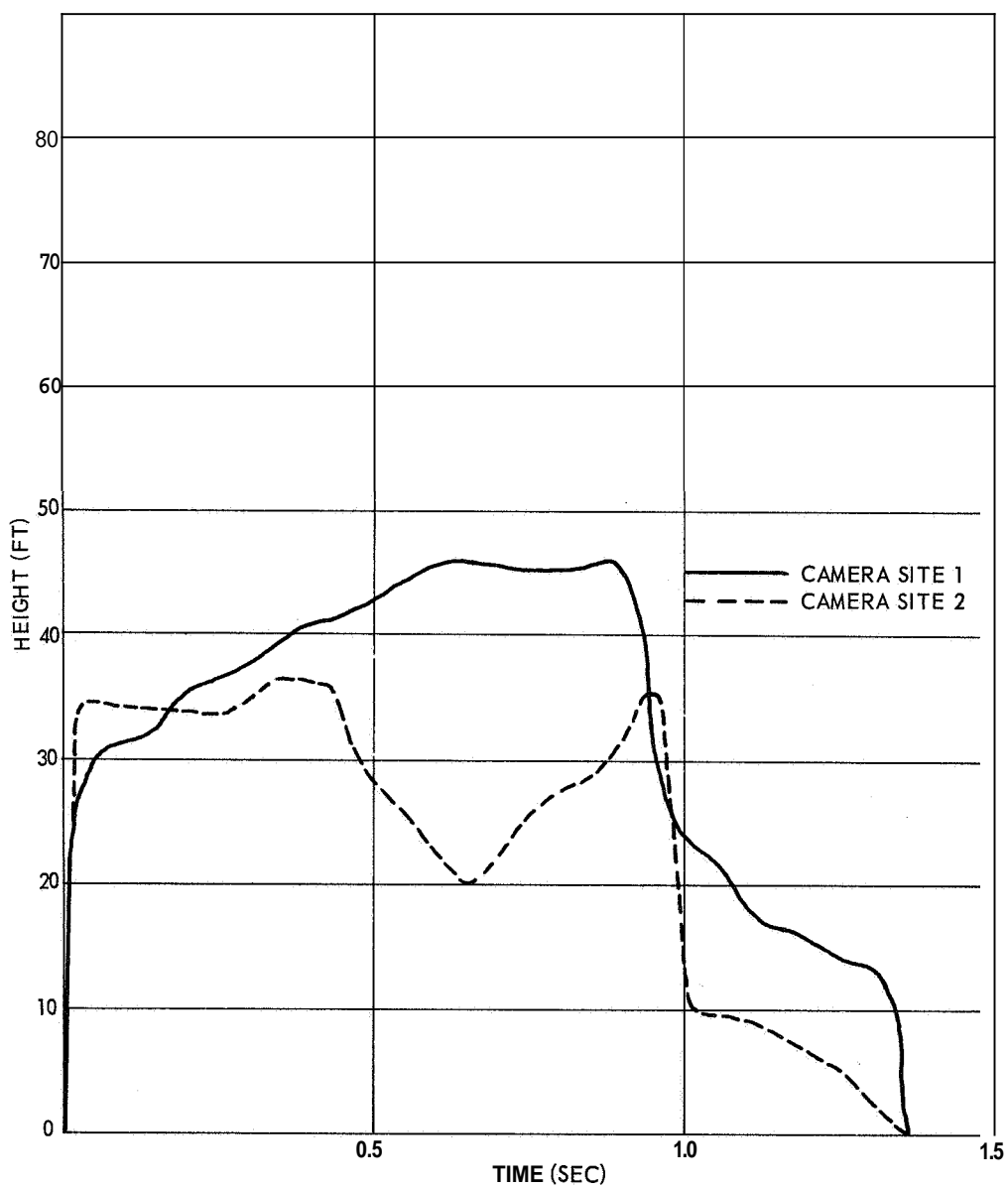
2828-30-1

Figure 30c. Fireball History - LOX/RP-1 - Height. Contact Area = 36.81 ft^2 (Test No. 10).

2828-30-1
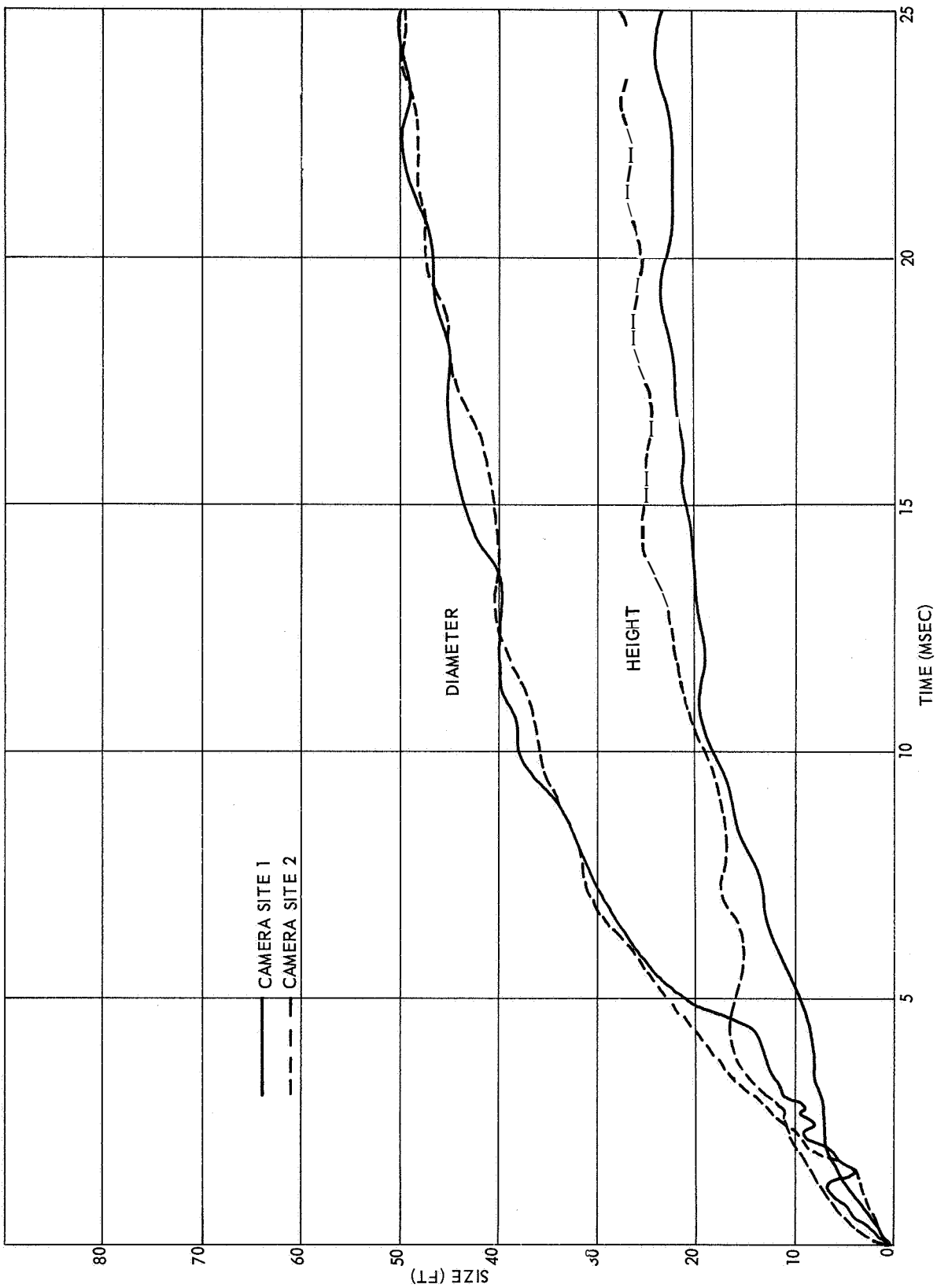
Figure 31a. Fireball History - N_2O_4/A-50 - Initial Growth. Contact Area = 36.81 ft2 (Test No. 9).
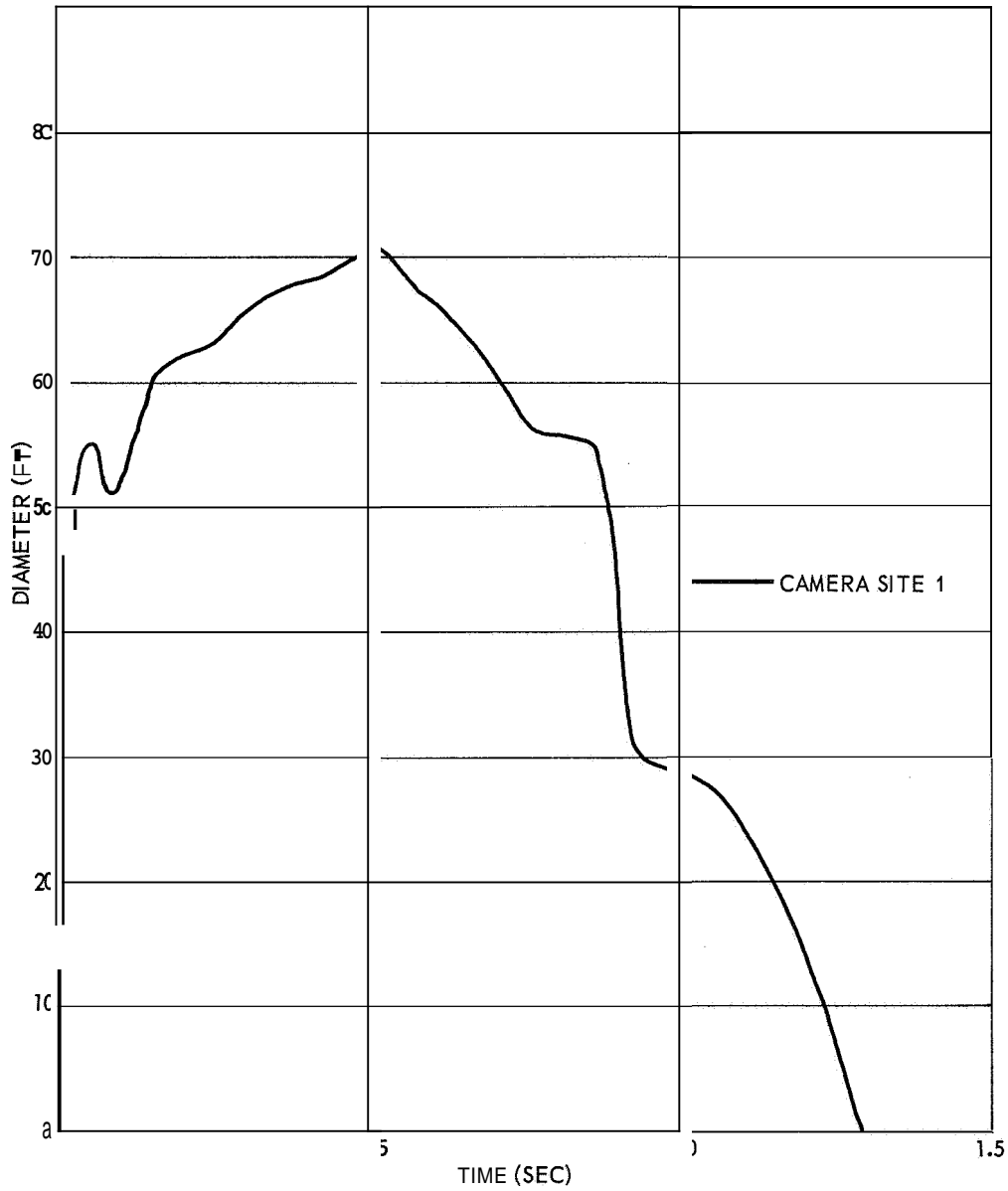
2828-31-1

Figure 31b. Fireball History – N_2O_4/A -50 – Diameter. Contact Area = 36.81 ft² (Test No. 9).
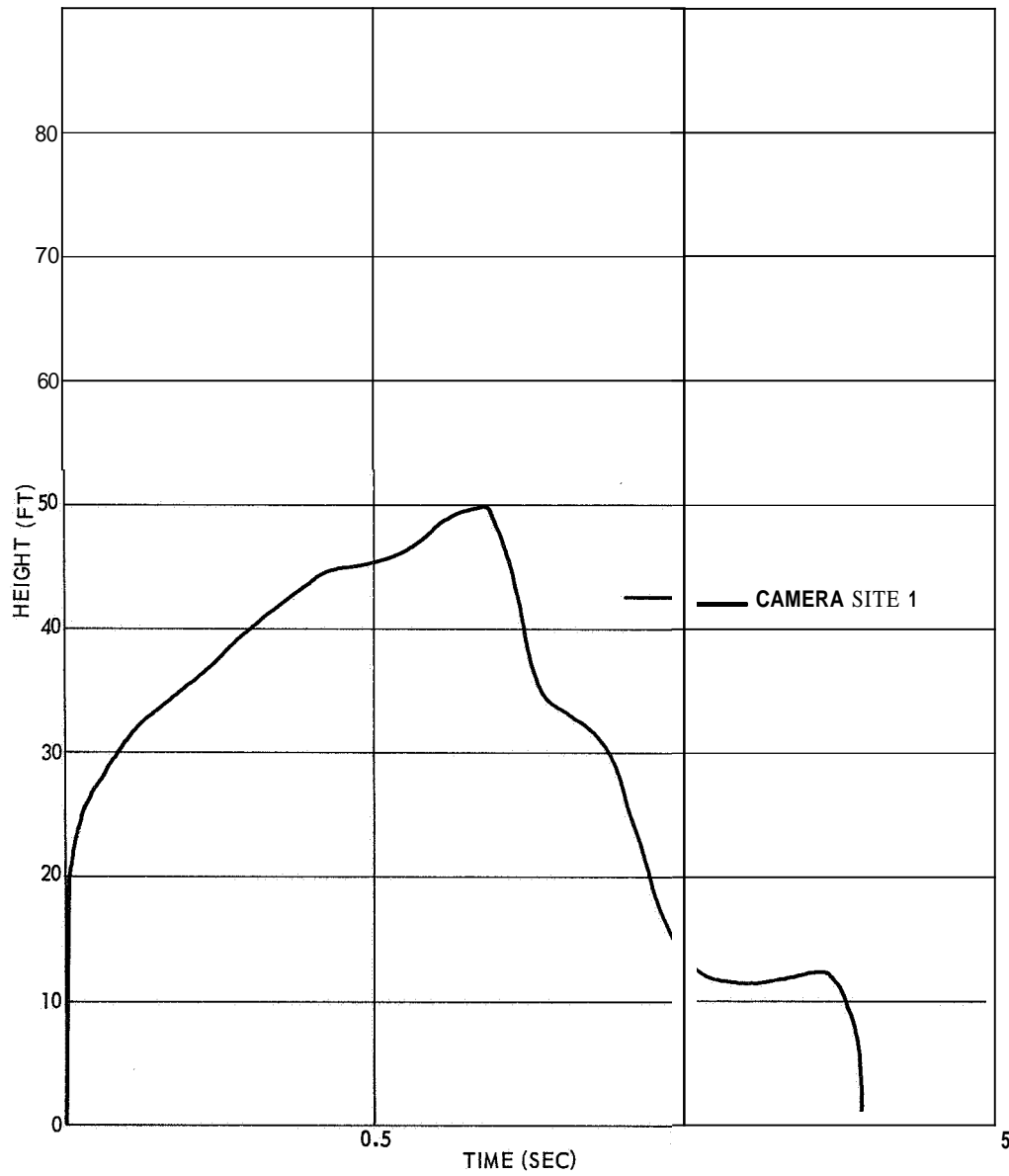
2828-31-1

Figure 31c. Fireball History – N_2O_4/A-50 – Height
Contact Area = 36.81 ft^2 (Test No. 9).

2828-31-31

Preliminary comparison of the initial LOX/LH_2 fireball growth rate data summarized in Figure 32 indicated that the greater the contact area, the faster the fireball propagation rate, except for the fireball height measurements for Test 6 which was side-initiated instead of bottom-initiated as in other tests. The curves shown in Figure 32 were plotted from the means of the camera data shown in Figures 23 through 28. Further analysis of the growth rate data by applying the cube root scaling law indicated that the scaled fireball propagation rate tends to be a constant value. Results of the scaling law analysis are shown in Figure 33 in the form of size (diameter and height)/weight (1/3) vs time. It is apparent from the scaling curve (Figure 33) that the variation of propellant quantities does not appreciably change the growth rate for the specified test conditions of a constant ratio of the contact area to the propellant weight.

Evaluation of the reduced fireball size data (Figure 33) for the LOX/LH_2 tests inidcated a growth rate of 0.92 ft/msec per $lb^{1/3}$ of propellant during the first 5 msec of diameter growth, 0.51 ft/msec per $lb^{1/3}$ of propellant during the second 5 msec, and appoximately 0.31 and 0.18 ft/msec per $lb^{1/3}$ of propellant for the third and fourth 5-msec periods. Similar analysis of the LOX/LH_2 fireball height data indicated growth rates of approximately 0.46, 0.28, 0.20, and 0.14 ft/msec per $lb^{1/3}$ of propellant for the first, second, third, and fourth 5-msec growth periods. No definite initial fireball growth rate analysis was made for the LOX/RP-1 and N_2O_4/A-50 tests due to limited amount of data available.

Observation of the initial fireball size data indicated the fireball diameter measurements were consistently larger than the fireball height measurements. This phenomenon was attributed to the configuration of the dewar pans; i.e., the pan had a greater width (24 to 44 in.) than height (16 in.).

A typical LOX/LH_2 propellant fireball sequence is shown in Figure 34. Examination of the sequence will show the growth of the hemispherical fireball which eventually rises from the ground before terminating.
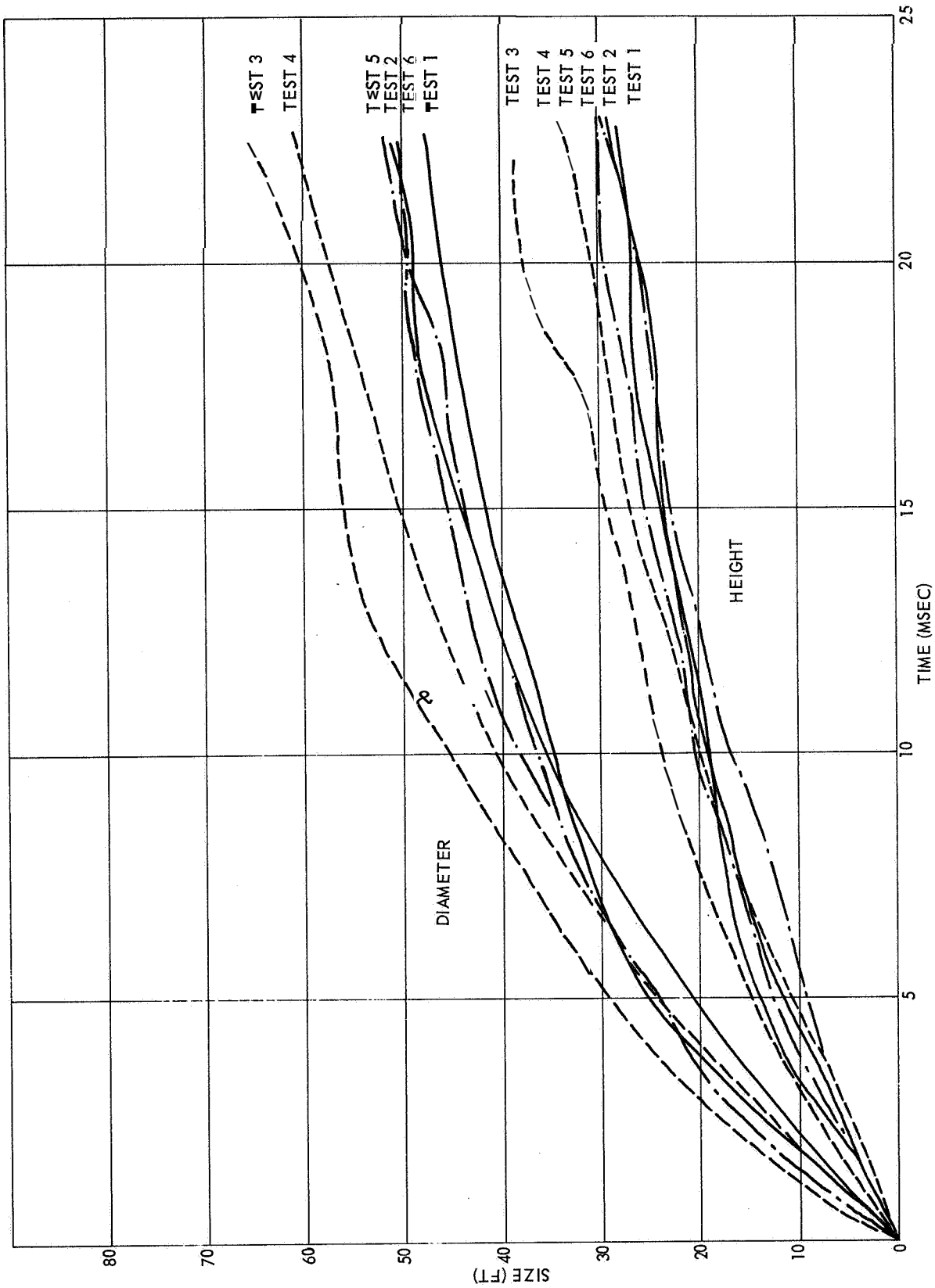
Figure 32. Summary of Fireball History Data for LOX/LH$_2$ Propellant.

2828-32-1

FIREBALL DIAMETER/W$^{1/3}$)
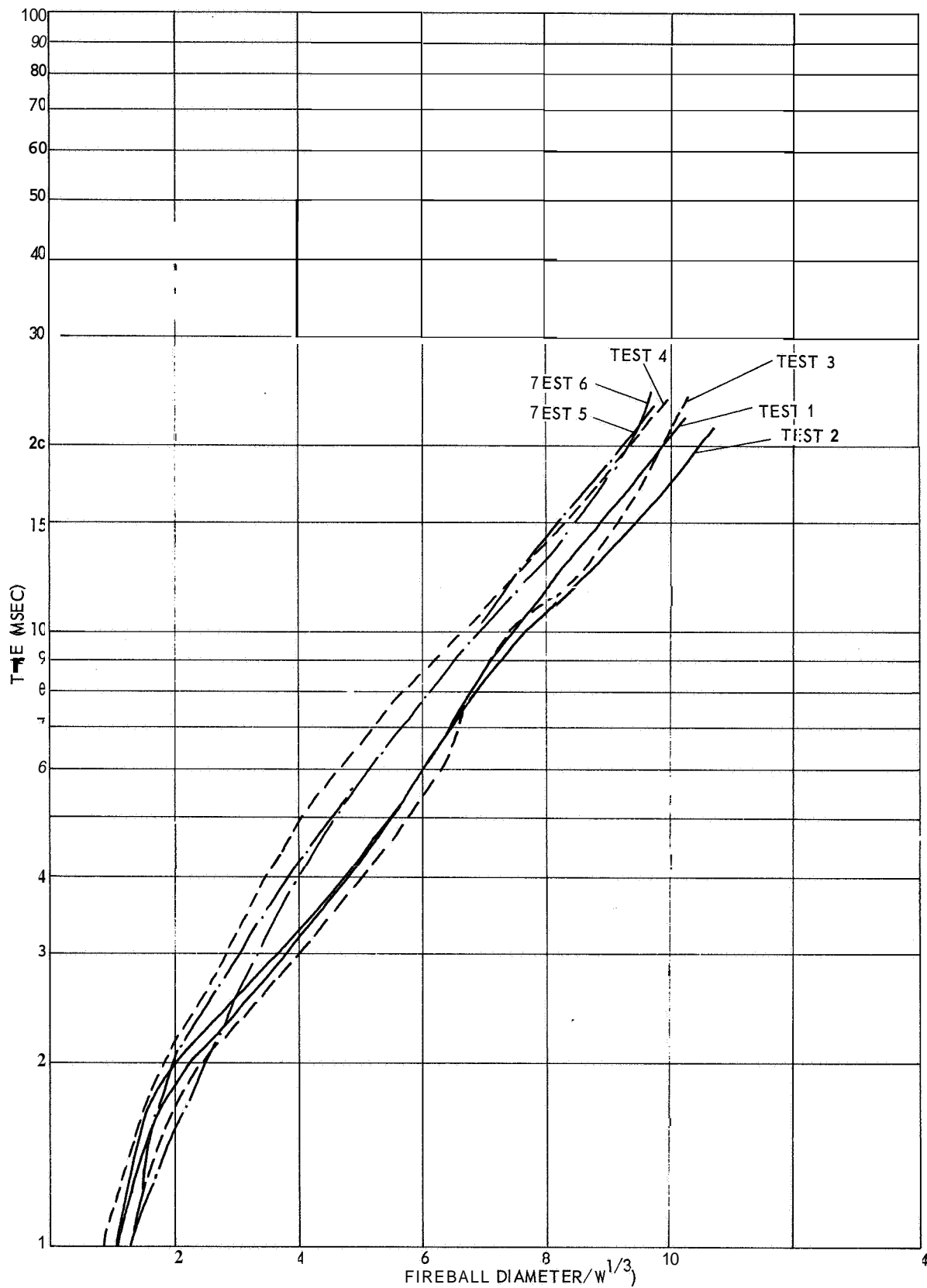
2828-33-1

Figure **33a.** Reduced Fireball History - Diameter.
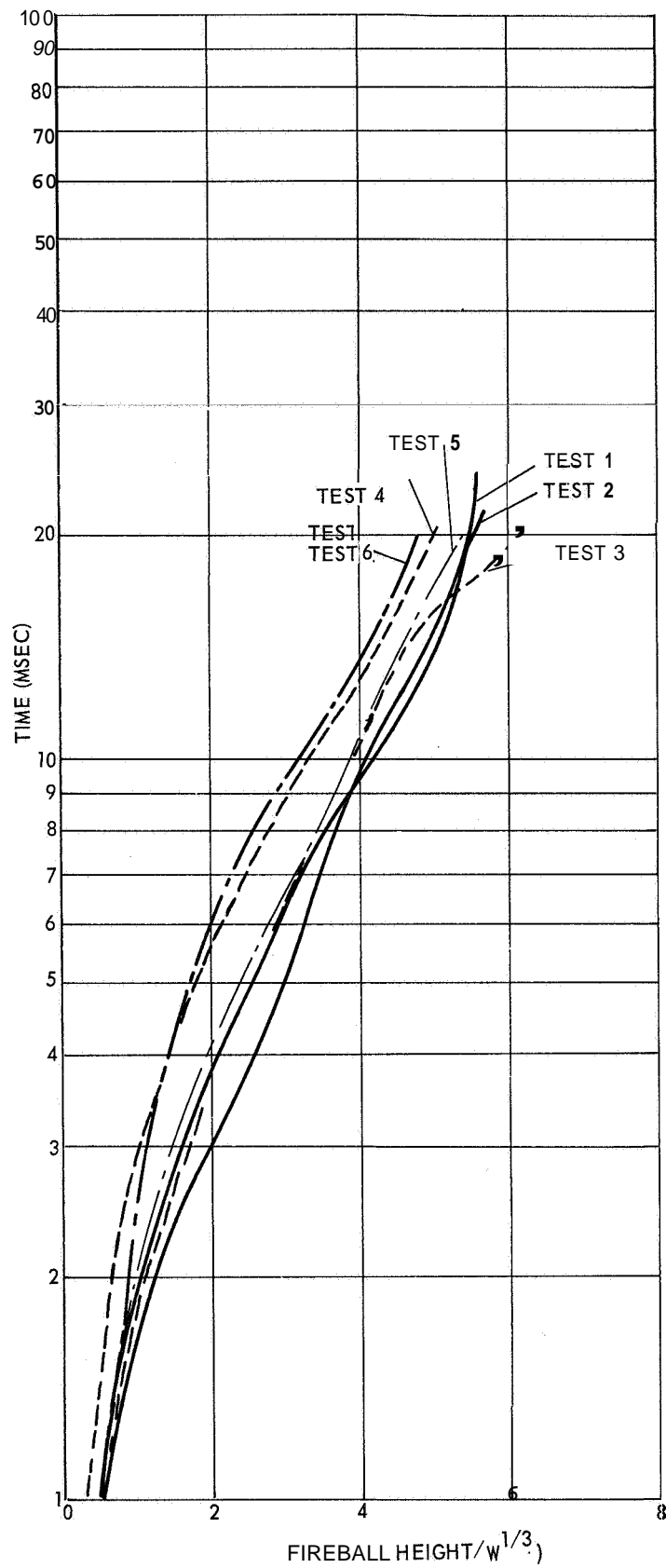
Figure 33b. Reduced Fireball History - Height.
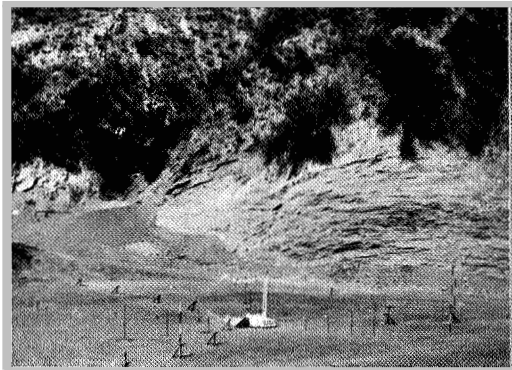
Still
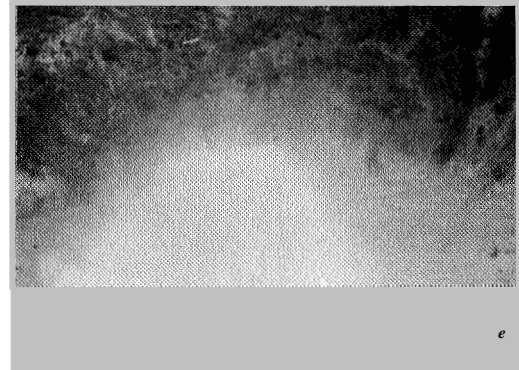
0.3 Seconds
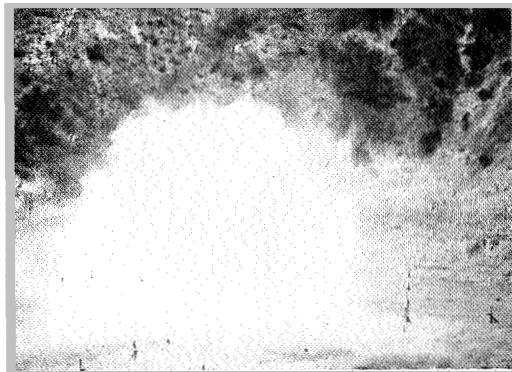
0.6 Seconds
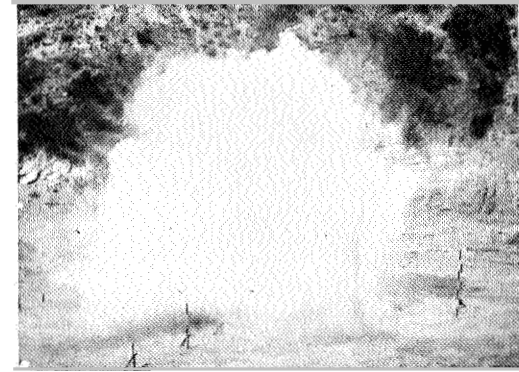
0.9 Seconds
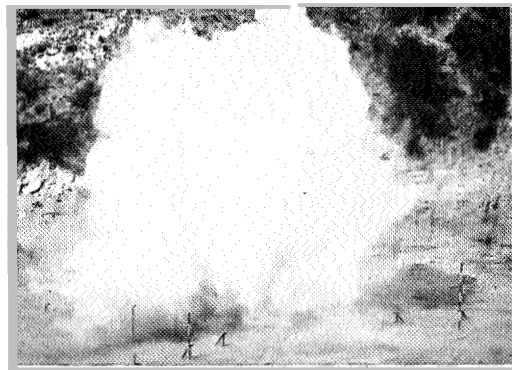
1.2 Seconds

1.5 Seconds
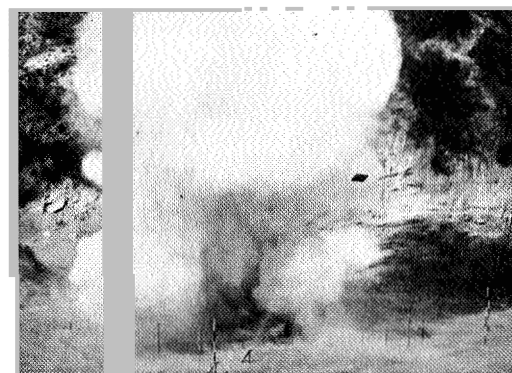
1.8 Seconds
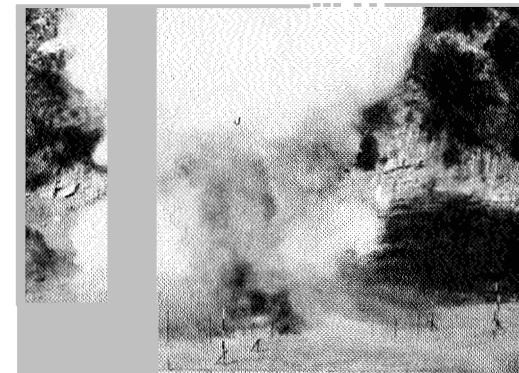
2.1 Seconds

Figure **34.** Fireball Growth.

2829-34-1

4.6. 5   Blast Results

Examination of the peak overpressure data for the LOX/LH_2 tests
(Table 5, Figures 13, 14, and 15) indicated TNT equivalences which
ranged from 0. 18 lb to 0. 5 lb of TNT per lb of propellant at the
25-ft gage stations to 0. 3 lb to 0. 8 lb of TNT per lb of propellant at the
80-ft gage stations.   The positive impulse data for the same propellants
(Figures 18, 19, and 20) indicated TNT equivalences which ranged from
a low of 0. 35 lb to a high of 0. 8 lb of TNT per lb of propellant at the
25-ft gage stations to 0. 5 lb to 1. 0 of TNT per lb of propellant at the 40,
60, and 80 ft stations.   As indicated previously in this report, all
LOX/LH_2 propellant tests utilized a 1:4 contact area to propellant
weight ratio.   Previous studies (Reference 9) indicated that a decrease
in the contact area with the same total propellant weight yielded cor-
respondingly lower TNT equivalences.   Therefore, the equivalences
indicated apply only to the specific test conditions involved in this series
of tests.

Direct comparison of the test data for the LOX/LH_2 propellant combina-
tions was impeded by the variation in total weight of propellants involved
in each test.   To clarify the analysis of the test results, both the peak
overpressure and impulse data were modified with the cube root scaling
law by dividing both sets of data by the cube root of the propellant weight.
Results of these computations are plotted in Figures 35 and 36 on a peak
overpressure vs reduced distance, $X(ft/W^{1/3})$, or range, basis for the
overpressure data and a reduced impulse $(I/W^{1/3})$ vs range basis for the
impulse data.   These two curves illustrate the change in LOX/LH_2 pro-
pellant TNT equivalences in relationship to distance from the test event.
The overpressure equivalences (Figure 35) increased as the range, X ,
increased to a value of 0.9 lb of TNT per lb of propellant at a range value
of 20.   The impulse data (Figure 36) indicated different results.   The im-
pulse equivalence for the LOX/LH_2 propellant tests increased from small
values of the range to a maximum of 0.90 lb of TNT per lb of propellant at
a range of 9 to 10 and then decreased with further increases in X.

Comparison of the composite overpressure curves for the three propellants
at the 80-ft gage stations indicated TNT equivalences of 0. 6 to 0. 8 lb of
TNT per lb of propellant for LOX/RP-1 propellant, 0.42 lb of TNT per
lb of propellant for N_2O_4/A-50 propellant and 0.6 to 0. 8 lb of TNT per lb
of propellant for the LOX/LH_2 tests.   A similar comparison of the
impulse data indicated equivalences of 0. 8 to 1.05 lb of TNT per lb
of propellant for LOX/RP-1 tests, 0.8 to 0. 9 lb of TNT per lb of
propellant for the LOX/LH_2 tests, and 0. 52 lb of TNT per lb   of pro-
pellant for the N_2O_4/A-50 tests.   Both the TNT overpressure and impulse
equivalences as stated above are for contact area to propellant weight ratios
of 1:4. 54 and 1:6. 25 for the LOX/RP-1 and N_2O_4/A-50 propellants
respectively.
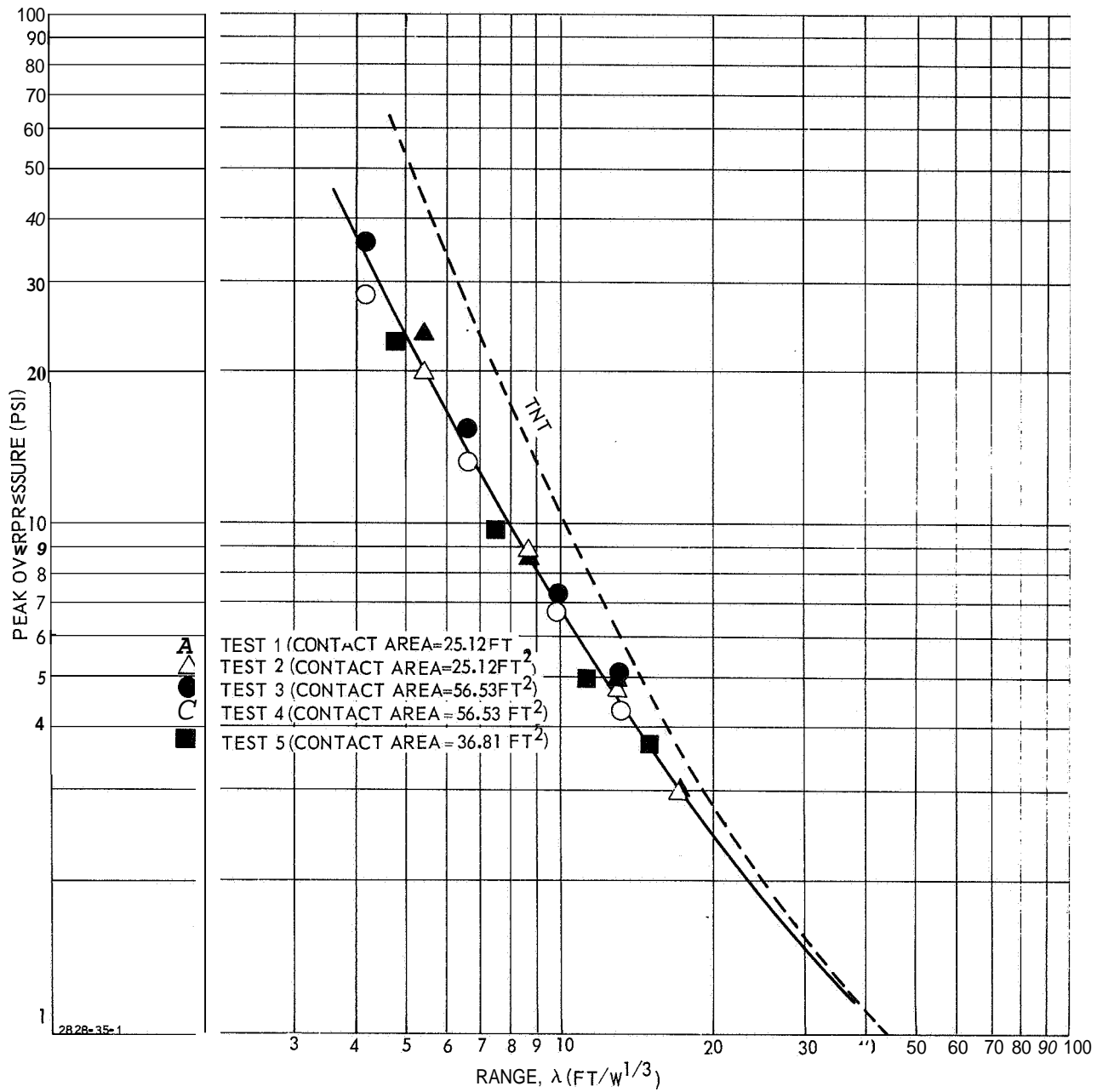
Figure 35. Peak Overpressure vs Scaled Distance for Liquid
Hydrogen/Liquid Oxygen.
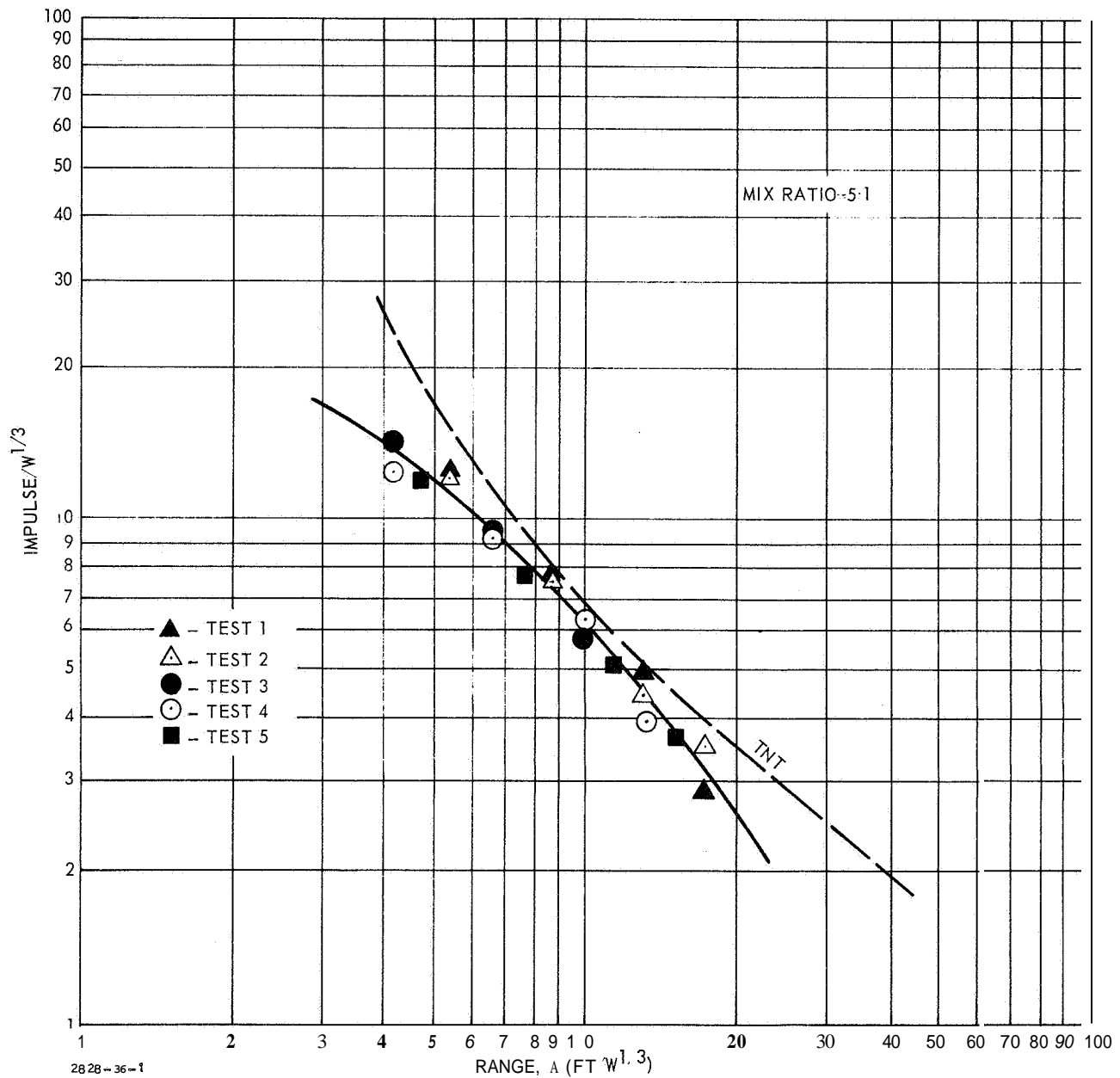
Figure 36.   Positive Impulse vs Scaled Distance **for** Liquid Oxygen/
Liquid Hydrogen.

Analysis of the second 150 lb LOX/LH_2 (Test 6) test data indicated low blast yields for both the overpressure and impulse measurements. Examination of the test records indicated the dewars were shattered by a safety destruction charge placed on the side of the dewar pan. This charge was programed to fire 0.1 sec after the explosive charge on the pan bottom in case of a malfunction in the primary firing system. Data from this test was not used in the compilation of the LOX/LH_2 composite curves due to the questionable contact area and mixing process of the two propellants.

A similar cube root law analysis was applied to the $LOX/RP-1$ and $N_2O_4/A-50$ data; i.e., the data was reduced to a one lb equivalent basis for direct comparison of the overpressure and impulse measurements with the LOX/LH_2 measurements. Results of these compilations are shown in Figures 37 and 38.

Least-squares analysis of the test results indicated the LOX/LH_2, $LOX/RP-1$ and $N_2O_4/A-50$ curves shown in Figures 35 through 38 were best represented by an equation of the type,

$$y = A_0 t A_1 \ln \lambda + A_2 (\ln\lambda)^2$$

where

$$y = \text{peak overpressure or impulse}/W^{1/3}$$

$$\lambda = \text{distance}/W^{1/3}$$

Results of the computations for each propellant type and condition are shown in Table 6 for the three equation coefficients A_0, A_1, and A_2. A measure of the relative accuracy of the equations is included in Table 6 as the average percent error in terms of the logarithmic pressure or logarithmic impulse scales. Use of the empirical equations or the composite curves (Figures 35 through 38) for small (<100 lb) or large (>230 lb) quantities of propellants should be applied with caution and consideration for the quantities and contact area of the propellants involved.

The results of the shock wave velocity measurements and the calculated overpressure are presented in Table 7. The calculated shock pressures are slightly higher than the measured shock pressures because the calculated shock velocities are average determinations over a known distance and the shock wave velocity does not attenuate at a linear rate, but rather at some exponential function depending on the distance from the event.

The meteorological conditions for the various test conditions are shown in Table 8.
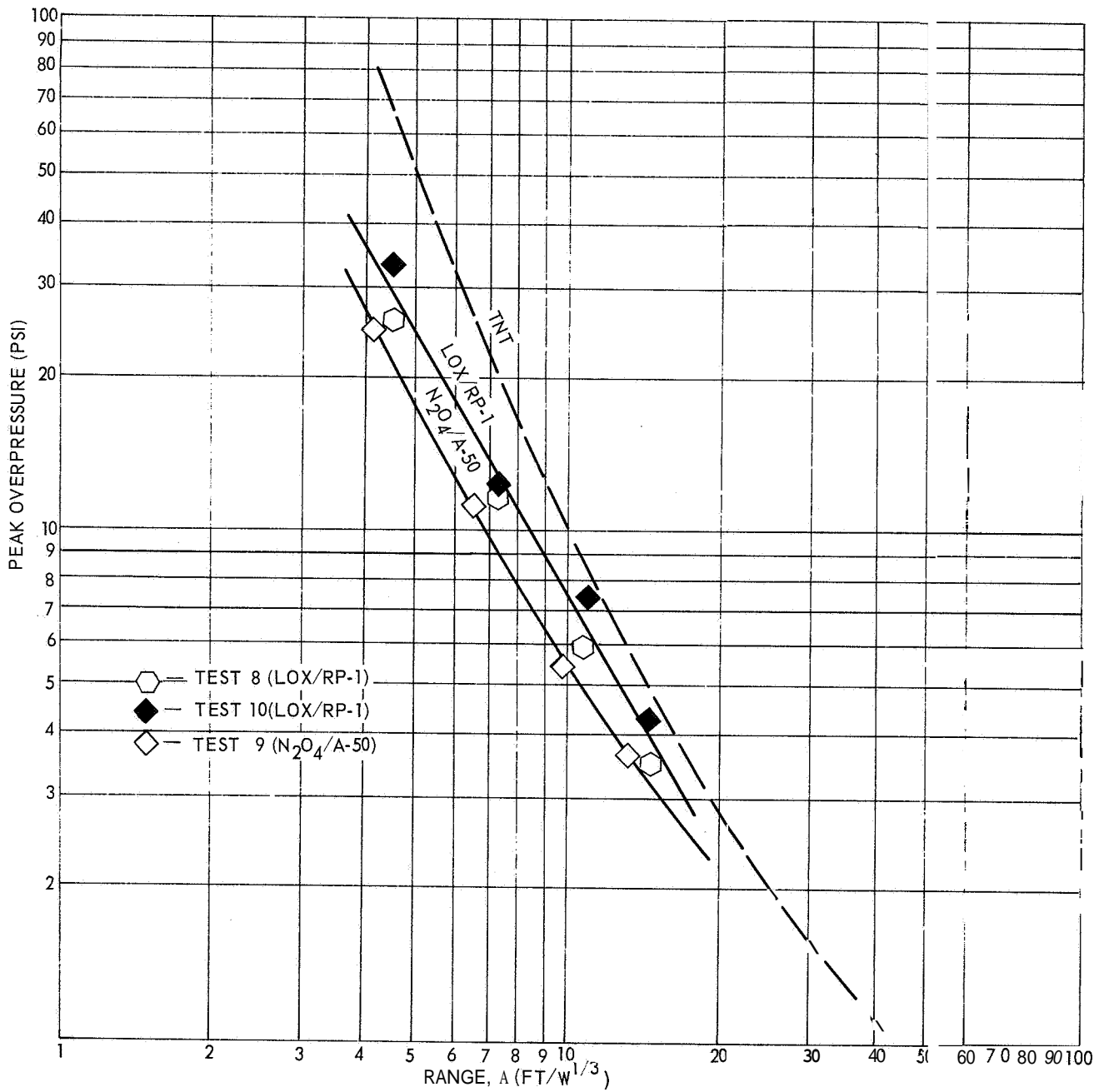
Figure **37.** Peak Overpressure vs Scaled Distance for
LOX/RP-1 and N_2O_4/A-50.
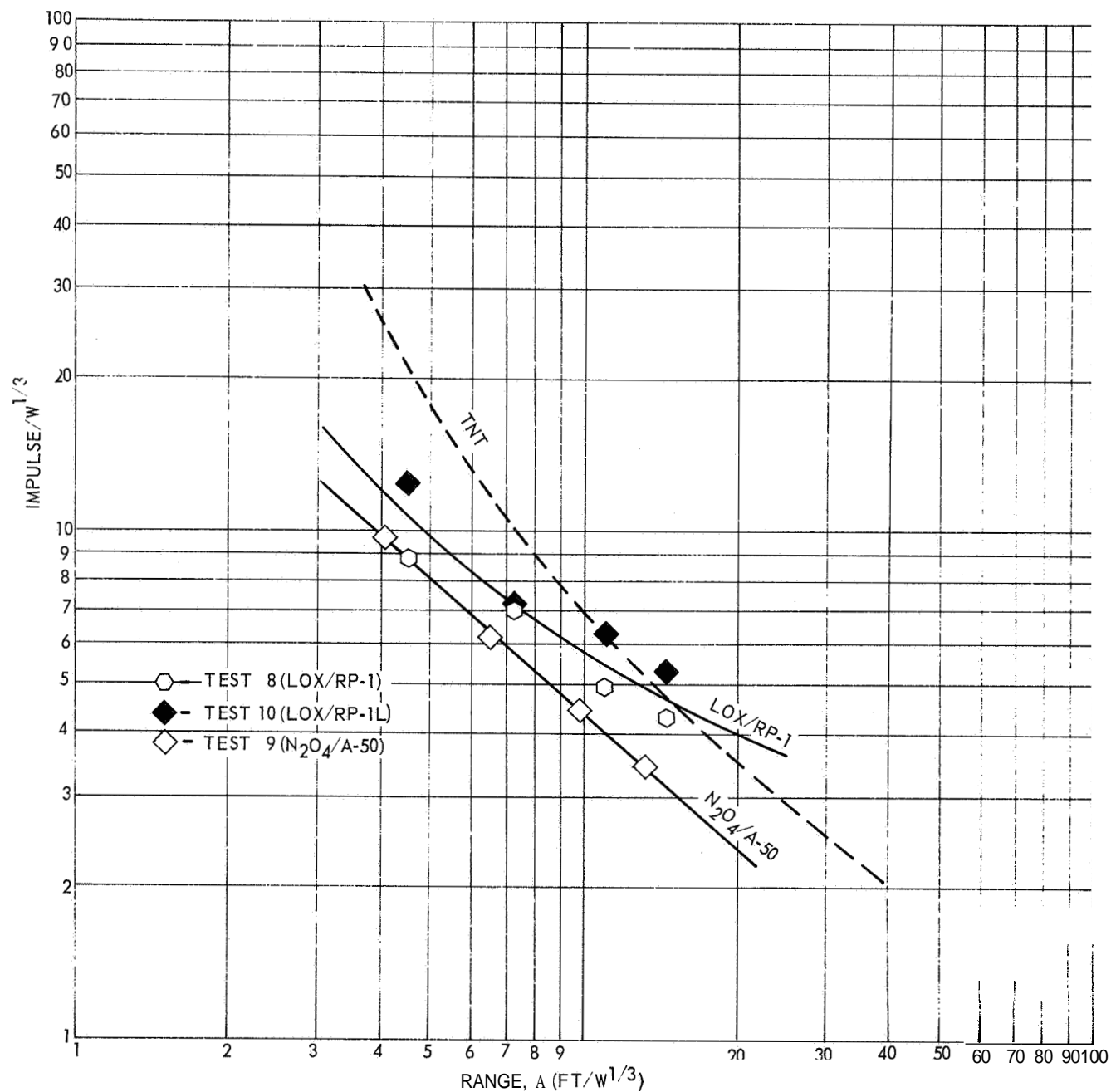
Figure **38.** Positive Impulse vs Scaled Distance **for**
LOX/RP-1 and N_2O_4/A-50.

5.   CONCLUSIONS

Rased on the results of the experimental studies conducted on this program the following conclusions are made.

5.1   BLAST YIELD

A comparison of the explosive yields of the three propellants on an overpressure basis utilizing the TNT calibration data (Figure 11) as reference indicated TNT equivalences of 0. 6 to 0. 8 lb of TNT per lb of propellant for LOX/LH_2 propellant, 0.42 lb of TNT per lb of N_2O_4/A-50 propellant and 0.6 to 0. 8 lb of TNT per lb of LOX/RP-1 propellant.   A similar comparison of the propellants on an impulse basis utilizing the TNT calibration data (Figure 12) **as** reference indicated 0. 8 to 0. 9 lb of TNT per lb of LOX/LH_2 propellant, 0. 8 to 1. 05 lb of TNT per lb of LOX/RP-1 propellant and 0. 52 lb of TNT per lb of N_2O_4/A-50 propellant.

The explosive yield of both the cryogenic and hypergolic propellants varied with distance from the event.   The variation was attributed to the basic characteristic of the shock wave produced by the propellants. The overpressure TNT-equivalences for the three types of propellant increased with increased distance from the propellant reaction within the limits of the program.   The impulse TNT-equivalences for the LOX/LH_2 increased with increased distance from the event to a distance of approximately 60 ft.   Beyond this distance the impulse TNT-equivalences decreased with further increases in distance within the limits of the test data.   The LOX/RP-1 and N_2O_4/A-50 impulse TNT-equivalences increased with increased distance from the test fixture within the limits of the measurements.   The TNT-equivalences of the LOX/LH_2 propellant were not affected by the weight of propellant within the range of 100 to 225 lb at a mixture ratio of 5:1.

5.2   FIREBALL SIZE AND DURATION

The fireballs produced by the three propellants indicated a correlation between the fireball duration and blast yield for most tests.   Analysis indicated the longer the fireball duration the lower the air blast yield.

The maximum fireball diameter for the various weight samples varied from 64 to 91 ft and the maximum height ranged from 38. 5 to 73 ft.   The fireball durations varied from 1.28 to 2.45 sec.

A similar initial fireball growth rate was observed for LOX/LH_2 pro-
pellant on a per $lb^{1/3}$ of propellant basis for the various test conditions.
Analysis of the initial fireball growth rate on a total propellant weight
basis indicated the larger the quantity of propellant, the greater the initial
growth rate for a constant ratio of contact area to propellant weight.
Initial growth rates of 0.92 and 0.46 ft/msec per $lb^{1/3}$ of propellant were
observed for the fireball diameter and height. The fireball growth rate,
was observed to attenuate to a growth rate of 0.18 and 0.14 ft/msec per
$lb^{1/3}$ of propellant for the diameter and height, respectively, after
approximately 15 msec. Observation of the fireball size vs time data
indicated that the majority of the growth occurred within 20 msec after
the initiation of the propellant reactions.

The fireball diameter and height were influenced by the dewar pan con-
figuration; i.e., the flat pan (height = 16 in., width = 24 to 44 in.)
produced a fireball with a greater diameter than width by a factor of
approximately 2 to 1.

Examination of the fireball film data indicated that the initial fragment
velocity was less than the initial shock wave velocity and initial growth
rate of the propellant fireballs. In all cases the pan and the controlled
fragments appeared and traveled beyond the edge of the fireball some
time after the initial fireball growth period.

REFERENCES

1.   Summary Report on a Study of the Blast Effect of a Saturn Vehicle,
      A. D. Little, Inc., Report C63850, Contract NAS 8-523, February
      1962 (Confidential).

2.   Titan II - Dyna-Soar Destruct Test and Analysis Report, Martin-
      Marietta Corporation, Report ER12269, Contract AF04(695)-54,
      15 March 1962.

3.   Research on Hazard Classification of New Liquid Rocket Propellants,
      Rocketdyne, a Division of North American Aviation, Inc., Final
      Report AF/SSD-TR-61-40, Volume II Contract AF33(616)-6939,
      October 1961.

4.   Storable Propellant Data for the Titan II Program, Bell Aerosystems
      Company, Report 8182-933001, AFBMD TR-61-55, Contract
      AF04(647)-846, July 1961.

5.   Storable Propellant Data for the Titan II Program, Bell Aerosystems
      Company, Report 8182-933002, AFBSD TR-61-35, Contract AF04(694)-
      72, November 1961.

6.   Final Report on An Investigation of Hazards Associated With the Storage
      of Liquid Hydrogen in Close Proximity to Liquid Oxygen and RP-1,
      A. D. Little, Inc., Report No. 61092, Contract No. AF18(600)-1687,
      July 1960 (Confidential).

7.   Explosive Potential of Atlas Propellants, Broadview Research Corp. ,
      Final Report No. MSD-6-483, June 1957.

8.   Final Report on An Investigation of Hazards Associated With the Storage
      and Handling of Liquid Hydrogen, A. D. Little, Inc., Report No. C-
      61092, Contract AF18(600)-1687, March 1960 (Confidential).

9.   Blast and Fireball Comparison of Cryogenic and Hypergolic Propellants,
      Aerojet-General Corp. , Final Report No. 0822-01(01)FP,
      Contract NAS 9-2055, June 1964.

REFERENCES   (Cont)

10.   Kalavski, P. A. , A High-speed Recording System Using the Velocity
       ,Method to Determine the Peak Pressure Produced in Air by
       Explosives, U. S. Naval Ordnance Laboratory, NAVORD Report 2167.

11.   Klein, V. W., C. E. Moeller, and E. T. Fago,   Determination of
       Transient Temperature During the Expansion of Fireballs, Midwest
       Research Institute, Final Report, MRI Project No. 2885-E, Contract
       No, NAS 9-4448, 25 May 1965 to 1 March 1966.

12.   Kingery, C. , and B. Pannil, Peak Overpressure vs Scaled Distance,
       BRL Memo Report 1518, April 1964.

13.   Operation Snow Ball Project Descriptions, Volume 1, DASA Data
       Center Special Report 24-1, DASA 1516-1.

APPENDIX A

BALLISTIC RESEARCH LABORATORY BLAST MEASUREMENTS

A-1. INTRODUCTION

The program objectives required a redundant method of measuring peak overpressure, positive impulse, and pressure pulse duration. The Ballistic Research Laboratories (BRL) have developed and used a self-contained mechanical pressure-time gage for obtaining blast measurements from explosive tests. This gage provided a contrast to the piezoelectric gages used elsewhere on the program and permitted a cross-check of the pressure-measuring instrumentation.

The Ballistic Research Laboratories provided eight gages for the duration of the test program.

A-2. GAGE DESCRIPTION

The BRL gage contains a single diaphragm sensor that scratch-records on a negator-spring motor recorder in response to the pressure phenomena. Sensors are fabricated of NiSpan C and are welded into a mounting ring. A section of thin-wall stainless steel tubing is bonded, by epoxy to the center of the diaphragm; the free end of the tube passing through an olive jewel bearing fixed to the top section of the mounting ring. A flat 5/16-in.-long section of phosphor bronze, containing an osmium-tipped 1/32-in.-long stylus, is soldered in the tubing. An O-ring serves as a pressure seal, and two alignment pins facilitate a mounting in the gage. Sensors are 1-5/16-in. in diameter and are interchangeable, covering a pressure spectrum of 9 to 1000 psi in 15 pressure ranges. A sensor is shown in Figure A-1.

The general characteristics of the pressure sensors are presented in Table A-1. Average deflection at rated pressure is 0.020 in., hysteresis is less than 1% and the nonlinearity is less than 5%. The natural frequency ranges from 1 to 7000 cps. Damping is accomplished by an orifice plate mounted in the face plate of the gage. Rise times of from 0.3 to 0.5 msec have been achieved in shocktube and field-test programs.
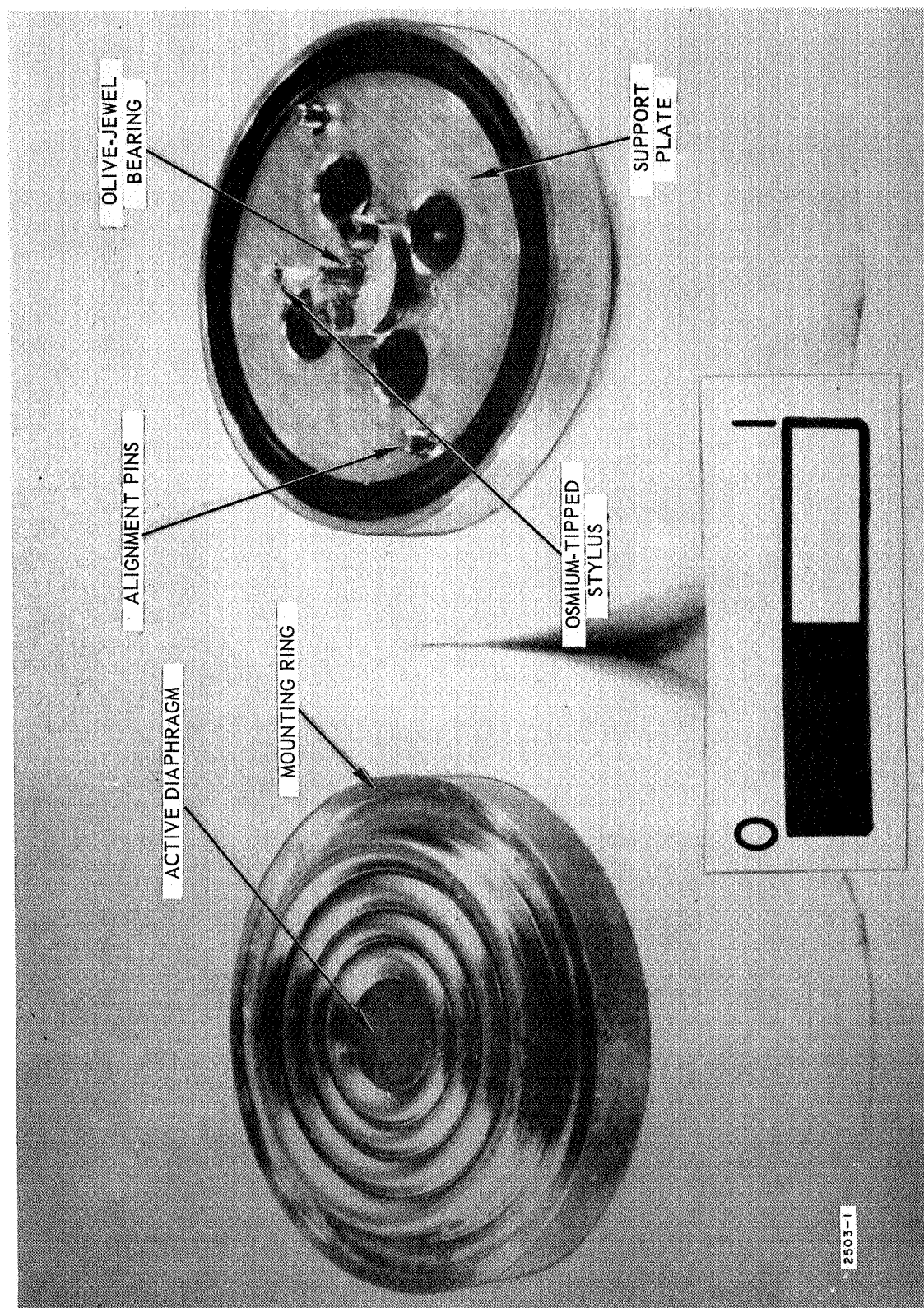
Figure A-1. Pressure Sensor.

Table A-1. Sensor Statistics,

Sensor Ranges (psi)	Sensor Natural Frequency (cps)	Sensor Characteristics		
		Deflection of Rated Pressure (mils)	Hysteresis (%)	Nonlinearity (Terminal-Based)
0-1	820	15-30	0.70	1, 60
0-2	1085	19.60	0. 87	1. 68
0-5	1570	20.20	0.00	1, 60
0-10	1895	26.80	0. 67	2.69
0-25	2726	23.90	0.20	0.70
0-50	2995	24-20	0. 30	2, 40
0-100	3615	28-60	0.35	0, 87
0-200	4351	31.35	0, 73	3.57
0-400	5105	23.17	0. 86	3.75
0-600	5955	20.82	0. 62	2, 16
0-1000	6990	20.10	0.59	0.45
0- 10 (Negative)	1915	25.70	0.20	0. 70
0-0.50	430	18.15	0.55	1.70
0-0.125	250	17.40	0. 60	4. 90
0-0.030	250	18.20	1-10	4, 20

The method of using a negator spring as both the drive motor and recorder was devised and patented by BRL. The negator spring motor has the inherent characteristic of providing a constant torque output during its entire running cycle. It consists basically of a supply or output drum, a recording drum, a storage drum, and a balanced frictional governor. The storage drum with the spring freely installed on it is mounted for free rotation about its fixed axis. With the outer end of the flat spring extended to pass over the recording drum and anchored to the output drum, the spring is reverse wound onto the output drum. Release of the output drum (the larger of the drums) at any degree of windup allows the material to revert to its natural prestressed curvature by returning to the smaller storage drum. Speed control of the spring to within 10% is provided by the governor through a gear coupling to the output drum. Speeds of 0.5 to **3** ips can be obtained by adjusting the governor. Springs are fabricated of stainless steel in 5/16-in. widths and in lengths of 30 to 60 in. The recording surface of the spring is vapor honed with a fine grit, preparing it for the scratch recording.

Arming, initiation, and shutoff are provided for in the gage system by associated gearing and switches. Two methods, either a solenoid with a balanced armature or an explosive piston actuator, are used for initiating the gage; both systems being triggered by a relay closure. The solenoid or the actuator releases a spring-loaded trigger arm that rapidly serves to bring the motor up to a constant speed. The startup time for the solenoid system is 18.8 msec, while the startup time for the explosive actuator system is 9.4 msec. A startup time of 4.4 msec can be achieved by using an explosive actuator as the sole means of initiation and by bringing the motor up to speed rapidly.

Three traces are recorded on the surface of the spring as it passes over the recording drum. These are the active pressure trace, the 50-cps squarewave timing trace, and the fixed reference trace. Timing is applied by solenoid-operated scribes in series with a 50-cps electro-mechanical oscillator. It operates from 12 v supplied by a nickel-cadmium battery mounted in the base of the gage canister.

Mounting of the motor-recorder, sensor, timing scribes, and release mechanism is made to a face plate 4.75 in. in diameter x 1.2 in. thick. A flange of matching dimensions is welded to a 3-1/2-in.-diameter x 4-in.-long aluminum canister. The timing oscillator, with the initiation relay, battery, and condenser, is mounted on a removable section at the base of the canister. Electrical connections between the removable halves of the gage are achieved by matching sections of a Cannon connector. The initiation cable enters the gage through a Microdot cable grip at the base of the gage. O-rings at the top and at the base of the gage provide pressure seals when installed in the canister. The gage is mounted flush with the ground surface. Figures A-2 to A-4 illustrate the gage.

TAKE UP DRUM

RECORDING DRUM

SUPPLY DRUM

CUTOFF ARM

MOTOR

REFERENCE SCRIBE

INITIATOR ASSEMBLY

TIMING SCRIBE

SENSOR SCRIBE

2503-1
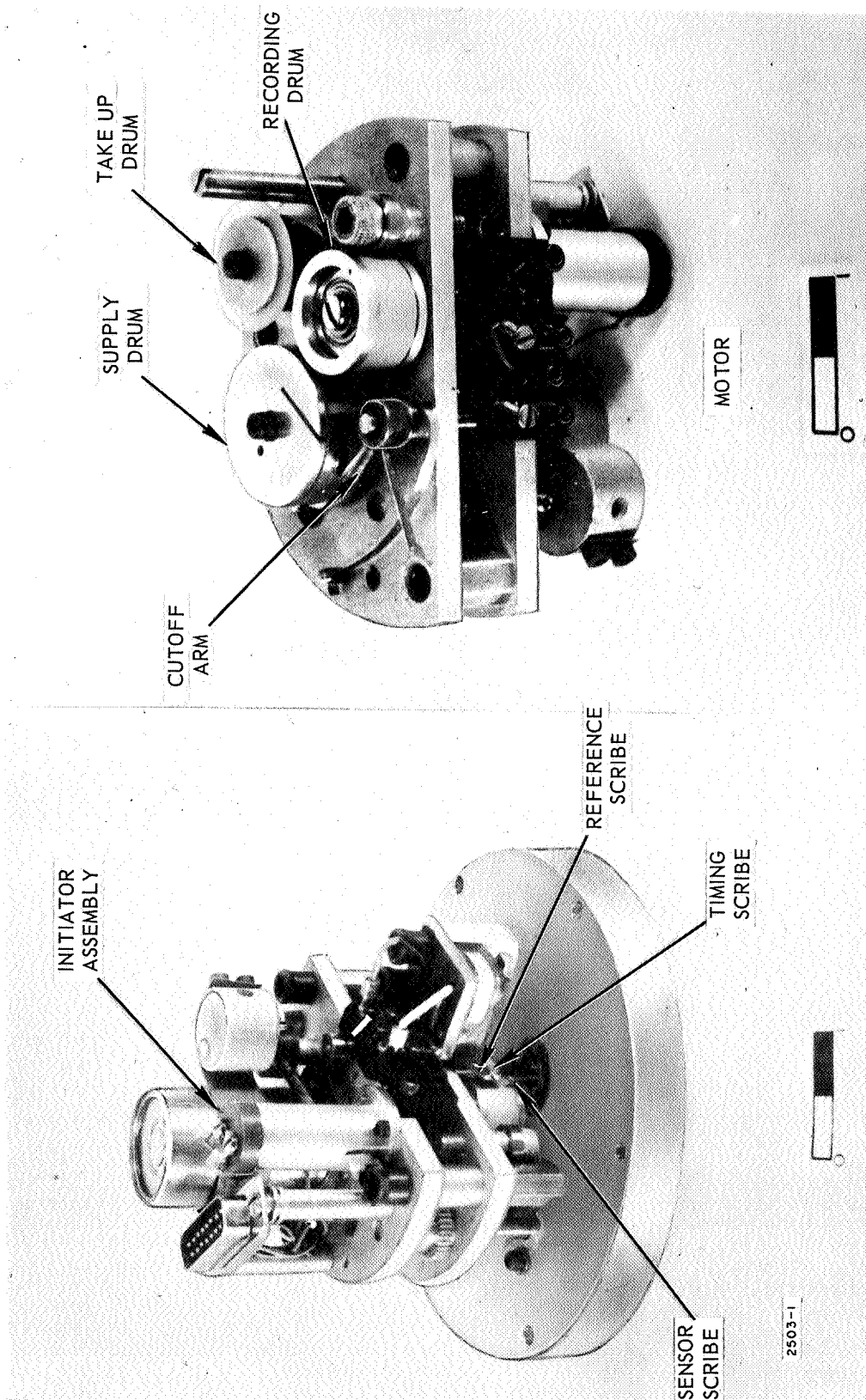
Figure A-2. Recording Assembly, PNS Gage.
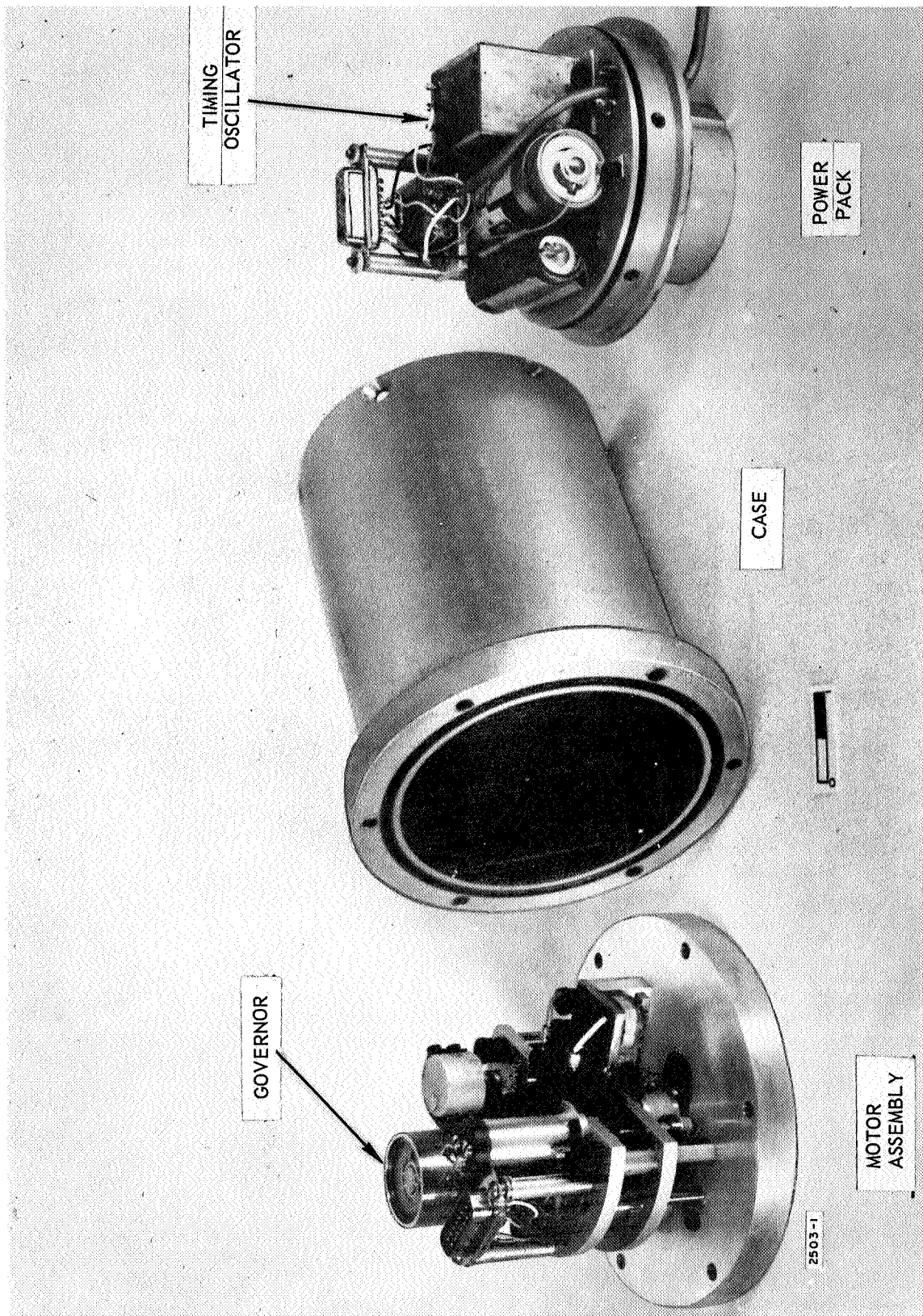
Figure A-3. Exploded View of PNS Gage.
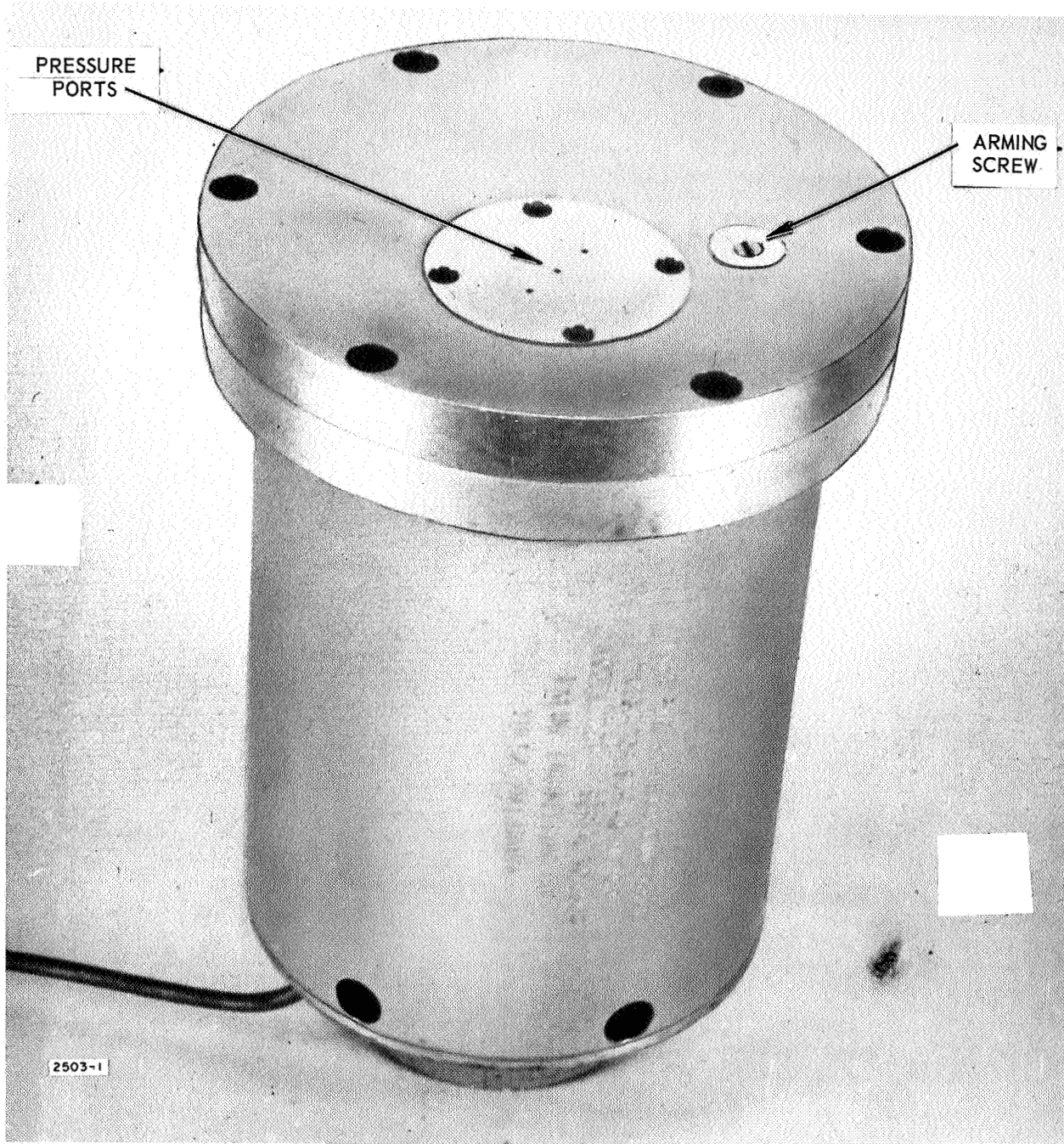
Figure A-4. Assembled Gage.

The deflection time traces recorded on the negator spring are converted
to real points with the aid of a specially equipped reading microscope.
Telecomputing digital readout heads, mounted on the reading equipment
for x and y measurements, furnish input to Telecordex accumulators
whose output is recorded by an automatic typewriter and a paper-tape
punch system.

These data, together with the calibration data, are fed into an auto-
matic computer for obtaining final pressure-time information. An
automatic plotter plots the final information.

A-3. GAGE POSITION

The original program plan provided for locating the BRL gages directly
underneath the piezoelectric gage positions and for flush mounting with
the ground. However, the blast shock wave characteristics necessitated
locating the gages at stations commensurate with sensor response charac-
teristics. Two gage rows were established at gage positions 2-3-4 and
10-11-12. Gage stations 13 and 14 were established on the ends of the
rows at a distance of 98 ft from the test fixture.

A-4. TEST RESULTS

The results of the blast measurements are presented in Tables A-2 and
A-3. No data was obtained for Test 7 due to the initiation of the
hypergolic propellants during the loading operation and for Test 9 due
to pretriggering of the gages before the event while checking out other
instrumentation.

Table A-2. LOX/LH$_2$ Test Results.

Contact Area (ft^2)	Test No.	Gage Distance from Event (ft)	Gage No.	Time (msec)	Overpressure (psi)	Impulse (psi-msec)
25. 12	1	40	10	0. 58	0.97	0. 29
				1. 06	0.89	0.73
				1.43	2. 25	1. 30
				1.75	5. 51	2. 58
				2. 28	5. 23	5. 43
				3.39	4. 83	10.97
				3.91	4.33	13.36
				4.11	4. 67	14.28
				4. 82	3.22	17.06
				5. 35	3.83	18.93
				6. 87	3.78	24.74
				7. 69	3. 33	27. 63
				8. 14	1.94	28. 83
				8.48	1.94	29.49
				8. 78	1.47	30.00
				11. 15	0. 83	32.73
				13. 16	0.44	34.01
				14. 21	0. 31	34.41
				17.69	0. 31	35.47
				20. 58	0. 31	36. 35
				21. 89	0. 17	36.66
				25. 14	0. 06	37.02
				29. 33	0. 00	37. 14
			2	No Data		
		60	3	0. 15	6.40	0. 51
				0. 24	4.85	1.00
				0. 58	3.01	2. 35
				0. 87	3.69	3. 29
				1.21	3.53	4. 53
				1.54	3. 18	5. 66
				2. 20	3.03	7. 71
				2. 81	2. 88	9. 50
				3.02	2. 55	10.07
				3. 31	2. 88	10.86
				3. 63	2. 08	11.65

Table A-2. (Continued)

Contact Area (ft²)	Test No.	Gage Distance from Event (ft)	Gage No.	Time (msec)	Overpressure (psi)	Impluse (psi-msec)
				4.11	2.12	12.66
				4. 35	1.84	13. 14
				4.74	1.82	13.84
				5. 60	1.76	15.39
				5. 77	1.55	15.67
				6. 03	1.66	16.09
				6. 29	1.32	16.47
				6. 59	1. 19	16.85
				7. 65	1. 13	18.08
				9. 09	1.04	19.64
				10.07	0.77	20.53
				10.70	0.49	20.93
				11.91	0. 31	21.41
				12.99	0. 25	21. 72
				13.80	0.10	21.86
				14.44	0. 00	21.90
			11	0. 39	5.64	1.12
				0.43	4.94	1.34
				0. 59	4.65	2. 09
				0. 64	4.02	2. 31
				1. 16	3.94	4. 39
				1. 67	3. 96	6. 40
				2. 03	3.86	7.79
				2.45	3.82	9.43
				3. 07	3. 52	11.68
				3.45	3. 26	12.99
				3.79	3. 29	14.08
				4. 03	3. 04	14.84
				4.20	3.10	15.38
				4.55	2.67	16.37
				5. 94	2. 61	20.06
				6. 35	2. 85	21. 17
				6.64	2.64	21. 97
				7.00	2.81	22.97
				7.73	2. 71	24.98
				8.62	2.35	27. 22
				8.91	2.44	27.92
				9. 80	1.90	29.86
				11.71	1.50	33.11

Table A-2. (Continued)

Contact Area (ft^2)	Test No.	Gage Distance from Event (ft)	Gage No.	Time (msec)	Overpressure (psi)	Impulse (psi-msec)
				12.96	1.18	34.78
				14.18	0.81	36.00
				15.11	0.63	36.66
				16.95	0.37	37.57
				21.02	0.12	38.55
				26.90	0.00	38.89
	80		4	No data		
			12	0.66	3.71	1.23
				1.04	2.37	2.38
				1.51	2.40	3.51
				2.28	2.20	5.28
				2.91	2.01	6.61
				3.49	1.93	7.75
				3.82	1.99	8.39
				4.11	1.71	8.93
				5.31	1.57	10.91
				6.50	1.30	12.61
				7.44	0.97	13.68
				9.02	0.73	15.02
				10.37	0.48	15.84
				11.52	0.26	16.27
				13.63	0.11	16.65
				15.30	0.02	16.75
				16.65	0.00	16.76
	98		13	No data		
			14	0.46	1.83	0.42
				0.96	2.31	1.45
				1.41	1.91	2.42
				2.31	1.87	4.10
				3.02	1.78	5.40
				3.40	1.73	6.08
				4.24	1.70	7.51
				4.85	1.57	8.50
				5.40	1.56	9.37
				5.88	1.46	10.09
				6.41	1.27	10.81
				8.03	1.18	12.80

Table A-2. (Continued)

Contact Area (ft^2)	Test No.	Gage Distance from Event (ft)	Gage No.	Time (msec)	Overpressure (psi)	Impulse (psi-msec)
				9.48	0.98	14.36
				11.72	0.90	16.47
				12.40	0.60	16.98
				13.39	0.58	17.56
				13.69	0.47	17.72
				16.48	0.38	18.90
				17.35	0.22	19.16
				19.40	0.22	19.60
				19.97	0.43	19.79
				21.30	0.43	20.36
				21.50	0.47	20.45
				23.01	0.00	20.80
25.12	2	40	2	0.42	7.62	1.62
				0.76	4.62	3.72
				1.19	4.35	5.63
				1.70	3.91	7.73
				2.12	3.37	9.28
				2.36	2.90	10.03
				2.70	3.30	11.07
				2.98	2.82	11.92
				3.35	3.62	13.11
				3.64	2.55	14.02
				4.00	3.10	15.04
				4.42	2.31	16.17
				5.63	1.82	18.67
				7.32	1.54	21.50
				8.60	1.20	23.26
				10.85	0.76	25.47
				12.90	0.32	26.56
				13.96	0.00	26.73

Table A-2. (Continued)

Contact Area (ft^2)	Test No.	Gage Distance from Event (ft)	Gage No.	Time (msec)	Overpressure (psi)	Impulse (psi-msec)
			10	0.56	4.69	1.32
				0.87	4.57	2.74
				1.09	4.78	3.80
				1.78	4.58	7.01
				3.11	4.53	13.07
				4.32	4.49	18.51
				4.76	4.12	20.41
				6.70	4.60	28.90
				7.66	3.99	32.99
				8.41	3.98	36.01
				9.42	2.45	39.24
				11.55	1.65	43.60
				13.81	1.44	47.08
				15.68	1.19	49.54
				19.17	1.00	53.35
				22.38	0.72	56.11
				26.79	0.29	58.34
				31.88	0.10	59.33
				35.23	0.00	59.50
	60		3	0.20	10.36	1.05
				0.33	0.69	1.78
				0.70	5.99	3.01
				0.80	6.72	3.68
				1.12	6.30	5.74
				1.60	5.89	8.64
				2.27	0.86	10.93
				2.60	4.88	11.86
				3.25	4.52	14.92
				3.72	3.88	16.88
				4.17	0.08	17.77
				4.52	3.53	18.40
				4.83	2.34	19.31
				5.16	3.10	20.22
				5.40	2.51	20.89
				6.34	1.99	23.00
				6.83	1.89	23.96
				7.23	1.51	24.63

Table A-2. (Continued)

Contact Area (ft²)	Test No.	Gage Distance from Event (ft)	Gage No.	Time (msec)	Overpressure (psi)	Impulse (psi-msec)
				8.48	1.39	26.45
				8.86	0.99	26.91
				10.37	0.75	28.22
				11.16	0.53	28.73
				11.96	0.14	29.00
				12.74	0.01	29.06
				13.57	0.00	29.07
			11	0.45	4.28	0.97
				1.63	4.25	6.01
				3.58	3.93	13.98
				5.27	3.62	20.31
				6.42	3.28	24.32
				8.57	2.78	30.82
				10.26	2.24	35.07
				12.17	1.77	38.91
				14.86	1.34	43.09
				18.44	0.91	47.11
				22.59	0.70	50.47
				25.13	0.48	51.97
				30.71	0.21	53.90
				38.41	0.13	55.23
				44.63	0.06	55.83
				49.80	0.00	55.98
		80	4	No data		
			12	0.43	4.36	0.95
				0.77	2.11	2.06
				1.14	2.89	2.99
				1.39	2.63	3.66
				1.51	2.45	3.96
				2.03	2.43	5.24
				2.56	2.32	6.49
				2.97	2.54	7.50
				3.28	2.30	8.25
				4.08	1.87	9.91
				4.21	2.08	10.18
				4.59	1.72	10.88
				5.86	1.62	13.01

Table A-2. (Continued)

Contact Area (ft^2)	Test No.	Gage Distance from Event (ft)	Gage No.	Time (msec)	Overpressure (psi)	Impulse (psi-msec)
				8.06	0.91	15.79
				9.98	0.59	17.24
				10.86	0.34	17.65
				12.27	0.17	18.01
				16.14	0.00	18.34
		98	13	No data		
			14	0.48	1.90	0.46
				0.93	2.33	1.41
				1.63	2.06	2.94
				2.59	2.00	4.90
				3.51	1.81	6.64
				3.98	1.68	7.46
				4.67	1.51	8.58
				6.08	1.23	10.51
				8.21	1.06	12.94
				8.88	1.04	13.65
				9.66	0.83	14.38
				11.49	0.76	15.84
				12.14	0.52	16.26
				13.89	0.52	17.17
				14.53	0.60	17.53
				16.62	0.55	18.74
				17.31	0.34	19.04
				19.40	0.27	19.67
				19.95	0.52	19.89
				21.75	0.49	20.80
				22.70	0.00	21.03
56.23	3	40	2	No data		
			10	0.60	20.18	6.06
				0.82	13.00	9.79
				0.92	9.64	10.88
				1.44	8.93	15.76
				2.70	6.85	25.65
				3.33	7.20	30.09
				3.85	5.59	33.45
				4.13	6.10	35.08
				4.54	4.09	37.16
				4.84	5.71	38.63

Table A-2.   (Continued)

Contact Area (ft²)	Test No.	Gage Distance from Event (ft)	Gage No.	Time (msec)	Overpressure (psi)	Impulse (psi-msec)
				5. 08	4.48	39.83
				5.94	2.47	42.85
				6. 34	3. 23	43.98
				7. 30	1. 98	46.49
				7. 68	2.84	47.40
				10. 50	0. 98	52. 77
				13. 11	0. 00	54. 04
		60	3	0. 72	0. 48	0. 17
				1.07	6.79	1.45
				1.35	6.98	*3.* 40
				1.74	6. 63	6. 05
				2. 17	6.45	8. 86
				2. 74	6. 41	12. 50
				3. 50	5. 84	17. 16
				3. 96	5. 05	19.65
				6. 37	4. 29	30.94
				8. 37	3. 76	38.99
				11.39	3. 13	49.37
				15. 11	2. 50	59. 85
				19. 19	1. 80	68.61
				22.39	1.21	73.43
				27.91	0. 72	78.76
				34.55	0. 35	82. 30
				39.57	0. 21	83.70
				46. 87	0. 08	84.76
				56.44	0. 00	85. 12
			11	0. 09	0. 05	0. 00
				0. 20	6. 81	0. *36*
				0.43	5. 65	1.84
				0. 61	6. 04	2. 87
				0. 87	5. 61	4. 36
				0. 98	5. 73	5.01
				1. 36	5. 38	7.11
				2. 20	5. 25	11.60
				2. 88	5. 00	15.07
				3.49	4.43	17.94
				3.98	4. 68	20.18
				4. 13	4. 13	20.84
				4. 52	3. 36	22. 29

Table A-2.   (Continued)

Contact Area (ft²)	Test No.	Gage Distance from Event (ft)	Gage No.	Time (msec)	Overpressure (psi)	Impulse (psi-msec)
				4.73	3.48	23.01
				4.90	2.92	23.58
				5.05	3.15	24.03
				5.45	2.57	25.16
				5.89	2.62	26.31
				6.26	2.03	27.16
				6.86	2.15	28.41
				7.98	2.09	30.78
				8.78	1.63	32.26
				9.92	1.25	33.91
				11.01	0.89	35.08
				11.18	0.89	35.23
				12.70	0.67	36.41
				14.40	0.52	37.41
				16.96	0.00	38.08
	80		4	1.10	5.75	3.18
				1.59	4.18	5.63
				2.40	4.11	8.95
				3.33	3.72	12.61
				4.37	3.37	16.29
				5.01	2.79	18.27
				7.24	2.59	24.27
				7.99	2.19	26.06
				8.47	2.15	27.11
				8.95	1.88	28.07
				10.11	1.76	30.18
				10.69	1.52	31.14
				14.05	1.29	35.85
				18.38	0.48	39.70
				21.11	0.27	40.72
				23.16	0.00	40.99
			12	No data		
	98		13	0.62	1.87	0.59
				1.24	3.06	2.10
				1.67	2.94	3.40
				1.79	2.97	3.74
				2.50	2.80	5.81
				3.29	2.74	7.99
				3.71	2.57	9.10

Table A-2.   (Continued)

Contact Area (ft^2)	Test No.	Gage Distance from Event (ft)	Gage No.	Time (msec)	Overpressure (psi)	Impulse (psi-msec)
				4.68	2.56	11.58
				5.59	2.45	13.87
				5.86	2.24	14.51
				6.57	1.91	15.97
				7.19	1.91	17.15
				7.51	1.80	17.74
				8.17	1.80	18.94
				8.75	1.68	19.94
				9.10	1.67	20.54
				9.38	1.58	21.00
				9.67	1.26	21.40
				12.37	1.24	24.77
				13.53	1.05	26.10
				14.05	0.98	26.63
				15.31	0.74	27.70
				18.98	0.68	3.0.32
				19.76	0.45	30.76
				21.22	0.27	31.29
				22.77	0.13	31.60
				24.17	0.02	31.70
				26.33	0.00	31.72
			14	1.80	2.39	2.16
				2.04	2.18	2.69
				2.28	2.20	3.22
				2.43	2.11	3.56
				2.60	2.20	3.91
				2.96	2.10	4.69
				3.21	2.13	5.22
				3.79	2.06	6.42
				4.62	2.05	8.14
				5.26	1.96	9.43
				6.06	1.93	10.98
				6.91	1.81	12.58
				7.83	1.66	14.16
				8.98	1.59	16.02
				10.02	1.53	17.65
				11.48	1.49	19.85
				12.37	1.40	21.14
				13.20	1.17	22.21

Table A-2.   (Continued)

Contact Area (ft^2)	Test No.	Gage Distance from Event (ft)	Gage No.	Time (msec)	Overpressure (psi)	Impulse (psi-msec)
				14. 12	1. 15	23. 29
				15.03	1. 23	24. 37
				16. 51	1. 15	26. 14
				16.87	0. 87	26. 51
				17.88	0. 87	27. 39
				18.37	0.79	27.80
				19.01	0. 86	28. 33
56. 23	4	40	2	No data		
			10	0.59	15.86	4. 69
				0. 71	12.33	6.42
				1. 51	11.40	15.92
				1. 89	8. 36	19.70
				3. 30	7.47	30.81
				3.76	6. 99	34.20
				4.39	6. 99	38.59
				5. 06	6. 04	42.93
				6. 15	4.73	48.83
				7. 20	3.69	53. 24
				7.41	4. 09	54.05
				9. 70	2. 80	61.94
				11.44	2.10	66.21
				13.42	1.34	69.62
				15.77	0. 58	71.88
				18.27	0.00	72.60
		60	3	1.00	5. 12	2. 57
				1. 64	5. 05	5. 84
				2. 40	4. 96	9. 63
				2. 78	5. 15	11.53
				3. 61	5. 05	15.80
				4.79	5.10	21.76
				6. 03	4.86	27.92
				7.42	4.33	34.32
				9. 16	3. 89	41.49
				11.67	3. 41	50.66
				13.84	3. 08	57.70
				16.07	2. 71	64.13
				18.97	2. 51	71.70
				21. 08	2. 31	76. 80
				24. 37	2.21	84. 23
				27. 11	2. 04	90. 04

Table A-2.   (Continued)

Contact Area (ft^2)	Test No.	Gage Distance from Event (ft)	Gage No.	Time (msec)	Overpressure (psi)	Impulse (psi-msec)
				31.11	1.85	97.82
				33.93	1.67	102.79
				37.82	1.53	109.01
				44.76	1.35	118.99
				51.93	1.26	128.33
				60.66	1.20	139.07
				62.89	1.23	141.79
				67.30	1.23	147.21
				Possible Zero Shift		
			11	0.57	7.23	2.07
				0.73	5.25	3.11
				0.98	5.68	4.46
				1.74	5.20	8.57
				1.80	4.92	8.89
				2.59	4.58	12.65
				3.19	3.93	15.20
				3.63	4.62	17.08
				4.07	3.67	18.90
				4.61	3.53	20.83
				5.20	3.19	22.84
				5.89	2.91	24.93
				6.15	2.59	25.63
				7.60	2.50	29.33
				8.24	2.23	30.85
				8.96	1.98	32.37
				9.81	1.73	33.93
				10.64	1.33	35.20
				10.90	1.06	35.52
				11.75	0.88	36.34
				11.95	1.23	36.55
				12.39	0.90	37.02
				13.42	0.57	37.78
				14.72	0.43	38.43
				15.55	0.19	38.69
				17.34	0.14	38.98
				19.20	0.00	39.10

Table A-2.   (Continued)

Contact Area (ft^2)	Test No.	Gage Distance from Event (ft)	Gage No.	Time (msec)	Overpressure (psi)	Impulse (psi-msec)
		80	4	1.57	5.07	3.99
				1.94	4.50	5.75
				3.20	3.99	11.10
				4.09	3.63	14.53
				4.97	3.32	17.56
				5.23	3.32	18.72
				6.10	2.69	21.08
				6.39	2.59	21.75
				7.17	2.40	23.78
				7.71	2.36	25.07
				9.54	1.91	28.96
				11.09	1.69	31.75
				12.64	1.40	34.13
				15.28	1.23	37.61
				16.23	0.87	38.61
				17.75	0.54	39.68
				19.79	0.47	40.72
				22.29	0.47	41.90
				24.39	0.41	42.83
				25.75	0.22	43.26
				27.99	0.16	43.69
				29.85	0.13	43.95
				23.51	0.09	44.24
				34.68	0.02	44.46
				35.46	0.02	44.55
				36.74	0.00	44.62
			12	0.46	2.47	0.58
				3.51	2.41	8.02
				5.92	2.43	13.85
				8.76	2.46	20.81
				11.30	2.48	27.07
				18.22	2.42	44.03
				22.23	2.43	53.57
				25.35	2.22	60.69
				29.40	2.08	69.40
				33.11	2.03	77.02
				37.49	1.98	85.78
				44.04	1.98	98.78
				47.69	1.96	105.96

Table A-2.   (Continued)

Contact Area (ft^2)	Test No.	Gage Distance from Event (ft)	Gage No.	Time (msec)	Overpressure (psi)	Impulse (psi-msec)
				53.44	1.93	117.14
				59.87	1.90	129.45
				63.43	1.83	136.08
				70.52	1.74	148.75
				74.40	1.70	155.44
.		98	13	0.12	4.23	0.26
				0.56	2.85	1.81
				0.74	2.68	2.31
				0.96	2.82	2.93
				1.72	2.74	5.04
				2.51	2.67	7.17
				3.45	2.54	9.61
				4.21	2.41	11.50
				5.04	2.27	13.44
				5.82	2.01	15.12
				7.53	1.85	18.42
				8.89	1.57	20.75
				10.59	1.37	23.26
				13.05	1.21	26.44
				13.61	0.92	27.04
				14.77	0.91	28.09
				15.58	0.70	28.75
				19.53	0.70	31.52
				23.04	0.65	33.91
				24.32	0.56	34.69
				25.29	0.42	35.17
				28.91	0.34	36.54
				33.37	0.23	37.81
				38.66	0.49	38.78
				54.92	0.06	39.52
				57.89	0.00	39.93
				59.14	0.00	39.94
			14	0.61	1.20	0.37
				0.85	1.40	0.68
				1.07	1.52	0.99
				2.00	1.59	2.44
				4.20	1.59	5.94
				5.60	1.61	8.17
				7.17	1.61	10.70

Table A-2. (Continued)

Contact Area (ft^2)	Test No.	Gage Distance from Event (ft)	Gage No.	Time (msec)	Overpressure (psi)	Impulse (psi-msec)
				9.18	1.59	13.92
				12.63	1.59	19.38
				15.74	1.61	24.34
				20.70	1.61	32.31
				22.80	1.55	35.62
				24.34	1.48	37.94
				25.40	1.36	39.46
				25.92	1.23	40.12
				26.28	0.97	40.52
				26.52	0.62	40.71
				26.74	0.35	40.82
				27.10	0.09	40.90
				28.80	0.00	40.98
36.81	5	40	2	0.60	10.69	3.26
				0.95	10.13	6.83
				1.67	9.20	13.83
				2.24	8.38	18.85
				2.86	7.53	23.78
				3.22	7.41	26.48
				3.57	6.68	28.90
				3.81	7.19	30.61
				4.17	6.88	33.09
				4.33	7.44	34.25
				4.94	4.75	37.97
				5.10	5.94	38.83
				5.40	6.56	40.68
				5.86	5.80	43.56
				6.23	5.14	45.59
				7.20	4.97	50.46
				8.21	4.81	55.44
				8.91	3.97	58.49
			10	0.54	13.38	3.62
				0.66	9.85	5.06
				0.90	9.85	7.39
				1.14	9.43	9.78
				1.19	7.38	10.16
				1.46	7.77	12.21
				2.18	6.46	17.34
				2.95	6.58	22.33

Table A-2. (Continued)

Contact Area (ft^2)	Test No.	Gage Distance from Event (ft)	Gage No.	Time (msec)	Overpressure (psi)	Impulse (psi-msec)
				3.95	6.19	28.73
				4.10	5.09	29.56
				4.29	5.51	30.57
				4.57	4.66	32.01
				4.75	5.15	32.89
				5.02	3.32	34.04
				5.16	4.09	34.54
				5.49	3.67	35.85
				5.71	2.84	36.55
				6.79	2.68	39.54
				7.86	2.35	42.23
				8.68	2.04	44.02
				9.33	1.25	45.10
				10.80	1.31	46.98
				11.96	0.91	48.27
				13.76	0.64	49.66
				15.23	0.18	50.27
				16.58	0.00	50.39
		60	3	No data		
			11	0.20	7.02	0.71
				0.70	4.00	3.47
				0.86	4.58	4.15
				1.24	4.63	5.94
				1.87	4.14	8.68
				2.08	4.29	9.57
				2.48	3.90	11.19
				3.08	3.35	13.39
				3.65	3.46	15.31
				4.11	2.81	16.77
				5.12	2.57	19.47
				6.15	2.31	21.99
				7.77	1.88	25.40
				10.33	1.27	29.35
				12.99	0.51	31.65
				15.97	0.21	32.73
				18.15	0.00	32.97

Table A-2.   (Continued)

Contact Area (ft²)	Test No.	Gage Distance from Event (ft)	Gage No.	Time (msec)	Overpressure (psi)	Impulse (psi-msec)
		80	4	0.78	1.91	0.75
				1.91	1.94	2.92
				3.91	1.91	6.77
				6.70	1.95	12.17
				7.85	1.83	14.35
				10.13	1.44	18.06
				12.96	1.17	21.76
				16.05	0.95	25.02
				16.56	0.79	25.47
				19.73	0.55	27.59
				23.21	0.42	29.29
				28.18	0.22	30.87
				29.18	0.22	31.09
			12	0.46	2.45	0.57
				1.65	2.40	3.44
				2.97	2.38	6.62
				5.40	2.40	12.41
				8.46	2.40	19.76
				10.08	2.36	23.62
				12.87	2.33	30.16
				15.14	2.28	35.37
				17.32	2.17	40.22
				21.49	2.10	49.11
				24.28	2.00	54.82
				27.10	1.91	60.33
		98	13	0.30	3.47	0.52
				0.44	3.03	1.00
				0.95	2.37	2.36
				2.01	2.36	4.86
				3.10	2.35	7.45
				3.76	2.27	8.97
				4.14	2.10	9.79
				5.07	2.07	11.74
				5.38	1.95	12.35
				5.92	1.89	13.39
				6.75	1.77	14.90
				7.08	1.70	15.46
				7.33	1.63	15.88
				8.62	1.47	17.87

Table A-2.   (Continued)

Contact Area (ft²)	Test No.	Gage Distance from Event (ft)	Gage No.	Time (msec)	Overpressure (psi)	Impulse (psi-msec)
				9.35	1.16	18.84
				10.86	1.07	20.53
				12.50	0.89	22.14
				14.53	0.72	23.78
				17.38	0.59	25.66
				22.28	0.49	28.32
				26.53	0.30	30.01
				29.53	0.22	30.77
				37.06	0.12	32.06
				41.96	0.11	32.65
				57.27	0.11	34.39
				65.71	0.09	35.25
				79.74	0.09	36.49
				97.99	0.05	37.76
				111.23	0.00	38.10
			14	0.41	0.28	0.06
				0.98	0.50	0.28
				1.55	0.59	0.59
				2.99	0.66	1.48
				5.50	0.66	3.14
				0.73	0.68	6.65
				15.07	0.68	9.60
				19.69	0.78	12.75
				23.22	0.66	15.12
				26.65	0.62	17.31
				28.28	0.58	18.28
				30.77	0.51	19.63
				34.22	0.42	21.25
				38.32	0.32	22.78
				43.96	0.24	24.37
				47.12	0.20	25.07
				53.85	0.16	26.28
				60.35	0.12	27.19
				64.26	0.09	27.58
				68.05	0.06	27.86
				72.23	0.03	28.04
				75.96	0.00	28.09

Table A-2. (Continued)

Contact Area (ft²)	Test No.	Gage Distance from Event (ft)	Gage No.	Time (msec)	Overpressure (psi)	Impulse (psi-msec)
36.81	6	40	2	0.49	5.82	1.43
				0.92	5.77	3.93
				1.23	5.91	5.79
				1.71	5.99	8.59
				2.33	5.51	12.18
				2.96	5.17	15.52
				3.26	4.81	17.05
				4.02	4.94	20.75
				4.79	4.17	24.26
				5.50	5.31	27.63
				6.25	4.14	31.17
				6.99	4.81	34.48
				7.84	3.69	38.08
			10	0.45	10.05	2.29
				0.50	6.40	2.68
				1.27	6.19	7.54
				2.32	4.51	13.16
				3.20	4.18	16.97
				3.96	3.96	20.06
				4.20	3.23	20.93
				4.81	3.23	22.90
				5.28	2.26	24.20
				6.10	1.65	25.79
				7.51	1.74	28.19
				8.23	1.28	29.27
			.	10.34	0.88	31.55
				12.52	0.43	32.98
				16.08	0.18	34.07
				18.77	0.03	34.35
		60	3	0.68	5.66	1.94
				0.80	2.73	2.45
				1.14	3.78	3.55
				1.47	2.92	4.66
				1.82	3.25	5.73
				1.89	2.94	5.95
				2.55	2.94	7.91
				3.14	2.65	9.56
				3.44	2.43	10.30
				3.65	2.69	10.84

Table A-2.   (Continued)

Contact Area (ft^2)	Test No.	Gage Distance from Event (ft)	Gage No.	Time (msec)	Overpressure (psi)	Impulse (psi-msec)
				3.95	1.88	11.53
				4.23	2.42	12.13
				4.43	1.96	12.56
				6.28	1.67	15.92
				7.20	1.50	17.39
				10.21	0.93	21.04
				10.55	1.47	21.45
				10.71	1.04	21.65
				13.80	0.61	24.21
				17.84	0.24	25.94
				21.02	0.00	26.33
			11	0.11	5.50	0.33
				0.63	2.57	2.40
				0.90	3.22	3.20
				1.46	3.17	4.97
				2.10	2.90	6.91
				2.74	2.78	8.73
				3.39	2.60	10.47
				3.93	2.00	11.73
				4.61	1.96	13.07
				5.40	1.75	14.54
				6.05	1.39	15.56
				6.32	1.50	15.95
				7.31	1.19	17.28
				9.04	0.76	18.96
				12.21	0.32	20.69
				15.28	0.14	21.39
				18.56	0.00	21.62
		80	4	0.45	3.74	0.86
				0.89	1.84	2.09
				1.41	1.82	3.03
				2.05	1.82	4.19
				2.56	1.82	5.13
				3.09	1.69	6.05
				3.47	1.62	6.69
				4.01	1.26	7.46
				5.01	1.15	8.67
				6.19	1.00	9.93
				7.76	0.77	11.33

Table A-2. (Continued)

Contact Area (ft²)	Test No.	Gage Distance from Event (ft)	Gage No.	Time (msec)	Overpressure (psi)	Impulse (psi-msec)
				9.43	0.59	12.47
				10.10	0.44	12.81
				12.64	0.27	13.70
				14.23	0.23	14.10
				15.01	0.00	14.18
			12	No data		
		98	13	0.45	2.46	0.56
				1.27	1.48	2.18
				2.00	1.46	3.26
				4.57	1.46	7.01
				6.82	1.46	10.29
				8.49	1.40	12.67
				10.04	1.29	14.76
				11.47	1.12	16.47
				13.46	1.17	18.75
				15.40	0.92	20.78
				18.47	0.77	23.39
				20.67	0.72	25.03
				22.95	0.67	26.61
				24.57	0.60	27.64
				25.67	0.53	28.27
				27.01	0.46	28.93
				32.00	0.43	31.14
				35.63	0.37	32.60
				38.14	0.29	33.43
				41.88	0.25	34.45
				46.37	0.19	35.45
				52.07	*0.09*	36.26
				58.13	0.05	36.70
				65.96	0.05	37.10
				72.89	0.00	37.27
			14	No gage		

Table A3.   LOX/RP-1 Test Results.

Contact Area (ft^2)	Test No.	Gage Distance from Event (ft)	Gage No.	Time (msec)	Over-pressure (psi)	Impulse psi-msec
36.81	8	40	2	0.75	10.25	6.10
				1.48	10.29	15.89
				1.85	10.72	19.76
				2.46	9.89	26.05
				2.95	9.03	30.62
			10	1.37	12.64	8.68
				1.60	2.35	10.41
				2.37	3.93	12.84
				2.83	6.29	15.20
				3.53	5.28	19.20
				4.53	2.87	23.29
				5.90	2.58	27.03
				6.68	0.72	28.30
				8.97	0.59	29.81
				9.70	0.39	30.17
				13.01	0.39	31.46
				15.83	0.39	32.55
				17.58	0.39	33.23
				18.48	0.07	33.44
				25.26	0.00	33.69
		60	3	0.57	8.72	2.52
				0.59	5.10	2.65
				0.71	5.53	3.27
				1.81	4.26	8.64
				2.23	5.50	10.71
				2.60	4.24	12.54
				2.91	4.02	13.81
				3.51	3.05	15.92
				3.83	3.93	17.03
				4.33	2.81	18.72
				4.54	3.41	19.38
				4.80	2.68	20.17
				5.20	3.00	21.32
				5.44	2.16	21.91
				5.73	2.45	22.60
				6.18	2.08	23.63
				6.58	3.18	24.66

Table **A3.** (Continued).

Contact Area (ft)	Test No.	Gage Distance from Event (ft)	Gage No.	Time (msec)	Over-pressure (psi)	Impulse psi-msec
				7. 03	2.22	25.88
				8.43	1.67	28. 60
				10.93	1.01	31.96
				13. 77	0.45	34. 03
				14. 27	1.51	34.51
				14.53	0. 40	34.76
				14.90	0. 63	34.95
				16. 28	0. 51	35.74
				16. 70	0. 15	35.88
				19.87	0.00	36.06
			11	0. 18	8. 76	0. 81
				0. 71	4. 60	4. 37
				1.42	3. 40	7. 20
				2. 18	2.47	9.44
				2. 54	1. 71	10. 19
				2. 79	4. 90	11.01
				3.34	3.00	13. 19
				3.54	4. 70	13.97
				3. 78	3.57	14.96
				4. 26	3.45	16. 63
				4. 60	2. 88	17. 71
				4. 86	2. 90	18.45
				5. 48	2. 19	20.02
				5. 86	1. 57	20.74
				6.06	3. 52	21.25
				6. 50	0. 78	22.32
				6. 85	1.76	22.67
				7. 28	1.96	23.48
				7.95	1.48	24. 63
				8. 27	1.66	25. 14
				9. 52	1. 10	26.86
				10. 73	1.00	28. 13
				11.09	0.57	28.41
				12.59	0.46	29.20
				14.54	0.37	30.01.
				15.34	0. 65	30.42
				16.37	0.57	31.04
				17.08	0.22	31.33
				19. 19	0.00	31.56

Table A3. (Continued).

ontact Area (ft)	Test No.	Gage Distance from Event (ft)	Gage No.	Time (msec)	Over-pressure (psi)	Impulse psi-msec
		80	4	0.55	5.36	1.48
				1.24	3.47	4.56
				1.94	3.34	6.93
				2.17	3.07	7.66
				2.35	3.11	8.22
				2.66	2.77	9.15
				3.42	2.78	11.24
				4.08	2.78	13.09
				4.76	2.41	14.84
				5.50	2.05	16.50
				6.42	1.95	18.33
				6.84	1.78	19.10
				7.03	1.84	19.46
				7.61	1.50	20.42
				8.81	1.42	22.18
				10.13	1.26	23.94
				12.27	0.81	26.17
				14.36	0.56	27.59
				17.12	0.53	29.10
				19.47	0.34	30.13
				23.57	0.02	30.86
				24.32	0.00	30.87
			12	0.19	4.142	0.41
				0.45	2.32	1.25
				0.70	2.40	1.84
				1.06	2.82	2.77
				1.81	2.71	4.85
				2.86	2.63	7.65
				3.94	2.53	10.45
				4.23	2.46	11.16
				5.05	1.88	12.95
				5.80	1.88	14.34
				6.10	1.73	14.88
				6.34	1.77	15.32
				6.68	1.49	15.86
				7.42	1.47	16.95
				7.86	0.90	17.47
				8.35	1.25	18.00
				8.39	1.81	18.07
				8.42	1.27	18.12
				9.06	0.70	18.74

Table A3. (Continued).

;ontact Area (ft)	Test No.	Gage Distance from Event (ft)	Gage No.	Time (msec)	Over-pressure (psi)	Impulse psi-msec
				10.58	0.75	19.84
				11.86	0.65	20.73
				13.21	0.50	21.50
				14.72	0.41	22.19
				18.56	0.41	23.74
				22.09	0.13	24.68
				23.55	0.00	24.77
		98	13	0.90	2.61	1.18
				1.37	1.96	2.26
				2.16	1.90	3.78
				2.67	2.18	4.81
				2.87	2.22	5.25
				3.32	1.97	6.20
				3.69	1.79	6.90
				4.64	1.39	8.42
				6.08	1.31	10.37
				6.65	1.12	11.06
				7.49	1.11	11.99
				8.29	0.92	12.81
				9.67	0.59	13.85
				10.74	0.50	14.44
				11.51	0.32	14.75
				13.36	0.28	15.31
				13.85	0.38	15.47
				17.40	0.32	16.72
				17.69	0.21	16.79
				19.72	0.08	17.09
				20.66	0.00	17.13
36.81	10	40	2	0.61	16.63	5.11
				0.72	11.22	6.59
				1.00	14.20	10.25
				1.20	12.34	12.80
				1.42	12.05	15.50
				1.67	10.53	18.32
				1.96	11.94	21.56
				2.43	9.85	26.69
				3.22	9.48	34.41
				3.67	8.49	38.38
				4.20	7.73	42.66
				4.84	6.53	47.25
				4.94	7.13	47.91
				5.36	7.13	50.92
				5.90	5.82	54.41

Table A3. (Continued)

ontact Area (ft)	Test No.	Gage Distance from Event (ft)	Gage No.	Time (msec)	Over-pressure (psi)	Impulse psi-msec
			10	0.72	19.46	7.04
				0.81	6.42	8.21
				1.39	5.34	11.60
				1.66	6.22	13.17
				2.35	4.36	16.82
				2.61	4.87	18.02
				3.07	3.98	20.07
				3.21	4.87	20.67
				3.53	3.73	22.09
				3.83	5.26	23.41
				4.24	3.03	25.09
				4.81	2.34	26.64
				5.50	1.97	28.13
				5.50	0.80	28.13
				6.69	1.80	29.67
				7.01	1.89	30.25
				7.33	1.02	30.73
				8.43	0.90	31.79
				9.42	0.45	32.46
				11.53	0.45	33.41
				12.80	0.33	33.90
				13.84	0.00	34.07
		60	3	0.39	1.95	0.39
				0.73	0.00	0.72
				1.83	0.00	0.40
				2.26	0.12	0.47
				2.62	0.00	0.57
				3.18	1.70	0.63
				3.65	0.00	0.85
				4.45	5.84	4.62
				5.96	5.29	13.44
				6.79	4.81	17.71
				8.12	3.07	23.46
				8.91	4.40	26.32
				9.74	2.50	28.95
				10.70	2.28	31.28
				11.80	2.62	33.47
				12.63	2.00	34.76

Table A3.   (Continued).

Contact Area (ft)	Test No.	Gage Distance from Event (ft)	Gage No.	Time (msec)	Over-pressure (psi)	Impulse psi-msec
				14.75	0.93	37.61
				16.18	0.58	38.72
				16.98	1.09	39.34
				18.83	0.28	40.50
				20.46	0.00	41.12
			11	0.32	1.54	0.25
				0.47	0.29	0.39
				0.55	8.51	0.73
				0.77	5.77	2.32
				1.05	4.99	3.84
				1.20	5.45	4.60
				2.06	5.21	9.18
				2.49	4.66	11.29
				3.38	4.15	15.25
				3.66	4.05	16.37
				4.05	3.78	17.89
				4.32	4,13	18.97
				4.94	3.62	21.39
				5.24	2.99	22.36
				5.55	3.09	23.31
				5.66	2.05	23.59
				6.08	2.15	24.46
				6.82	1.87	25.95
				7.89	2.00	28.03
				9.22	1.35	30.26
				10.46	0.98	31.70
				11.70	0.59	32.68
				13.40	0.54	33.64
				14.29	0.32	34.02
				15.63	0.26	34.41
				17.12	0.00	34.61
		80	4	0.36	1.64	0.30
				0.68	0.62	0.48
				0.86	0.34	0.40
				1.44	0.00	0.07
				1.57	0.27	0.09
				1.82	0.17	0.09
				2.61	0.09	0.01
				3.33	0.30	0.01

Table A3.   (Continued).

ontact Area (ft)	Test No.	Gage Distance From Event (ft)	Gage No,	Time (msec)	Over- pressure (psi)	Impulse psi-msec
				4. 03	0.00	0. 12
				4.97	0.97	0. 04
				5. 42	0.46	0. 15
				6. 06	1.27	0.29
				6. 34	0. 68	0.21
				6. 88	0.29	0. 03
				7.00	0.00	0. 05
				8. 52	6.90	0. 19
				8. 98	3.36	2. 52
				9. 62	3. 68	5.22
				9.97	3.97	6. 54
				11.02	3.33	10.46
				11. 61	3. 19	12.39
				11.95	3.21	13.41
				12.31	1.99	14.36
				13.03	2.21	16.05
				13. 19	2. 54	16.42
				14. 70	2. 07	19.88
				15.00	1.69	20.45
				15. 54	1.07	21.38
				15.69	1.54	21.58
				16.80	0.92	23.08
				17. 03	1.21	23.32
				19.49	0.74	25.66
				20.00	0. 50	25.97
				22.01	0.41	26. 64
				22.45	0. 13	26.77
				23.32	0. 19	27. 18
				25. 16	0.00	27.36
			12	0.35	4.20	0.74
				1.43	4. 25	5.32
				3. 23	4. 25	12.96
				5. 29	4. 25	21.71
				7. 42	4. 17	30. 69
				8. 67	4. 17	35.91
				9.33	1.07	37.64
				12. 62	1.07	41. 17
				15.92	1.07	44.71
				20.72	1.07	49. 8?
				27. 17	0.92	56.30
				27.57	0. 72	56.62
				27.72	0.00	56.67

Table A3. (Continued).

Contact Area (ft)	Test No.	Gage Distance from Event (ft)	Gage No.	Time (msec)	Over-pressure (psi)	Impulse psi-msec
		98	13	0.40	1.35	0. 28
				1. 10	0.00	0.75
				1.59	0. 30	0. 67
				4.01	0.23	0.03
				4. 28	0.12	0.02
				6. 76	0. 12	0. 32
				6. 95	0.00	0.33
				7. 78	0.00	0.33
				8. 13	0. 30	0. 28
				8. 63	0.28	0. 13
				9. 81	0.00	0. 03
				13. 78	0.00	0.03
				14.25	4. 72	1. 16
				14. 61	4.20	2.77
				14. 78	3.49	3.40
				15. 54	3.35	5.98
				16.23	2. 89	8. 14
				17.01	2.95	10.40
				17. 24	2. 79	11.05
				18.43	2. 61	14. 28
				18.91	2. 38	15.47
				19.95	2.35	17.93
				20.49	1.92	19.07
				21.52	1.92	21.07
				21.99	1. 64	21.90
				23.26	1.43	23. 85
				24.38	1. 11	25. 27
				26.02	0. 80	26.82
				28. 15	0. 67	28.38
				30.45	0.55	29.79
				33.83	0.52	31. 59
				35.75	0.47	32.57
				36.66	0. 34	32.94
				40.07	0. 16	*33*. 78
				41.91	0.02	33.95
				45.95	0. 02	34.04
				49.75	0.00	34.09